HANSEN SOLUBILITY PARAMETERS AS A QUANTIFIABLE TOOL TO STUDY 12HSA SELF-ASSEMBLY

By

SONGWEI WU

A thesis submitted to the

Graduate School - New Brunswick

Rutgers, The State University of New Jersey

In partial fulfillment of the requirements

For the degree of

Master of Science

Graduate Program in Food Science

Written under the direction of

Michael A. Rogers

And approved by

_____

_____

_____

New Brunswick, New Jersey

October 2014

ABSTRACT OF THE THESIS

HANSEN SOLUBILITY PARAMETERS AS AQUANTIFIABLE TOOL TO STUDY 12HSA SELF-ASSEMBLY

By SONGWEI WU

Thesis Director:

Michael A. Rogers

Organogels are thermal reversible semisolid materials that show great potential for use in foods to replace saturated fats and *trans* fats in processed foods. They are comprised of an organic liquid and low concentration (~ 2 wt%) of low molecular-mass organogelators (LMOGs) that spontaneously undergo formation of three-dimensional (3-D) self-assembled fibrillar networks (SAFiNs) capable of entrapping the solvent among the entangled nanofibers.

SAFiNs formation requires the meticulous balance between contrasting solvent-gelator interactions. To elucidate the role of solvent properties on molecular gels formation, Hansen solubility parameters (HSPs) are used to correlate the nature of solvents to the gelation behavior of 12-hydroxystearic acid (12HSA). The hydrogen-bonding HSP (δ_h) is found to be particularly useful in studying and predicting the solvent effect on 12HSA self-

assembly and ultimately on gelation ability. Transparent 12HSA organogels only form in the solvents studied with hydrogen-bonding HSP less than 4.7 $MPa^{1/2}$ while solution remains when $\delta_h > 5.1 MPa^{1/2}$. A strong linear correlation has also been established between δ_h and critical gelator concentration (CGC).

The macroscopic properties, microstructure and nanostructure of 12HSA molecular gels illustrate the importance of the nature of solvents that greatly affect SAFiN properties including: crystallinity, thermal properties, polymorphic forms, carboxylic dimer structure, domain size, fiber morphology and microstructure. Each of the aforementioned properties is influenced by δ_h and to a lesser extent the polar component of the HSPs (δ_p). 12HSA in solvents with a $\delta_h < 4.4 MPa^{1/2}$ form transparent organogels that contain fibrillar crystal aggregates with the hexagonal polymorpic form. As the δ_h of the solvent increases, the polymorph of 12HSA organogels undergoes transition from the hexagonal form to triclinic parallel form, which corresponds to the transitions observed in dimer structure, crystal morphology and the decrease in crystallinity.

This thesis is dedicated to:

My parents

Dong Wu & Hong Zheng

ACKNOWLEDGEMENTS

I have been grateful in the past two years of my graduate study and for all the encouragement and assistance that I have received from a numerous people. Without their love and support, it would have been more difficult and perhaps even impossible for me to finish this research project. Given such an opportunity, I would like to send my most sincere appreciation to those who have contributed to this accomplishment.

First and foremost, I would like to express my deepest gratitude to my advisor, Dr. Rogers for his supervision, guidance and support throughout the whole research process and his instructions on my thesis writing. He first introduced me to this research area on molecular gels and gave me the opportunity to work in his lab. The research topic is very intriguing but it was totally new to me, which made it a great challenge. I really appreciate Dr. Rogers for his great patience, time and efforts spent on guiding me through from the very beginning. Without his dedication, I could still be lost in the mist of confusions and frustrations. More than just being an academic advisor, Dr. Rogers is also a great mentor. He always encourages us to get exposed to different opportunities that help me keep refreshing my mind and see myself clearly not only in the current work but in the future planning. I will definitely taking his advice into my future study and work to better improve myself because what he said always turns out to be right.

I also would like to extend my sincere gratitude to Dr. Thomas J. Emge for his technical support in our research. His vast knowledge in crystallography and generous assistance in X-ray scattering has added tremendous value to this study and greatly facilitated the whole research process. I also would like to say thanks to Jie Gao, my research partner. Jie is a wonderful person and there were lots of memories and fun times in the past two years collaborating with her. Her assistance and encouragements are one of the important factors

that propelled me forward. We always discussed our problems and confusions which we encountered during the research, which was a great experience to learn from each other and inspire each other.

Last but not least, I would like to express my great appreciation to my parents. I know it is not easy for them to let their only child travel all the way across the world to study in another country. Thanks for allowing me to chase my dream and supporting me to come to the states to receive such a great education. Thank you for always being there for me through the good times and bad. Thanks for constantly encouraging me to do my best and bravely face the difficulties. My gratitude for their loving supports and great patience is way beyond description. Without their selfless love and faith in me, I could not have been who I am today. Also, my thanks go to my dear friends who always stand by me to cheer me up and give me support. I am so lucky and grateful to have these people in my life.

There may be others whom I have neglected to mention and please accept apologies. Thank you all for your contributions.

PREFACE

The results presented in this thesis are based on my research at Rutgers, The State University of New Jersey between September, 2011 and April, 2013. Instructed and supervised by Dr. Michael A. Rogers, work described in Chapter 4 and 5 were performed by Jie Gao and I with assistance from other collaborators. Experiments were mainly conducted in the Department of Food Science and Department of Chemistry and Chemical Biology at Rutgers, The State University of New Jersey.

Co-authored by Dr. Michael A. Rogers, Chapter 4 and 5 have been previously published. Chapter 4 was published as Gao, J.; Wu, S.; Rogers, M. A., Harnessing Hansen Solubility Parameters to Predict Organogel Formation. *Journal of Materials Chemistry* **2012,** *22*, 12651-12658. Chapter 5 was published as Wu, S.; Gao, J.; Emge, T. J., Rogers, M. A., Influence of Solvent on the Supramolecular Architectures in Molecular Gels, *Soft Matter* **2013,** *9*, 5942-5950.

TABLE OF CONTENTS

LIST OF FIGURES

LIST OF TABLES

LIST OF APPENDICES

1.0 INTRODUCTION

Lipids are a large, diverse group of naturally occurring compounds important to living organisms. More than just fatty acids and triglycerides (TAGs), lipids also include many other compounds including: waxes, sterols, phospholipids, vitamins A, D, E, and K.[1,2] Depending on the presence or absence of double bonds in their aliphatic chain, lipids can be either classified as saturated (without double bonds) or unsaturated (with double bonds) fats. The unsaturated fatty acids, are also classified based on their geometric isomerization as either *cis* or *trans* unsaturated fats.

Saturated fats occur naturally in animal-derived lipids such as meat and dairy products and also in seeds oil such as coconut oil and palm oil.[3,4,5] The naturally occurring *trans* unsaturated fats (or *trans* fats), on the other hand, can only be found in small amounts in dairy products due to the biohydrogenation of the naturally-occurring microbiota in ruminants.[6,7] Due to the more desirable properties of saturated fats (e.g. higher melting point, better oxidative stability, more pleasant mouthfeel), the food industry has shifted towards engineered lipids.[3,8] For example, liquid vegetable oils that contain *cis* unsaturated fatty acids are converted to semisolid hydrogenated fats through partial hydrogenation. Accompanied with the generation of *trans* form unsaturated fatty acids, partial hydrogenation causes the original unsaturated fats to become less unsaturated or completely saturated.[7,9,10] Due to the higher degree of saturation, hydrogenated fats have higher melting point and greater oxidative stability.[3,10] They become appealing in food industry for their role as an economical structural element used in artificial shortening and margarine,[11] a heat transfer medium due to their heat stability,[10] and as texture and palatability enhancers in baked goods.[12] It has been reported that the average consumption of *trans* fats is estimated to be 2 to 3 percent of total energy consumed in the United States.[9,13]

Saturated fats and *trans* fats have drawn lots of attention due to the reported increase in health risks associated with the consumption of these fatty acids. One of the concerns is the elevated risk of coronary heart disease.[3,9,14] It has been reported that the combined effects of saturated fats and *trans* fats mediate the blood cholesterol level by decreasing the level of high density lipoprotein (HDL), a kind of cardioprotective cholesterol, and increasing the level of low density lipoprotein (LDL), which can build up in blood vessels and narrow the arteries causing atherosclerosis.[6,14,15,16] Other health concerns also include the metabolic syndrome such as impaired insulin sensitivity, obesity and hypertension, which may further promote other subsequent health issues like type 2 diabetes.[17,18] As a result, related regulations and dietary guidelines have been proposed to control the public's dietary intake of these fats. According to American Heart Association's Diet and Lifestyle Recommendations (2006 Revision), intake of saturated fats should be limited to < 7 % of total calories consumed each day, and of *trans* fats should be limited to < 1 % of energy.[19] This statement is consistent with the current Dietary Guidelines for Americans, which is published by U.S. Department of Health and Human Services (HHS) and the U.S. Department of Agriculture (USDA) every 5 years.[20] As well, legislation requires manufacturers, to declare the amount of *trans* fats on the Nutrition Facts label for all conventional foods and supplements.[21] Recently, the Food and Drug Administration (FDA) announced a proposal that intends to eliminate *trans* fats from food supply.[22]

Increased awareness of the health effects of consuming saturated fats and *tran*s fats as well as stricter regulations, has caused the food industry to initiate reductions in the use of these hardstock fats in producing fat-based food products and finding their substitutes. There are several approaches proposed to remove *trans* fats but preserving the appeal is difficult through modified hydrogenation, interesterification, fractionation and blending.[23,24] Our

present study is focused on a non-conventional solution for replacing saturated fats and *trans* fats by using the molecular organogels technique to structure edible vegetable oil.

Molecular organogels, as a kind of soft materials, have attracted lots of interests recently for their versatile utilization in numerous industrial applications.[25,26] They are thermal reversible quasi-solid materials mainly comprised of organic liquid phase different from hydrogels comprised of water. The solute or gelator often functions at low concentrations (as low as 0.5%), which are most often low molecular-mass compounds that spontaneously undergo formation of three-dimensional (3-D) self-assembled fibrillar networks (SAFiNs) capable of entrapping solvents among the nanofibers.[26,27,28,29,30] Focused on food research, organogels can be considered as a novel structural material for their solid-like rheological properties as well as their ability to incorporate liquid edible oils.[3,31] Numerous studies have focused on low molecular-mass organogelators (LMOGs) and the formation of organogel matrix; however, these studies are hindered mainly due to the inability to predict and/or manipulate the microstructure of fibrillar network.[25] The formation of organogels relies on the self-assembly of LMOGs facilitated by weak non-covalent interactions between gelator-gelator, and gelator-solvent.[32] This aggregation process is affected not only by the organogelator properties but also the external conditions including temperature, presence of co-surfactants and solvent properties.[33,34] However, the vast majority of studies are only focused on the gelators and neglect the role of solvent in the self-assembled network.[35]

In this study, we analyze the effects of solvents on organogel formation by using Hansen solubility parameters (HSPs). Widely used in polymer science, HSPs are recently introduced by Raynal and Boueiller to be the most promising technique in studying the relationship between solvents and gelator properties. 12-hydroxystearic acid (12HSA), a simple organogelator, was selected for this study, which is derived from castor oil and has

been demonstrated to be a kind of simple yet effective organogelators.[36] By using a broad group of solvents and modifying the chain length within the same solvent class (i.e., pentane, hexane, heptane, octane, nonane, decane, dodecane, tetradecane), the relationship between the HSPs of the solvent and the physical properties of 12HSA organogels can be examined.

2.0 OBJECTIVES

In order to understand the precise role of solvents in the formation of 3-D SAFiNs, the objectives are:

1) To examine HSPs as the useful tool in predicting 12HSA organogels formation and to analyze any correlation between the individual HSP and the critical gelator concentration
2) To examine HSPs as the useful tool in studying the solvents effects on the nanostructure, microstructure and supramolecular structure of 12HSA SAFiNs

3.0 LITERATURE REVIEW

3.1 Gels

3.1.1 Concept and Definition

Gels are functional materials found in numerous applications including: toothpastes, hair gels, moisturizers, sanitizers, etc.[37,38] Food and/or food ingredients such as egg white, surimi, jams and jellies are also produced via gelation. Gels also have applications in numerous other fields, such as in transdermal or mucoadhesive drug delivery,[39,40,41] and tissue engineering.[42] Innovative synthesized soft materials are attracting more interest in materials science, in part because of their natural role in biological organisms,[37,43] which include mucus,[41] cartilage, tendons,[44] etc.

The concept of "gels" has been evolving for more than a hundred years since Thomas Graham first attempted to define such a material in 1861: "While the rigidity of the crystalline structure shuts out external expressions, the softness of the gelatinous colloid partakes of fluidity, and enables the colloid to become a medium for liquid diffusion, like water itself".[30,45] The definition at that time was vague and inaccurate and it was not until 65 years later that Dr. Dorothy Jordon Lloyd stated a more comprehensive description of gels.[46] Her definition addressed the structural aspects of gels by proposing the idea of "two components - the gelators and the solvent" that constituted gels system and she also commented on their viscoelastic properties.[30,46] These definitions are solely based on the qualitative macroscopic observations reflecting the limited analytical techniques of that time.[30] Over the next couple of decades, the definition of gels progressed and several other definitions have appeared. In 1949, Hermans was the first to relate the macroscopic properties of gels to the microscopic characteristics.[26,47] He depicted gels as "a coherent colloid systems composed of at least two components that exhibit mechanical properties of

solid states and each component is extended continuously throughout the entire system".[30,47] Due to the complexity of gels, Ferry further refined the definition of gels to be less rigid but more descriptive - "a substantially diluted system which exhibits no steady state flow".[30,48] Generally, as stated in a review by Terech and Weiss, a gel is defined as a substance with: 1) a continuous structure that has macroscopic dimensions, which is permanent on the time scale of an analytic experiment; and 2) that is solid-like in its rheological behavior.[26]

3.1.2 Gel Classifications

Various ways have been proposed to categorize gels by different criteria such as optical, thermal and mechanical properties.[49] A general classification applied for both organic and inorganic gels was proposed by Flory based on the structural criteria that has included gels into 4 categories: 1) well-ordered lamellar structure, 2) covalent polymeric network, 3) polymer network constructed upon physical aggregation, 4) particulate, disordered structure.[49,50]

According to Flory's description, gels are formed through the cross-linking of the molecules randomly distributed in space to create a 3-D network and such description has since become widely accepted as a typical model for gels.[51,52] Flory's gels can be obtained either by chemical or physical cross-linking process.[51]

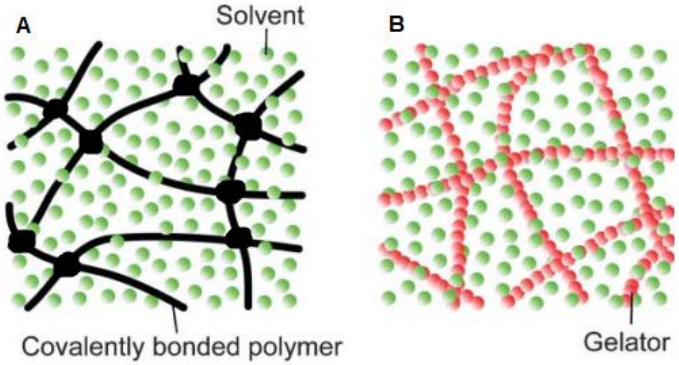

Figure 3-1 A schematic description of chemical gels network (A) with junction points and physical gels network (B) (Adapted from Kato et al., 2007).[53]

When chemical cross-linking (or formation of covalent bonds) is involved in the gelation process, a certain numbers of junction points are formed via covalent interactions in the cross-linking regions, which are not affected by the variation of external conditions such as temperature, pH, and stress due to the nature of covalent bonds.[54,55] Therefore, such gels formed are thermally irreversible and establish attributes of being robust and have a relatively high degree of elasticity.[37,56] Many industrial synthetic materials are found to fall within this category of gels such as polyester, polyacrylamide, and polyethylene.[38,57]

Conversely, physical non-covalent interactions (which may include intermolecular, intramolecular or a combination of both), result in gels that are sensitive to the external environment and undergo a gel-sol transition in response to changes in temperature.[54] The formation of cross-linking regions, in physical gels, is based on non-covalent interactions including: ionic interactions, hydrophobic interactions, hydrogen-bonding interactions, van der Waals interactions, and π-π stacking.[54,58] This kind of gel includes most naturally occurring gelators (i.e., collagen, starch, and agar) and are widely used in the food industry as thickening agents to modify viscosity.[38] They also include many synthetic materials such as polyvinyl chloride (PVC), polyacrylate, and polymethacrylate.[38,57]

3.2 Molecular Gels

3.2.1 Introduction

Although the vast majority of gels are formed using polymeric macromolecules, there are several gels comprised of small monomers or LMOGs and typically termed molecular gels.[30,59] Unlike Flory's prototypical cross-linked gel model, molecular gels are constructed based on molecular self-recognition or self-assembly of LMOGs. Cross-linking networks are not typically required in their microstructure.[51] LMOGs typically have a molecular weight less than 3000 Daltons and tend to self-assemble into extended fibers at low concentrations

(usually ≤ 2 wt % and can occur at concentrations as low as 0.5 wt %) in the appropriate solvent.[26,29,30]

The initial step, to form a molecular gel, is typically to dissolve LMOGs in the solvent at an elevated temperature above the melting temperature of the gelator to produce a solution. After which, the sol is cooled below its characteristic gelation transition temperature (T_{gel}).[29,51] The solution becomes super-saturated and the gelator molecules self-assemble to form a SAFiN that further self-aggregates to build up the supramolecular 3-D matrix, which immobilizes the liquid component. Unlike nucleation for typical spherulitic crystals, SAFiNs undergo microscopic phase separation, via stochastic nucleation once the solution is super-saturated and not macroscopic phase separation.[30]

3.2.2 Self-Assemble Firbillar Networks (SAFiNs)

SAFiNs formation is driven and stabilized by weak non-covalent interactions between gelator and gelator, gelator and solvent such as hydrogen bonding, π-π stacking, dipole-dipole interactions, electrostatic forces, metal-ligand coordination, hydrophobic effects and van der Waals interactions.[26,37,38,59,60] The highly specific interactions facilitate the preferential 1-D growth of crystal-like structure including fibers, strands and tapes. These aggregates serve similar functions of polymer chains in the polymer gels.[30,32,61] They further entangle and interact with each other to construct the higher order 3-D porous matrix. The strong entanglement and highly branched structures within the matrix render supramolecular structures that are rigid and able to entrap the fluid component by surface tension and capillary forces.[60,62,63]

To better explain the mechanism of the SAFiNs formation, a hierarchical model has been proposed to describe the self-assembly process of LMOGs from the microscopic scale

to the macroscopic scale.[62,64] There are three levels of structure involved in this transformation as described in Fig. 3-2.

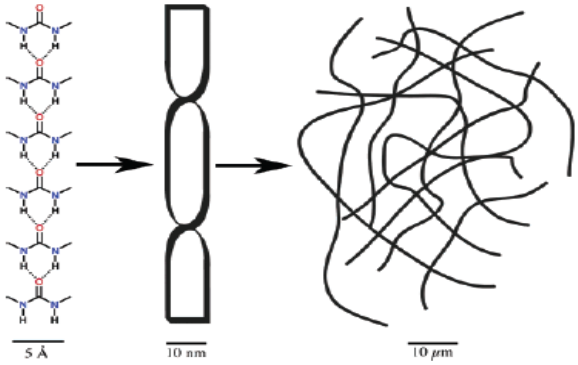

Figure 3-2 From left to right: the primary, secondary and tertiary structure of the self-assembled physical gels network (Taken from Estroff et al., 2004).[62]

The primary structure of SAFiNs is built upon the aggregation of the gelator molecules via non-covalent interactions.[62,65] Self-organization of the primary structures occurs through weak, non-covalent interactions creating the secondary 3-D structure such as fibers, rods, ribbons, sheets or other aggregates with large aspect ratio.[58,62,65] The formation of the different morphologies for this level of structure relies on physical interactions (i.e., strength and directions) as well as the structure of LMOGs.[30,60,62]

The aggregation process for both primary and secondary structures are greatly affected by different factors that control the axial and epitaxial growth of fibers[30,32,58] and the meticulous balance between factors that control solubility and precipitation.[28,66] The final tertiary supramolecular network comprised of individual SAFiN interacts forming the final porous gel system, which also determines the macroscopic properties of the materials.[32,65,67] The large solid-solvent interfacial area allows for the effective entrainment of the liquid component in pores of the network.[29,30,68] Unlike the primary and secondary structure, the tertiary structure is determined by the type of interactions between SAFiNs.[62,65] Junction

zones are the regions of interactions between the polymer-like SAFiNs strands, which connect these fibers into the 3-D supramolecular structure.[29,30]

Junction zones can be either transient or permanent as displayed in Fig. 3-3.[64] The transient junction zones rely on fiber entanglement and two major non-covalent interactions: hydrogen bonding and van der Waals forces, which are affected by the nature of the solvent.[32,64] The permanent junction zones, on the other hand, arise due to crystallographic mismatches at the interface of growing fiber crystals.[64,69] Driven by the degree of supersaturation and undercooling, crystallographic mismatches are governed by the nucleation and growth mechanism of the gel network.[64,65] The occurrence of crystallographic mismatch branching results in branched points along the fiber leading to either side-branching or tip-branching from the growing fibers.[64] Due to the division, permanent junction zones provide mesh-like networks that are effective at entraining liquids.[64,69]

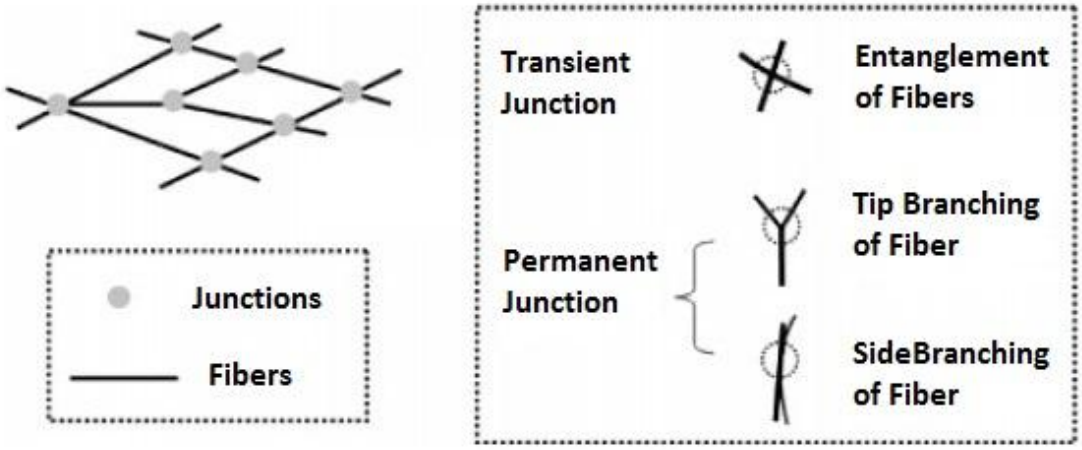

Figure 3-3 Fiber network with the illustration of two kinds of junction zones: transient junction zones and permanent junction zones (Taken from Wang et al., 2006).[64]

3.3 Organogels

Depending on the entrapped solvent properties within the fibrous network, molecular gels can be further classified as: organogels and hydrogels.[37,59] Organogels contain organic liquids immobilized as the solvent and hydrogels contain water as the liquid component.

Organogels formation process is mainly affected by two important factors. One is the chemical structure of organogelators.[70] Even the mechanism for linking the molecular structure of a gelator to its gelation capacity and its influence on SAFiNs is not clear yet, it has been observed that the subtle changes in a gelator's structure have great impacts on the nanoscopic crystal packing, which renders changes in organogels' formation and properties.[70,71,72] The other factor is the nature of solvents. Many studies have stated that solvent polarity plays an important role in the gelation efficiency of many LMOGs to construct SAFiNs. When the gelators interact more with the solvent, the active binding sites on gelators are more likely to be solvated, which impedes the gelator-gelator interactions and therefore affects the rigidity of molecular gels network.[73,74]

3.3.1 Applications

Two comprehensive reviews done on organogels (Abdallah & Weiss, 2000; Terech & Weiss, 1997) have outlined their current and future roles in many areas.[26,29] For example, in the lubrication industry, 12-hydroxyoctadecanoic acid has been studied for its use in restricting and maintaining the oil component in lubricating greases applied on various mechanical surfaces.[26,75] Divalent or trivalent metal soaps have been used as thickening agents.[26,76] In the petrochemical industry, phase selective gelation with organogelators has been shown to be effective in the crude oil spill recovery.[26,38] Drug and vaccine delivery using organogels have shown advantages due to their ability to incorporate not only the hydrophilic drug materials but also lipophilic ones that are usually difficult to be delivered and released by the traditional carriers.[77,78] Depending on the chemical properties of the organogelator and solvent, as well as the processing conditions, organogels can be designed with various physical-chemical properties for drug delivery via oral and topical routes.[77,79] Industrial applications of organogels in food may exploit them as a *trans* and saturated fat

replacer.[27] For example, organogelation makes it possible to restrict oil migration between lipid phases in food products such as cream-filled chocolates or baked cakes due to their oil binding capacity.[27,80,81] Other examples of potential applications of organogels also include: aviation fuel,[26] energy transfer and light harvesting,[82] protein crystallization,[26] cosmetics,[26,27] artwork preservation,[29,30,60,83] heat insulation or acoustic applications of xerogel,[26] purification and separation tools,[26] molecular devices as sensors or actuators,[26,38] templates for assembling nanoparticles[38,84,85] and batteries and electrochemical competitors.[86]

3.3.2 Low Molecular Weight Organogelators (LMOGs)

Considering the various potential applications of organogels, numerous studies have been conducted to discover LMOGs with desirable molecular structures and properties. Numerous LMOGs have been reported to be able to effectively immobilize various kinds of organic solvents ranging from n-alkanes to the complex substituted steroids or salts.[26,70] Slight changes in the molecular structure many result in significant changes in the crystal structures.[70]

Long chain n-alkanes only self-aggregate driven by the London dispersion forces due to the lack of any functional group in their structure.[70] However, the addition of functional groups to the long alkyl chain offers an opportunity to increase other non-covalent interactions. For example, terminal substitution of alkyl chain with a carboxylic acid functional group introduces hydrogen-bonding interactions to the total intermolecular forces besides the London dispersion forces (i.e., stearic acid).[70,87] However, these organogelators are still weak.[87] To further enhance the intermolecular interactions, other functional groups can be incorporated into the interior structure of gelator molecules.[70,87]

Research has focused on discovering different LMOGs, which are focused on the organogel structure, gelation modes in specific solvents and current or future applications.

LMOGs, can be classified into different groups to aid in the understanding and design of new LMOGs. For example, Terech and Weiss have grouped many of the known LMOGs into several classes, which are fatty acid derivatives, steroid derivatives, anthryl derivatives, amino acid types, organometallic compounds, steroidal and condensed aromatic rings contained molecules, two-component systems and other miscellaneous types.[26]

3.3.3 12-Hydroxystearic Acid (12HSA)

12HSA is derived from ricinoleic acid, a naturally occurring material obtained from castor seed oil, in which ~ 90% of the total fatty acids content is ricinoleic acid.[87,88]

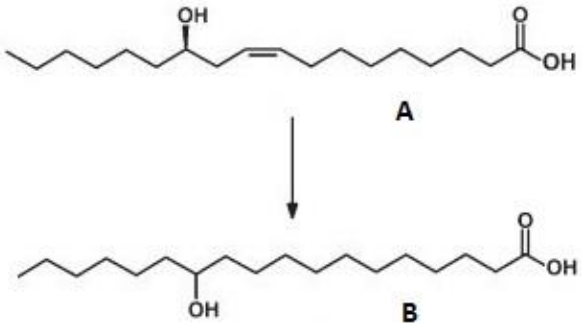

Figure 3-4 Ricinoleic acid (A) converted to 12HSA (B) by hydrogenation (Taken from Mutlu et al., 2010).[88]

As shown in Fig. 3-4, ricinoleic acid is an unsaturated ω-9 18-carbon fatty acid with a hydroxyl group attached to the C-12 position.[89] 12HSA is obtained by completely hydrogenating ricinoleic acid. The conformation of 12HSA was first clearly discussed by the work of Kuwahara et al., which is displayed in Fig. 3-5.[17,89,90]

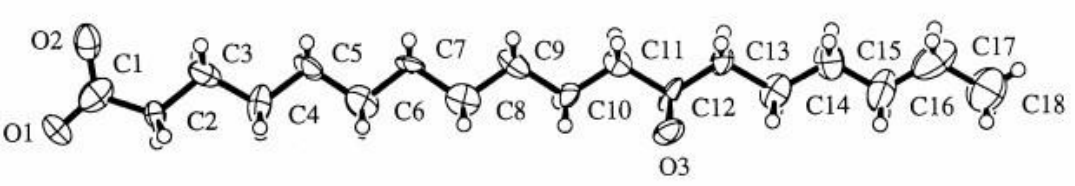

Figure 3-5 Numbering of atoms and conformation of DL-12-hydroxystearic acid (Taken from Kuwahara et al., 1996).[90]

With a hydroxyl group attached to C-12 position, 12HSA strands interact with each other and arrange into lamellar structures via hydrogen bonds between the hydroxyl groups at position C-12 along the α-axis as displayed in Fig. 3-6.[17,65,90] The distance between the O3-O3 (on 12-hydroxyl group) physical bond is 2.87 Å.[90] The aggregation results in a zig-zag pattern with a 107 ° angle of C12-O3-O3 (on 12-hydroxyl group).[17,90] The twist in pattern is due to the all-trans configuration adopted by hydrocarbon chain in the molecules along with the 12-hydroxyl group.[17,90] There is a deviation observed at C10-C11-C12-C13 with an angle of 107.3 ° only found in 12HSA instead of stearic acid, which may also partly account for the twisted helical structure.[17,90] Carboxylic head groups from two neighboring 12HSA molecules form dimers through hydrogen-bonding interactions.[17,87] The overall structure of 12HSA aggregates in organic solvent is shown in Fig. 3-7 with the hydrogen-bonding network displayed both vertically and horizontally. It is the gel network of one of the enantiomer forms of 12HSA ((*R*)-12HSA) molecules that form cyclic carboxylic dimers between molecules.[87]

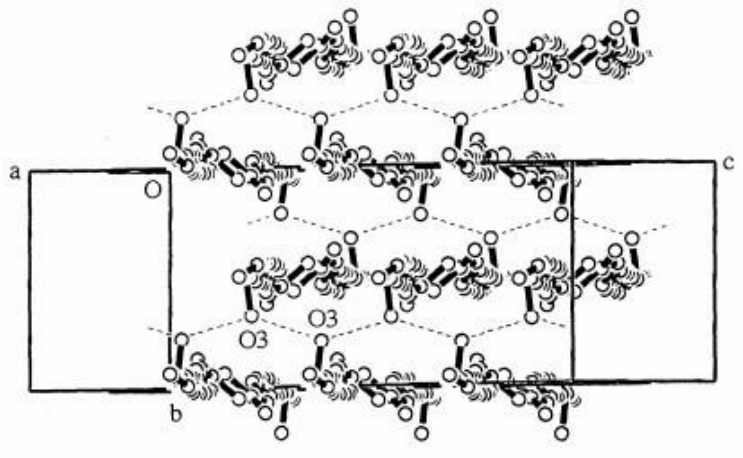

Figure 3-6 Crystallographic structure of 12HSA showing the hydrogen bond sequence along the α-axis (Taken from Kuwahara et al., 1996).[90]

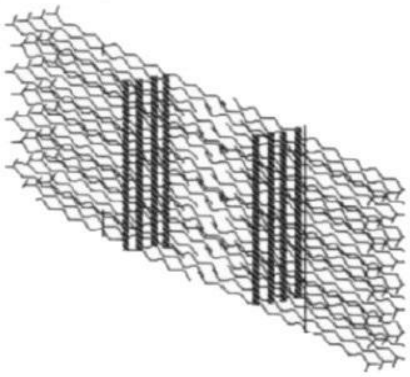

Figure 3-7 Structural model of the (*R*)-12HSA aggregates in organic solvents (Taken from Mallia et al., 2013).[87]

Currently, 12HSA has not obtained GRAS status for its use in foods, but it has potential for future use in food due to its naturally-derived nature. 12HSA is non-toxic when compared to other toxic gelators studied.[89] The simple structure and non-toxic properties were the main reasons why 12HSA was selected for further studies into its gelling behavior in different solvents. Other reasons that have driven our interest towards this kind of gelator also include: 12HSA can be easily obtained in large quantities in its (*R*) enantiomer form,[70,89] Extensive studies have been conducted on 12HSA gels and it is well documented that 12HSA efficiently gels organic solvents including carbon tetrachloride, benzene, toluene, methanol,

chloroform, mineral oil[65,91,92] and edible oil such as safflower oil and soybean oil.[25,87,93] It is documented that the microstructure of 12HSA organogels is solvent dependent. Therefore, solvents can greatly affect the gel network having significant effects on the macroscopic properties of the gel such as hardness, degree of crystallinity.[25,35]

3.4 Solubility Parameters

In an attempt to correlate solvent's properties to the gelation behavior and macroscopic properties of organogels, various approaches have been proposed. The simplest approach utilizes the dielectric constant (ε) of the solvent to quantitatively investigate the influence of solvents on gelation of specific gelators.[94,95,96] Other bulk solvent parameters such as Reichardt's E_T parameter scale have been widely used since they are simple ways to quantify and measure the solvent's properties.[94,97] However, these approaches have poor correlations to gelation ability and do not accurately reflect the specific interactions required on the molecular level.[96,98] To solve this problem, multi-parameter approaches have been developed such as the Kamlet-Taft parameters that have been used to investigate the specific solvent-gelator interactions.[96,98,99] Kamlet-Taft parameters account for different solvent-solute interactions including the hydrogen bond donation ability (α), hydrogen bond acceptor ability (β) and dipolarity-polarizability (π^*). However, previous studies indicated that Kamlet-Taft parameters only apply to some LMOGs and are not universal parameters.[97,98]

Solubility parameters, although a new tool for organogels, have been well established in polymer science.[100,101] They have found their greatest use in polymers, co-polymers, and multi-component solvents systems.[102,103,104] For example, solubility parameters are applied in the coating industry for selecting compatible solvents and surface characterization of pigments, fibers and fillers.[102] Based on the basic principle "like-dissolve-like", solubility parameters serve as a useful tool to measure the similarities between solvents, polymers,

pigments, substrates, etc.[102] A recent study by Raynal and Bouteiller, on the other hand, proposed a more promising technique using Hansen solubility parameters to assess the gelation behaviors of numerous LMOGs.[36] It was shown to correlate well with gelation behavior with only a few exceptions.[36,105]

3.4.1 Hildebrand Solubility Parameters

First introduced by Hildebrand and Scott, the Hildebrand solubility parameter was developed to describe the miscibility behaviors of solvents,[102,106,107,108] which is based on the fact of dissolution governed by the free energy change during mixing of polymer and solvent as described in the following equation:[104]

$$\Delta G_m = \Delta H_m - T\Delta S_m \quad \text{(Equation 3-1)}$$

where the Gibbs free energy change on mixing (ΔG_m) is dependent on the enthalpy change (ΔH_m) and the entropy change (ΔS_m) on mixing. Mixing occurs spontaneously when the free energy change is negative. Phase separation, which results in demixing, contributes a positive value to the free energy change. Based on the assumption in polymer science that the dissolution of the polymer is accompanied by a minor increase in entropy, enthalpy then becomes the deciding factor in determining the sign of the Gibbs free energy change.[104,105] Therefore, the solubility parameters were developed solely based on the change in the enthalpy of mixing.[104]

Hildebrand and Scott[107] and Scatchard[109] proposed the following equation to describe the enthalpy change in the mixing process:

$$\Delta H_m = V((\frac{\Delta E_1^v}{V_1})^{1/2} - (\frac{\Delta E_2^v}{V_2})^{1/2})^2 \phi_1 \phi_2 \quad \text{(Equation 3-2)}$$

where V is the volume of the mixture, V_i is the molar volume of species i, ϕ_i is the volume fraction of i in the mixture and ΔE_i^v is the energy of vaporization of species i under isothermal vaporization of the saturated liquid. ΔE_i^v , when denoted as the energy of vaporization per volume (cm^3), is the cohesive energy density (CED).[104] Vaporization occurs when the intermolecular non-covalent bonds between molecules are broken, therefore CED is a direct measure of the total attractive strengths between molecules.[102,104] The Hildebrand solubility parameter (δ_i) is derived from CED and has been defined as the square root of CED:[102]

$$\delta_i = \left(\frac{\Delta E_i^v}{V_i}\right)^{1/2} \quad \text{(Equation 3-3)}$$

There is an assumption that similar CEDs are correlated with mutual solubility, so Hildebrand solubility parameter can be viewed as an important tool in predicting solubility relationships reflecting the affinity between molecules.[102,104] However, Hildebrand solubility parameter fails to elucidate the different interactions between molecules and the association between each other.[102]

3.4.2 Hansen Solubility Parameters (HSPs)

Generally, three kinds of interactions are present in common organic solvents that include the dispersion, polar and hydrogen-bonding forces. Dispersion forces are the most common intermolecular interactions and are the only attractive forces present in non-polar symmetrical molecules such as alkanes.[110] The permanent dipole-dipole interactions give rise to a second type of intermolecular forces and are found in most molecules to various strength and extent. Hydrogen-bonding forces can be viewed as the special dipole-dipole interactions that occur between polar molecules where the hydrogen atom attached to an electronegative

atom is attracted to another electronegative atom in a different polar molecule such as fluorine, nitrogen or oxygen. The large difference in electronegativity between hydrogen and the electronegative element renders hydrogen-bonding forces the strongest intermolecular interactions.[102] HSPs, decompose the total cohesive energy (*E*) into three individual energies that represent the contributions from each of the three most basic intermolecular interactions,[102] as shown in the following equation:

$$E = E_d + E_p + E_h \quad \text{(Equation 3-4)}$$

where E_d is the dispersion cohesive energy, E_p is the polar cohesive energy, E_h is the hydrogen bonding cohesive energy. And the following equation can be derived by dividing Equation 3-4 by the molar volume of the solvent:[102]

$$\delta_i^2 = \delta_d^2 + \delta_p^2 + \delta_h^2 \quad \text{(Equation 3-5)}$$

where δ_d is the Hansen dispersion force component, δ_p is Hansen polar component, and δ_h is Hansen hydrogen-bonding component with the unit dimension of ($MPa^{1/2}$).

3.4.3 Group Contribution Methods (GSMs)

Solubility parameters can be approximated through various methods such as direct measurement, indirect methods or correlations with other physical parameters.[104] For low molecular weight materials including solvents, it can be directly calculated by measuring the energy of vaporization.[104,111] However, for polymers and other larger molecular weight materials, instead of direct measurements, indirect methods are used based on solvency testing, determination of osmotic pressure of polymer solutions and swelling values.[104,111] Correlations are also used by relating the physical parameters of polymers such as refractive index to the calculations of solubility parameters.[112]

The group contribution methods (GSMs), an alternative to experimentally determine HSPs, has been used extensively to estimate solubility parameters.[113,114,115] This method is based on the assumption that the contributions of each functional group of the molecules to the overall thermodynamic property are additive when there is only one polar or hydrogen-bonding functional group present.[102,104] As shown in following equations, the three Hansen components can be estimated by Hoftyzer and van Krevelen's method:[104]

$$\delta_d = \frac{\sum F_{di}}{V} \quad \text{(Equation 3-6)}$$

$$\delta_p = \frac{\sqrt{\sum F^2_{pi}}}{V} \quad \text{(Equation 3-7)}$$

$$\delta_h = \sqrt{\frac{\sum E_{hi}}{V}} \quad \text{(Equation 3-8)}$$

where F_{di} is the dispersive functional group value, F_{pi} is the polar functional group value, E_{hi} is the hydrogen-bonding functional group value; V is the molar volume.

3.4.4 Hansen Space

To visually display the three HSPs of solvents or polymers, Hansen space utilizes a 3-D presentation that has been proposed by Hansen.[102] A 3-D coordinate axis is constructed with the three HSPs (δ_h, δ_d, δ_p) serving as the X, Y, Z axis respectively. As shown in Fig. 3-8, each random solvent or polymer thus can be treated as a point where their HSPs vectors converge in Hansen space.[116]

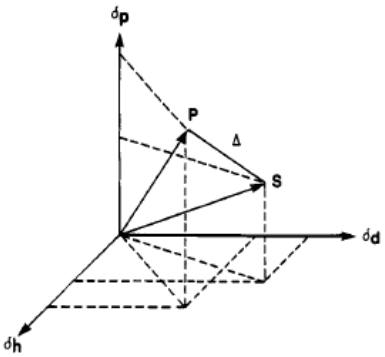

Figure 3-8 Plot of solvents (S) and polymers (P) in Hansen's 3-D model with each axis representing the individual HSPs (Adapted from Archer et al., 1991).[102,116]

Lots of observations have shown that good solvents, for a specific polymer, tend to cluster within a region away from immiscible solvents in Hansen space.[102] The specific region where solute-solvent combinations exist as a solution is termed the "*solubility sphere*".[102,117,118,119] Through trial and error, solvents tested are plotted in Hansen space to construct the solubility sphere with the radius of the sphere indicated, which is known as the "*interaction radius"* and denoted as R_0.[102]

When the interaction radius of a specific polymer is obtained, the corresponding solubility sphere can be developed in Hansen space with the HSPs of the polymer corresponding to the center of the solubility sphere. Generally, for a polymer to dissolve, the solvents must lie within the solubility sphere.[120] In order to compare the distance between solvents and the polymer with known R_0, an equation has been developed by Skaarup to determine the straight-line distance (R_a) between two points, which represent the two materials, in Hansen space.[102]

$$(R_a)^2 = 4(\delta_{d2} - \delta_{d1})^2 + (\delta_{p2} - \delta_{p1})^2 + (\delta_{h2} - \delta_{h1})^2 \quad \text{(Equation 3-9)}$$

where δ_{d1}, δ_{p1}, δ_{h1} and δ_{d2}, δ_{p2}, δ_{h2} are HSPs of the two materials respectively. The constant "4" is used to correctly illustrate the solubility data as a sphere in Hansen space.[102]

Therefore, by comparing R_a with R_0 of the polymer, the favorable solvents should be those with R_a less than R_0.

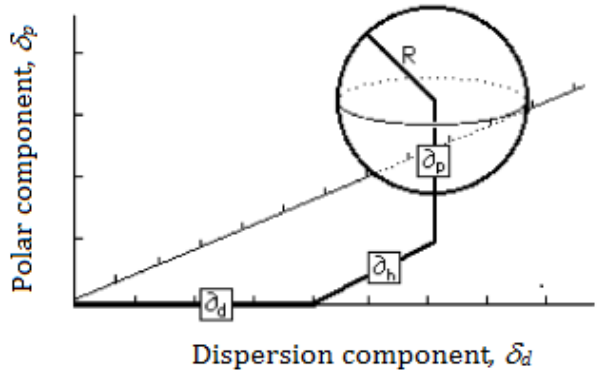

Figure 3-9 The Solubility sphere in Hansen's 3-D model with interaction radius R_0 depicted (Adapted from Hansen et al., 1971).[121]

3.4.5 Teas Plot

Another graphical technique widely used for displaying HSPs is a triangle plot developed by Teas that helps visualize all three parameters on a two-dimensional ternary graph, whereby each solvent can be interpreted as a point.[122]

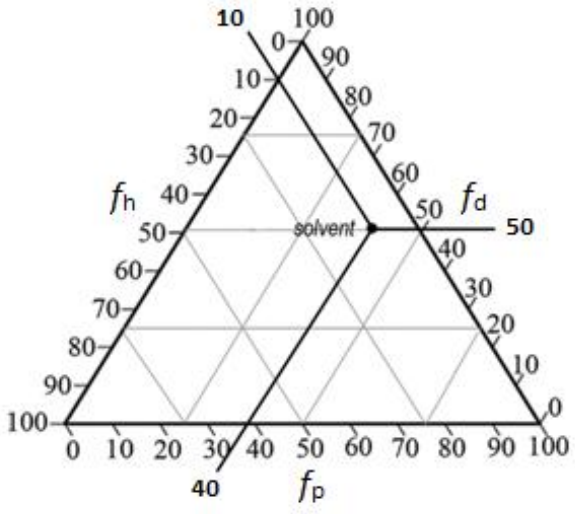

Figure 3-10 Solubility parameters of any solvent or polymer can be displayed in the ternary Teas plot.

Instead of using original HSPs, "*fractional parameters*" are applied in a Teas plot, which are generated by dividing each original HSPs by their sum as shown in the following equations.[28,102,119] In this way, three component forces are correlated to each other and the information on how much each constituted force is contributing to the overall cohesive energy can be displayed.

$$f_d = \frac{\delta_d}{\delta_d + \delta_p + \delta_h} \quad \text{(Equation 3-10)}$$

$$f_p = \frac{\delta_p}{\delta_d + \delta_p + \delta_h} \quad \text{(Equation 3-11)}$$

$$f_h = \frac{\delta_h}{\delta_d + \delta_p + \delta_h} \quad \text{(Equation 3-12)}$$

where f_d , f_p , f_h are Teas parameters that represent dispersive interactions, polar interactions and hydrogen-bonding interactions respectively.

Teas plots can be a very useful tool to study the solubility of solvents or polymers. Similar to Hansen's solubility sphere, many studies previously done have shown that the "good solvents", which show active interactions with the polymer can be marked out in a specific region separated from the "bad solvents" in Teas plot.[31] Therefore, a Teas plot can be a useful tool to study the solubility behavior of a specific polymer in untested solvents by determining the solvent's position with respect to the polymer's position in Teas plot.[111,123] Meanwhile, this plotting technique also plays an important role in aiding solvent blending to create solvent mixtures that exhibit selective solubility properties for some specific applications.[111] One of the examples is the application in art conservation where old paintings are restored by removing the old varnish while protecting the original masterpiece that stays intact.[102,124,125,126]

3.5 References

1. Fahy, E.; Subramaniam, S.; Murphy, R. C.; Nishijima, M.; Raetz, C. R. H.; Shimizu, T.; Spener, F.; van Meer, G.; Wakelam, M. J. O.; Dennis, E. A., Update of the LIPID MAPS Comprehensive Classification System for Lipids. *The Journal of Lipid Research* **2009,** *50* (Supplement), 9-14.
2. Subramaniam, S.; Fahy, E.; Gupta, S.; Manish, S.; Bymes, R. W.; Cotter, D.; Dinasarapu, A. R.; Maurya, M. R., Bioinformatics and Systems Biology of the Lipidome. *Chemical Reviews* **2011,** *111* (10), 6452-6490.
3. Botega, D. C. Z. Application of Rice Bran Wax Organogel to Substitute Solid Fat and Enhance Unsaturated Fat Content in Ice Cream. University of Guelph, Ontorio, Canada, 2012.
4. Mangels, R. Heart Healthy Eating Tips: The Vegetarian Way. http://www.vrg.org/nutshell/hearthealth1.pdf.
5. O'Brien, R. D., In *Fats and Oils: Formulating and Processing for Applications.*, 2 ed.; CRC Press Boca Raton, USA, 2004.
6. Mensink, R. P.; Katan, M. B., Effect of Dietary Trans Fatty Acids on High-Density and Low-Density Lipoprotein Cholesterol Levels in Healthy Subjects. *The New England Journal of Medicine* **1990,** *323* (7), 439-445.
7. Hunter, J. E., Dietary Levels of Trans-Fatty Acids Basis for Health Concerns. *Nutrition Research* **2005,** *25* (5), 499-513.
8. Ascherio, A.; Stampfer, M. J.; Willett, W. C. *Background and Scientific Review on Trans Fatty Acids and Coronary Heart Disease*; Harvard School of Public Health, Harvard University: 1999.
9. Mozaffarian, D.; Katan, M. B.; Ascherio, A.; Stampfer, M. J.; Willett, W. C., Medical Progress: Trans Fatty Acids and Cardiovascular Disease. *The New England Journal of Medicine* **2006,** *354* (15), 1601-1613.
10. Remig, V.; Franklin, B.; Margolis, S.; Kostas, G.; Nece, T.; Street, J. C., Trans Fats in America: A Review of Their Use, Consumption, Health Implications, and Regulation. *Journal of the American Dietetic Association* **2010,** *110* (4), 585-592.
11. Rogers, M. A., Novel Structuring Strategies for Unsaturated Fats-Meeting the Zero-Trans, Zero-Saturated Fat Challenge: A Review. *Food Research International* **2009,** *42* (7), 747-753.
12. Ghotra, B. S.; Dyal, S. D.; Narine, S. S., Lipid shortenings: A Review. *Food Research International* **2002,** *35* (10), 1015-1048.
13. Allison, D. B.; Eqan, S. K.; Barraj, L. M.; Caughman, C.; Infante, M.; Heimbach, J. T., Estimated Intakes of Trans Fatty and other Fatty Acids in the US Population. *Journal of the American Dietetic Association* **1999,** *99* (2), 166-174.
14. Astrup, A.; Dyerberg, J.; Elwood, P.; Hermansen, K.; Hu, F. B.; Jakobsen, M. U.; Kok, F. J.; Krauss, R. M.; Lecerf, J. M.; LeGrand, P.; Nestel, P.; Risérus, U.; Sanders, T.; Sinclair, A.; Stender, S.; Tholstrup, T.; Willett, W. C., The Role of Reducing Intakes of Saturated Fat in the Prevention of Cardiovascular Disease: Where Does the Evidence Stand in 2010? *The American Journal of Clinical Nutrition* **2011,** *93* (4), 684-688.
15. Judd, J. T.; Clevidence, B. A.; Muesing, R. A.; Wittes, J.; Sunkin, M. E.; Podczasy, J. J., Dietary trans Fatty Acids: Effects on Plasma Lipids and Lipoproteins of Healthy Men and Women. *The American Journal of Clinical Nutrition* **1994,** *59* (4), 861-868.

16. Judd, J. T.; Baer, D. J.; Clevidence, B. A.; Kris-Etherton, P.; Muesing, R. A.; Iwane, M., Dietary cis and trans Monounsaturated and Saturated Fatty Acids and Plasma Lipids and Lipoproteins in Men. *Lipids* **2002,** *37* (2), 123-131.
17. Rogers, M. A. Nanostructuring Fiber Morphology in 12HSA Organogels and the Development of a Food Grade Organogelator. University of Guelph, Ontorio, Canada, 2008.
18. Riccardi, G.; Giacco, R.; Rivellese, A. A., Dietary Fat, Insulin Sensitivity and the Metabolic Syndrome. *Clinical Nutrition* **2004,** *23* (4), 447-456.
19. Lichtenstein, A. H.; Appel, L. J.; Brands, M.; Carnethon, M.; Daniels, S.; Franch, H. A.; Franklin, B.; Kris-Etherton, P.; Harris, W. S.; Howard, B.; Karanja, N.; Lefevre, M.; Rudel, L.; Sacks, F.; Van Horn, L.; Winston, M.; Wylie-Rosett, J., Diet and Lifestyle Recommendations Revision 2006: A Scientific Statement from the American Heart Association Nutrition Committee. *Circulation* **2006,** *114* (1), 82-96.
20. U.S. Department of Agriculture and U.S. Department of Health and Human Services. *Dietary Guidelines for Americans, 2010.* 7th Edition, Washington, DC: U.S. Government Printing Office, December 2010.
21. "Tentative Determination Regarding Partially Hydrogenated Oils; Request for Comments and for Scientific Data and Information," *78 Federal Register 217* (8 Nov 2013), pp. 67169-67175.
22. "Food Labeling: Trans Fatty Acids in Nutrition Labeling, Nutrient Content Claims, and Health Claims," *68 Federal Register 133* (11 July 2003), pp. 41434 -41506.
23. Wassell, P.; Young, N. W. G., Food Applications of Trans Fatty Acid Substitutes. *International Journal of Food Science and Technology* **2007,** *42* (5), 503-517.
24. Klonoff, D. C., Replacements for Trans Fats-Will There Be an Oil Storage? *Journal of Diabetes Science and Technology* **2007,** *1* (3), 415-422.
25. Rogers, M. A.; Marangoni, A. G., Solvent-Modulated Nucleation and Crystallization Kinetics of 12 Hydroxystearic Acid: A Nonisothermal Approach. *Langmuir* **2009,** *25* (15), 8556-8566.
26. Terech, P.; Weiss, R. G., Low Molecular Mass Gelators of Organic Liquids and the Properties of Their Gels. *Chemical Reviews* **1997** *97* (8), 3133-3160.
27. Hughes, N. E.; Marangoni, A. G.; Wright, A. J.; Rogers, M. A.; Rush, J. W. E., Potential Food Applications of Edible Oil Organogels. *Trends in Food Science & Technology* **2009,** *20* (10), 470-480.
28. Wu, Y.; Wu, S.; Zou, G.; Zhang, Q., Solvent Effects on Structure, Photoresponse and Speed of Gelation of a Dicholesterol-linked Azobenzene Organogel. *Soft Matter* **2011,** *7* (19), 9177-9183.
29. Abdallah, D. J.; Weiss, R. G., Organogels and Low Molecular Mass Organic Gelators. *Advanced Materials* **2000,** *12* (17), 1237–1247.
30. Weiss, R. G.; Terech, P., Introduction. In *Molecular Gels: Materials with Self-Assembled Fibrillar Networks*, Weiss, R. G.; Terech, P., Eds. Springer: Dordrecht, The Neatherlands, 2006; pp 1-13.
31. Rogers, M. A.; Wright, A. J.; Marangoni, A. G., Oil Organogels: the Fat of the Future? *Soft Matter* **2009,** *5* (8), 1594-1596.
32. Rogers, M. A.; Wright, A. J.; Marangoni, A. G., Engineering the Oil Binding Capacity and Crystallinity of Self-Assembled Fibrillar Networks of 12-Hydroxystearic Acid in Edible Oils. *Soft Matter* **2008,** *4* (7), 1483-1490.
33. Nomura, R.; Yamada, K.; Tabei, J.; Takakura, Y.; Takigawa, T.; Masuda, T., Stumuli-Responsive Organogel Based on Poly (N-Propargylamide). *Macromolecules* **2003,** *36* (18), 6939-6941.

34. Wright, A. J.; Marangoni, A. G., Vegetable Oil-Based Ricinelaidic Acid Organogels-Phase Behavior, Microstructure and Rheology. In *Edible Oleogels: Structure and Health Implications*, Marangoni, A. G.; Garti, N., Eds. AOCS Press: 2011; pp 81-97.
35. Xu, H.; Song, J.; Tian, T.; Feng, R., Estimation of Organogel Formation and Influence of Solvent Viscosity and Molecular Size on Gel Properties and Aggregate Structures. *Soft Matter* **2012,** *8* (12), 3478-3486.
36. Raynal, M.; Bouteiller, L., Organogel Formation Rationalized by Hansen Solubility Parameters. *Chemical Communications* **2011,** *47* (29), 8271-8273.
37. Rao, M. R.; Sun, S.-S., Supramolecular Assemblies of Amide-Derived Organogels Featuring Rigid π-Conjugated Phenylethynyl Frameworks. *Langmuir* **2013,** *29* (49), 15146-15158.
38. Sangeetha, N. M.; Maitra, U., Supramolecular Gels: Functions and Uses. *Chemical Society Reviews* **2005,** *34* (10), 821-836.
39. Carvalho, F. C.; Calixto, G.; Hatakeyama, I. K.; Luz, G. M.; Gremião, M. P. D.; Chorilli, M., Rheological, Mechanical, and Bioadhesive Behavior of Hydrogels to Optimize Skin Delivery Systems. *Drug Development and Industrial Pharmacy* **2013,** *39* (11), 1750-1757.
40. Sun, F.; Sui, C.; Zhou, Y.; Liu, X.; Shi, Y.; Wu, Y.; Li, Y., Preparation, Characterization and Pharmacological Evaluation of Tolterodine Hydrogels for the Treatment of Overactive Bladder. *International Journal of Pharmaceutics* **2013,** *454* (1), 532-538.
41. Tsibouklis, J.; Middleton, A. M.; Patel, N.; Pratten, J., Toward Mucoadhesive Hydrogel Formulations for the Management of Xerostomia: The Physicochemical, Biological, and Pharmacological Considerations. *Journal of Biomedical Materials Research Part A* **2013,** *101* (11), 3327-3338.
42. Gutowska, A.; Jeong, B.; Jasionowski, M., Injectable Gels for Tissue Engineering. *The Anatomical Record* **2001,** *263* (4), 342-349.
43. Steed, J. W., Supramolecular Gel Chemistry: Developments Over the Last Decade. *Chemical Communications* **2011,** *47* (5), 1379-1383.
44. Thiele, H. F. Process of Reconstructing Tendons, Cartilage ,Nerve Sheaths, and Products. U.S Patent 3551560, Dec 29, 1970.
45. Graham, T., Liquid Diffusion Applied to Analysis *Philosophical Transactions of the Royal Society of London* **1861,** *151*, 183-224.
46. Lloyd, D. J., In *Colloid Chemistry*, Alexander, J., Ed. The Chemical Catalog Company Inc: New York, 1926; Vol. 1, pp 767-782.
47. Hermans, P. H., Gels. In *Colloid Science, Vol. II*, Kruyt, H. R., Ed. Elsevier: Amsterdam, The Netherlands, 1949; pp 483-651.
48. Ferry, J. D., In *Viscoelastic Properties of Polymers*, John Wiley & Sons: New York, 1961; p 391.
49. Nishinari, K., Some Thoughts on the Definition of a Gel. In *Progress in Colloid and Polymer Science-Gels: Structure, Properties, and Functions: Fundamentals and Applications*, Tokita, M.; Lishinari, K., Eds. Springer: 2009; Vol. 136, pp 87-94.
50. Pierre, A. C., Gels. In *Introduction to Sol-Gel Processing* Springer: 1998; pp 205-220.
51. Raghavan, S. R.; Douglas, J. F., The Conundrum of Gel Formation by Molecular Nanofibers, Wormlike Micelles, and Filamentous Proteins: Gelation without Cross-Links? *Soft Matter* **2012,** *8* (33), 8539-8546.
52. Stauffer, D.; Aharony, A., In *Introduction To Percolation Theory*, CRC Press: 1994.
53. Kato, T.; Hirai, Y.; Nakaso, S.; Moriyama, M., Liquid-crystalline physical gels. *Chemical Society Reviews* **2007,** *36* (12), 1857-67.

54. Kato, K.; Ito, K., Side-Ring Materials Using Polyrotaxane. In *Supramolecular Polymer Chemistry*, Harada, A., Ed. WILEY-VCH Verlag GmbH & Co. kGaA, 2012; pp 205-229.
55. Song, J. Y.; Wang, Y. Y.; Wan, C. C., Review of Gel-Type Polymer Electrolytes for Lithium-Ion Batteries. *Journal of Power Sources* **1999,** *77* (2), 183–197.
56. Overstreet, D. J.; Dutta, D.; Stabenfeldt, S. E.; Vernon, B. L., Injectable Hydrogels. *Journal of Polymer Science Part B: Polymer Physics* **2012,** *50* (13), 881-903.
57. Grassino, S. B. Gel: A Short Word with a Long Meaning. http://pslc.ws/macrog/property/gel/gel.htm.
58. Suzuki, M.; Nakajima, Y.; Yumoto, M.; Kimura, M.; Shirai, H.; Hanabusa, K., Effects of Hydrogen Bonding and van der Waals Interactions on Organogelation Using Designed Low-Molecular-Weight Gelators and Gel Formation at Room Temperature. *Langmuir* **2003,** *19* (21), 8622-8624.
59. Buerkle, L. E.; Rowan, S. J., Supramolecular Gels Formed from Multi-Component Low Molecular Weight Species. *Chemical Society Reviews* **2012,** *41* (18), 6089-6102.
60. George, M.; Weiss, R. G., Molecular Organogels. Soft Matter Comprised of Low-Molecular-Mass Organic Gelators and Organic Liquids. *Accounts of Chemical Research* **2006** *39* (8), 489-497.
61. Terech, P.; Furman, I.; Weiss, R. G., Structures of Organogels Based upon Cholesteryl 4-(2-Anthryloxy)butanoate, a Highly Efficient Luminescing Gelator: Neutron and X-ray Small-Angle Scattering Investigations. *The Journal of Physical Chemistry* **1995,** *99* (23), 9558-9566.
62. Estroff, L. A.; Hamilton, A. D., Water Gelation by Small Organic Molecules. *Chemical Reviews* **2004,** *104* (3), 1201-1218.
63. Suzuki, M.; Hanabusa, K., Polymer Organogelators That Make Supramolecular Organogels through Physical Cross-Linking and Self-Assembly. *Chemical Society Reviews* **2009,** *39* (2), 455-463.
64. Wang, R.-Y.; Liu, X.-Y.; Narayanan, J.; Xiong, J.-Y.; Li, J.-L., Architecture of Fiber Network: From Understanding to Engineering of Molecular Gels. *The Journal of Physical Chemistry B* **2006,** *110* (51), 25797-25802.
65. Rogers, M. A.; Wright, A. J.; Marangoni, A. G., Nanostructuring Fiber Morphology and Solvent Inclusions in 12-Hydroxystearic Acid/Canola Oil Organogels. *Current Opinion in Colloid & Interface Science* **2009,** *14* (1), 33-42.
66. Zhu, G.; Dordick, J. S., Solvent Effect on Organogel Formation by Low Molecular Weight Molecules. *Chemistry of Materials* **2006,** *18* (25), 5988-5995.
67. Wang, R.-Y.; Liu, X.-Y.; Xiong, J.; Li, J., Real-Time Observation of Fiber Network Formation in Molecular Organogel: Supersaturation Dependent Microstructure and Its Related Rheological Property. *The Journal of Physical Chemistry B* **2006,** *110* (14), 7275-7280.
68. de Loos, M.; Feringa, B. L.; van Esch, J. H., Design and Application of Self-Assembled Low Molecular Weight Hydrogels. *European Journal of Organic Chemistry* **2005,** *2005* (17), 3615-3631.
69. Lam, R.; Quaroni, L.; Pederson, T.; Rogers, M. A., A Molecular Insight Into the Nature of Crystallographic Mismatches in Self-Assembled Fibrillar Networks under Non-Isothermal Crystallization Conditions. *Soft Matter* **2009,** *6* (2), 404-408.
70. Mallia, V. A.; George, M.; Blair, D. L.; Weiss, R. G., Robust Organogels from Nitrogen-Containing Derivatives of (R)-12-Hydroxystearic Acid as Gelators: Comparisons with Gels from Stearic Acid Derivatives†. *Langmuir* **2009,** *25* (15), 8615-8625.

71. Burrows, A. D., In *Structure and Bonding*, Mingos, D. M. P., Ed. Springer-Verlag: Berlin, 2004; Vol. 108, pp 55-96.
72. George, M.; Tan, G.; John, V. T.; Weiss, R. G., Urea and Thiourea Derivatives as Low Molecular-Mass Organogelators. *Chemistry-A European Journal* **2005,** *11* (11), 3243-3255.
73. Krishnan, A. S.; Roskov, K. E.; Spontak, R. J., Nanostructured Organogels via Molecular Self-Assembly. In *Advanced Nanomaterials*, Geckeler, K. E.; Nishide, H., Eds. WILEY-VCH: 2010; pp 791-834.
74. Wilder, E. A.; Hall, C. K.; Khan, S. A.; Spontak, R. J., Effects of Composition and Matrix Polarity on Network Development in Organogels of Poly(ethylene glycol) and Dibenzylidene Sorbitol. *Langmuir* **2003,** *19* (15), 6004-6013.
75. Boner, C. J., In *Manufacture and Application of Lubricating Greases*, Robert E. Krieger Publishing Company: New York, 1954.
76. Pilpel, N., Properties of Organic Solutions of Heavy Metal Soaps. *Chemical Reviews* **1963,** *63* (3), 221-234.
77. Vintiloiu, A.; Leroux, J.-C., Organogels and Their Use in Drug Delivery - A Review. *Journal of Controlled Release* **2008,** *125* (3), 179-192.
78. Lupi, F. R.; Gabriele, D.; Baldino, N.; Mijovic, P.; Parisi, O. I.; Puoci, F., Olive Oil/Policosanol Organogels for Nutraceutical and Drug Delivery Purposes. *Food & Function* **2013,** *4* (10), 1512-1520.
79. Kang, L. F.; Cheong, H. H.; Chan, S. Y.; Fung, P. C. L., Application of Small-Molecular Gels - Drug Delivery. In *Soft Fibrillar Materials: Fabrication and Applications*, Li, J.-L.; Liu, X. Y., Eds. Wiley-VCH Verlag GmbH & Co. KGaA: Weinheim, Germany, 2013; pp 115-117.
80. Nakano, A.; Masaki, N. Migration Inhibitor for Fats and Oils for Baked Cakes and Process for Producing Composite Baked Cakes with the Use of the Same. U.S Patent 04855152, Aug 8, 1989.
81. Marty, S.; Baker, K.; Dibildox-Alvarado, E.; Rodrigues, J. N.; Marangoni, A. G., Monitoring and Quantifying of Oil Migration in Cocoa Butter Using a Flatbed Scanner and Fluorescence Light Microscopy. *Food Research International* **2005,** *38* (10), 1189–1197.
82. Ajayaghosh, A.; Praveen, V. K.; Vijayakumar, C., Organogels as Scaffolds for Excitation Energy Transfer and Light Harvesting. *Chemical Society Reviews* **2008,** *37* (1), 109-122.
83. Carretti, E.; Deia, L.; Weiss, R. G., Soft Matter and Art Conservation. Rheoreversible Gels and Beyond. *Soft Matter* **2005,** *1* (1), 17–22.
84. Simmons, B.; Li, S.; John, V. T.; McPherson, G. L.; Taylor, C.; Schwartz, D. K.; Maskos, K., Spatial Compartmentalization of Nanoparticles into Strands of a Self-Assembled Organogel. *Nano Letters* **2002,** *2* (10), 1037-1042.
85. Kimura, M.; Kobayashi, S.; Kuroda, T.; Hanabusa, K.; Shirai, H., Assembly of Gold Nanoparticles into Fibrous Aggregates Using Thiol-Terminated Gelators. *Advanced Materials* **2004,** *16* (4), 335-338.
86. Chatterjee, J.; Liu, T.; Wang, B.; Zheng, J. P., Highly Conductive PVA Organogel Electrolytes for Applications of Lithium Batteries and Electrochemical Capacitors. *Solid State Ionics* **2010,** *181* (11-12), 531-535.
87. Mallia, V. A.; Weiss, R. G., Self-assembled Fibrillar Networks and Molecular Gels Employing 12 Hydroxystearic Acid and Its Isomers and Derivatives. In *Journal of Physical Organic Chemistry*, 2013.
88. Mutlu, H.; Meier, M. A. R., Castor Oil as a Renewable Resource for the Chemical Industry. *European Journal of Lipid Science and Technology* **2010,** *112* (1), 10-30.

89. Co, E.; Marangoni, A. G., The Formation of a 12-Hydroxystearic Acid/Vegetable Oil Organogel Under Shear and Thermal Fields. *Journal of the American Oil Chemists' Society* **2013,** *90* (4), 529-544.
90. Kuwahara, T.; Nagase, H.; Endo, T.; Ueda, H.; Nakajima, M., Crystal structure of DL-12-Hydroxystearic Acid. *Chemistry Letters* **1996,** *25* (6), 435-436.
91. Grahame, D. A. S.; Olauson, C.; Lam, R. S. H.; Pedersen, T.; Borondics, F.; Abraham, S.; Weiss, R. G.; Rogers, M. A., Influence of Chirality on the Modes of Self-assembly of 12-Hydroxystearic Acid in Molecular Gels of Mineral Oil. *Soft Matter* **2011,** *7* (16), 7359-7365.
92. Li, J.-L.; Wang, R.-Y.; Liu, X.-Y.; Pan, H.-H., Nanoengineering of a Biocompatible Organogel by Thermal Processing. *The Journal of Physical Chemistry B* **2009,** *113* (15), 5011–5015.
93. Eloundou, J. P.; Girard-Reydet, E.; Gérard, J. F.; Pascault, J.-P., Calorimetric and Rheological Studies of 12-Hydroxystearic Acid/Digycidyl Ether of Bisphenol A Blends. *Polymer Bulletin* **2005,** *53* (5-6), 367-375.
94. Zhao, C.; Wang, H.; Bai, B.; Qu, S.; Song, J.; Ran, X.; Zhang, Y.; Li, M., Organogels from Unsymmetrical π-Conjugated 1,3,4-Oxadiazole Derivatives. *New Journal of Chemistry* **2013,** *37* (5), 1454-1460.
95. Makarević, J.; Jokić, M.; Perić, B.; Tomišić, V.; Kojić-Prodić, B.; Žinić, M., Bis(Amino Acid) Oxalyl Amides as Ambidextrous Gelators of Water and Organic Solvents: Supramolecular Gels with Temperature Dependent Assembly/Dissolution Equilibrium. *Chemistry-A European Journal* **2001,** *7* (15), 3328-3341.
96. Hirst, A. R.; Smith, D. K., Solvent Effects on Supramolecular Gel-Phase Materials: Two-Component Dendritic Gel. *Langmuir* **2004,** *20* (25), 10861-10867.
97. Bielejewski, M.; Kowalczuk, J.; Kaszyńska, J.; Łapiński, A.; Luboradzki, R.; Demchuk, O.; Tritt-Goc, J., Novel Supramolecular Organogels Based on a Hydrazide Derivative: Non-Polar Solvent-Assisted Self-assembly, Selective Gelation Properties, Nanostructure, Solvent Dynamics. *Soft Matter* **2013,** *9* (31), 7501-7514.
98. Edwards, W.; Lagadec, C. A.; Smith, D. K., Solvent-Gelator Interactions-Using Empirical Solvent Parameters to Better Understand the Self-assembly of Gel-Phase Materials. *Soft Matter* **2011,** *7* (1), 110-117.
99. Lagalante, A. F.; Hall, R. L.; Bruno, T. J., Kamlet-Taft Solvatochromic Parameters of the Sub- and Supercritical Fluorinated Ethane Solvents. *The Journal of Physical Chemistry B* **1998,** *102* (34), 6601-6604.
100. Barton, A. F. M., Applications of Solubility Parameters and Other Cohesion Parameters in Polymer Science and Technology. *Pure and Applied Chemistry* **1985,** *57* (7), 905-912.
101. Sperling, L. H., *Introduction to Physical Polymer Science*. John Wiley & Sons, Inc.: Hoboken, New Jersey, 2006.
102. Hansen, C. M., In *Hansen Solubility Parameters: A User's Handbook, Second Edition* CRC Press: New York, 2007.
103. Ham, H. T.; Choi, Y. S.; Chung, I. J., An Explanation of Dispersion States of Single-Walled Carbon Nanotubes in Solvents and Aqueous Surfactant Solutions Using Solubility Parameters. *Journal of Colloid and Interface Science* **2005,** *286* (1), 216-223.
104. Grulke, E. A., Solubility Parameter Values. In *Polymer Handbook, 4th Ed.*, Brandrup, J.; Immergut, E. H.; Grulke, E. A., Eds. Wiley, John & Sons, Incorporated: 1999; pp 675-627.
105. Gao, J.; Wu, S.; Rogers, M. A., Harnessing Hansen Solubility Parameters to Predict Organogel Formation. *Journal of Materials Chemistry* **2012,** *22* (25), 12651-12658.

106. Belmares, M.; Blanco, M.; Goddard, W. A.; Ross, R. B.; Caldwell, G.; Chou, S. H.; Pham, J.; Olofson, P. M.; Thomas, C., Hildebrand and Hansen Solubility Parameters from Molecular Dynamics with Applications to Electronic Nose Polymer Sensors. *Journal of Computational Chemistry* **2004,** *25* (15), 1814-1826.
107. Hildebrand, J.; Scott, R. L., In *The solubility of Nonelectrolytes, 3rd Ed.* , Reinhold: New York, 1950.
108. Hildebrand, J.; Scott, R. L., In *Regular Solutions* Prentice Hall: Englewood Cliffs, 1962.
109. Scatchard, G., Equilibrium in Non-Electrolyte Mixtures. *Chemical Reviews* **1949,** *44* (1), 7–35.
110. Stefanis, E.; Panayiotou, C., Prediction of Hansen Solubility Parameters with a New Group-Contribution Method. *International Journal of Thermophysics* **2008,** *29* (2), 568-585.
111. Miller-Chou, B. A.; Koenig, J. L., A review of Polymer Dissolution. *Progress in Polymer Science* **2003,** *28* (8), 1223-1270.
112. Koenhen, D. M.; Smolders, C. A., The determination of Solubility Parameters of Solvents and Polymers by Means of Correlation with other Physical Quantities. *Journal of Applied Polymer Science* **1975,** *19* (4), 1163-1179.
113. Jang, M.; Kamens, R. M.; Leach, K. B.; Strommen, M. R., A Thermodynamic Approach Using Group Contribution Methods to Model the Partitioning of Semivolatile Organic Compounds on Atmospheric Particulate Matter. *Environmental Science & Technology* **1997,** *31* (10), 2805-2811.
114. Lindvig, T.; Michelsen, M. L.; Kontogeorgis, G. M., A Flory-Huggins Model Based on the Hansen Solubility Parameters. *Fluid Phase Equilibria* **2002,** *203* (1-2), 247-260.
115. Fedors, R. F., A method for Estimating Both the Solubility Parameters and Molar Volumes of Liquids. Supplement. *Polymer Engineering & Science* **1974,** *14* (6), 472-472.
116. Archer, W. L., Determination of Hansen Solubility Parameters for Selected Cellulose Ether Derivatives. *Industrial & Engineering Chemistry Research* **1991,** *30* (10), 2292-2298.
117. Barton, A. F. M., In *Handbook of Solubility Parameters and other Cohesion Parameters, 2nd ed.*, CRC Press: Boca Raton, FL, 1991.
118. Hansen, C. M., In *The Three Dimensional Solubility Parameter and Solvent Diffusion Coefficient*, Copenhagen Danish Technical Press: Denmark, 1967; pp 33-38.
119. Barton, A. F. M., Solubility parameters. *Chemical Reviews* **1975,** *75*, 731–753.
120. Burke, J. Solubiity Parameters: Theory and Application *The Book and Paper Group ANNUAL* [Online], 1984. http://cool.conservation-us.org/coolaic/sg/bpg/annual/v03/bp03-04.html.
121. Hansen, C. M., Solubility in the Coatings Industry. *Färg och Lack* **1971,** *17* (4), 69-77.
122. Teas, J. P., Graphic Analysis of Resin Solubilities. *Journal of Paint Technology* **1968,** *40* (516), 19-25.
123. Xu, H. S., J.; Tian, T.; Feng, R., Estimation of Organogel Formation and Influence of Solvent Viscosity and Molecular Size on Gel Properties and Aggregate Structures. *Soft Matter* **2012,** *8* (12), 3478-3486.
124. Smith, G. D.; Johnson, R., Strip 'Tea' - Solubility Data for the Removal (and Application) of Low Molecular Weight Synthetic Resins Used as Inpainting Media and Picture Varnishes. *WAAC Newsletter* **2008,** *30* (1), 11-19.
125. Hedley, G., Solubility Parameters and Varnish Removal: A Survey. *The Conservator* **1980,** *4* (1), 12-18.
126. Phenix, A., Solubility Parameters and the Cleaning of Paintings: An Update and Review. *Zeitschrift für Kunsttechnologie und Konservierung* **1998,** *12* (2), 387-409.

4.0 HARNESING HANSEN SOLUBILITY PARAMETERS TO PREDICT ORGANOGEL FORMATION

Gao, J., Wu, S., and Rogers, M. A.

**This chapter is published in *Journal of Material Chemistry* (DOI: 10.1039/c2jm32056h), Received: April 2, 2012 / Published: July 7, 2012.

4.1 Abstract

HSPs predict the capacity of molecular gels to form in a vast array of organic solvents. The prediction ability for 12HSA is closely associated with the hydrogen-bonding HSP (δ_h). Solvents with a hydrogen-bonding HSP less than 4.7 $MPa^{1/2}$ produce clear organogels, opaque organogels formed between 4.7 $MPa^{1/2} < \delta_h < 5.1$ $MPa^{1/2}$ and solution remains when the hydrogen-bonding HSP is greater than 5.1 $MPa^{1/2}$. Furthermore, the critical gelator concentration (CGC) is linearly correlated with the hydrogen-bonding HSP. Solvents with the same functional group, which varied only by chain length, have correlations between the static relative permittivity, total HSP, dispersive HSP, polar HSP and hydrogen-bonding HSP and the CGC**.**

4.2 Introduction

Organogels are thermal reversible quasi-solid materials mainly comprised of organic liquids that undergo spontaneous formation of SAFiNs.[1,2,3] The non-covalent interactions within these small molecules are capable of structuring fluids, preventing flow and improving the mechanical properties of some solids.[4,5] Numerous practical applications of organogels are being investigated pertaining to photovoltaics,[6] light harvesting,[7] templating reactions,[7] controlled drug release,[8] and reversible photoisomerization.[9]

SAFiNs, in organic solvents, require a meticulous balance between contrasting parameters including solubility and those intermolecular forces that control epitaxial growth into axially symmetric elongated aggregates.[2,10,11] The precise ratio of gelator-gelator interactions to gelator-solvent interactions is established to play a central role in the formation of an organogel; however, the direct effects of solvents on the physical properties are not well understood.[9,12] As solvent-gelator interactions increase, the likelihood of directional gelator-gelator interactions decreases leading to thicker fibers.[9,13] In general,

optimal gelation is achieved when the solvent and gelator are unable to form intermolecular hydrogen bonds and the SAFiN is comprised of thin entangled fibers.[13] Typically, the intermolecular forces that drive aggregation are non-covalent in nature and include hydrogen-bonding,[14,15,16,17] π-π stacking, dipole-dipole,[18,19] and London dispersion forces,[20] however, the vast majority of reported organogelators are driven to spontaneously self-assemble by hydrogen bonding.[9, 21]

Due to the interplay between solvent and gelator, numerous attempts have been made to correlate solvent parameters to gelation ability.[11,22] The most promising technique was recently presented by Raynal and Bouteiller where they preformed a meta-analysis, applying the HSPs to numerous LMOGs evaluating gelation behavior.[22] Their meta-analysis revealed that the solvents which gelled had similar HSPs with only a few exceptions.[22] Numerous other measures of solubility have been applied to individual organogels which include dielectric constants,[23,24] Hildebrand solubility parameter[22] and the aforementioned HSPs.[22,24,25] Solubility parameters, although a new tool for organogels, have been well established for polymers, co-polymers, and systems employing multi-component solvents.[26,27,28] From an industrial perspective, understanding the interactions between solvents and gelating molecules is of utmost importance. The objective of this manuscript is to scrutinize HSPs for a much wider class of solvents and to observe if significant trends exist that may correlate the individual HSPs to the CGC.

4.3Materials and Methods

4.3.1 Materials

Several classes of organic solvents were sub-divided into solvents capable of hydrogen-bonding, apolar and polar solvents (Table 4-1). The selection criteria for solvents were maintained as simple as possible with the aliphatic chain being linear, saturated, the

functional group located in the primary position and the solvent must be in a liquid state between 10 ℃ and 30 ℃. The only exceptions to these selection criteria were the ethers and ketones where the functional group was located in the exact middle of the molecule. Apolar solvents included aliphatics (pentane, hexane, heptane, octane, nonane, decane, dodecane and tetradecane), cycloalkanes (cyclopentane, cyclohexane and cyclooctane) and methyl halides (carbon tetrachloride, dichloromethane and chloroform). Polar solvents were subdivided into four categories: aldehydes (hexanal, octanal, nonanal and decanal), ketones (2-propone, 3-pentone, 4-nonanone, and 6-undecanone), ethers (diethyl ether, dipropyl ether, dibutyl ether and dipentyl ether) and nitriles (ethanenitrile, propanenitrile, pentanenitrile, and hexanenitrile). Hydrogen-bonding solvents were also divided into four groups, alcohols (1-butanol, 1-pentanol, 1-hexanal, 1-heptanol, 1-octanol, 1-nonanol, and 1-decanol), carboxylic acids (1-propanoic acid, 1-butanoic acid, 1-pentanoic acid, 1-hexanoic acid, 1-heptanoic acid, 1-octanoic acid, and 1-nonanoic acid), thiols (1-pentanethiol, 1-hexanethiol, 1-heptanethiol, and 1-octanethiol) and amines (1-butamine, 1-pentanamine, 1-hexamine, and 1-octanamine). All solvents and (*R*)-12HSA were obtained from Sigma-Aldrich (Cherry Hill, NJ, USA) with purity greater than 95%.

4.3.2 Methods

Gel Test: 12HSA was dispersed in each solvent at varying concentrations not exceeding 3 wt%, heated to 100 ℃ for 20 min, and stored for 24 h at 20 ℃; the vial was inverted for 1 h and if the material did not flow it was considered to be gelled.

Solubility Parameters: Dielectric constants were obtained from literature and were reported between 20 ℃ and 25 ℃.[29] HSPs were obtained from literature[26] or were calculated from GCMs, which is a widely accepted technique for approximating HSPs.[30,31,32,33]

4.4 Results and Discussion

The ability to predict gelation behavior of organogels has been elusive due to the meticulous balance of contrasting parameters including solubility and the intermolecular forces controlling epitaxial growth. The solubility parameters, of the selected organic solvents, cover a vast breadth of static relative permittivities (1.82 to 37.5) (Table 4-1) as well as a large portion of Hansen space (Table 4-1 and Fig. 4-1). Due to the apolar nature of the solvents, the dispersive component of Hansen space is restricted, even though almost all of solvents fall within a narrow range of dispersive components (14 $MPa^{1/2}$ < δ_d < 20 $MPa^{1/2}$).[27] Typically, if the solvent has a dispersive component below 14 $MPa^{1/2}$, it is in the gaseous state at atmospheric pressure and above 20 $MPa^{1/2}$, the solvent is a solid at 20 ℃ to 30 ℃. The dispersive component of HSPs is linearly correlated to the carbon length, while the polar and hydrogen-bonding HSP are inversely correlated.

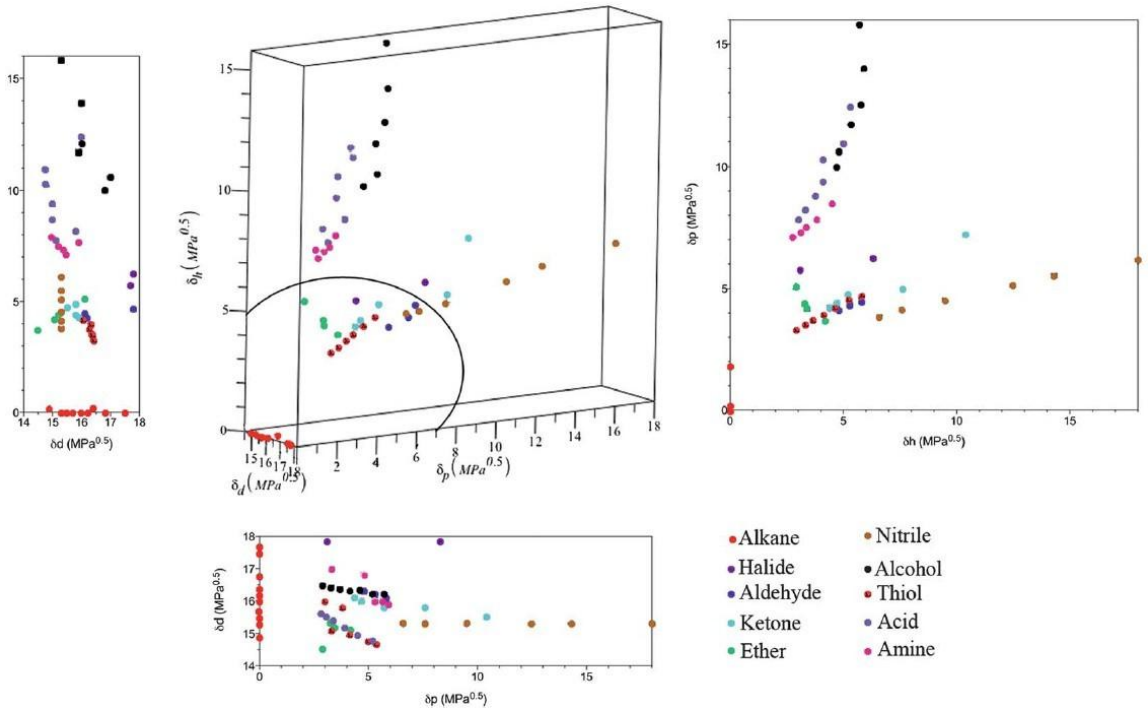

Figure 4-1 Hansen space of the selected solvents categorized by functional group located in the primary position with varying aliphatic chain lengths. Lower left area was the region of Hansen space where solvents gelled.

Table 4-1 Static relative permittivities (ε_r) obtained at 20 ℃,[29] HSPs estimated using the GCMs,[26] and distance in Hansen space from 12HSA (δ_d = 16.59 MPa$^{1/2}$, δ_p = 2.86 MPa$^{1/2}$, δ_h = 6.77 MPa$^{1/2}$), CGC and appearance of 12HSA in various solvents.

Organic Solvent	Chemical Structure	ε_r	δ_T	δ_d	δ_p	δ_h	R_{ij}	CCG	State
		Unitless	MPa$^{1/2}$	MPa$^{1/2}$	MPa$^{1/2}$	MPa$^{1/2}$	MPa$^{1/2}$	WT%	
Apolar									
Pentane	$CH_3(CH_2)_3CH_3$	1.82	14.90	14.90	0.00	0.00	9.11	0.5	Clear
Hexane	$CH_3(CH_2)_4CH_3$	1.89	14.90	15.30	0.00	0.00	9.11	0.4	Clear
Heptane	$CH_3(CH_2)_5CH_3$	1.91	15.30	15.50	0.00	0.00	8.66	0.3	Clear
Octane	$CH_3(CH_2)_6CH_3$	1.95	15.50	15.70	0.00	0.00	8.45	0.3	Clear
Nonane	$CH_3(CH_2)_7CH_3$	1.99	15.70	15.70	0.00	0.00	8.26	0.25	Clear
Decane	$CH_3(CH_2)_8CH_3$	2.00	15.70	16.00	0.00	0.00	8.26	0.2	Clear
Dodecane	$CH_3(CH_2)_{10}CH_3$	2.04	16.00	16.20	0.00	0.00	8.01	0.2	Clear
Tetradecane	$CH_3(CH_2)_{12}CH_3$	2.06	16.20	16.40	0.00	1.80	7.86	0.2	Clear
Cyclopentane	C_5H_{10}	1.96	16.50	16.80	0.00	0.20	6.21	0.5	Clear
Cyclohexane	C_6H_{12}	2.01	16.80	17.50	0.00	0.00	7.34	0.4	Clear
Cyclooctane	C_8H_{16}	2.11	17.50	17.70	0.00	0.00	7.35	0.4	Clear
Dichloromethane	CH_2Cl_2	8.51	20.23	17.80	3.10	5.70	3.69	2.5	Clear
Chloroform	$CHCl_3$	4.81	18.94	18.20	6.30	6.20	1.17	N/A	No Gel
CCl_4	CCl_4	2.24	19.64	17.80	8.30	0.60	8.23	0.4	Clear
Polar									
Hexanal	$CH_3(CH_2)_4CHO$	9.50	18.32	15.90	7.40	5.30	5.85	N/A	No Gel
Octanal	$CH_3(CH_2)_6CHO$	8.60	17.75	16.10	5.80	4.70	4.67	2.8	Opaque
Nonanal	$CH_3(CH_2)_7CHO$	7.60	17.62	16.20	5.28	4.50	4.33	2.5	Opaque
Decanal	$CH_3(CH_2)_8CHO$	6.80	17.53	16.30	4.80	4.30	4.06	1.6	Opaque
2-Propone	$CH_3(CHO)CH_3$	17.00	19.94	15.50	10.40	7.00	2.65	N/A	No Gel
3-Pentone	$CH_3CH_2(CHO)CH_2CH_3$	11.20	18.15	15.80	7.60	4.70	2.17	N/A	No Gel
4-Heptone	$CH_3(CH_2)_2(CHO)(CH_2)_2CH_3$	10.60	17.50	15.80	5.70	4.90	2.21	N/A	No Gel
5-Nonanone	$CH_3(CH_2)_3(CHO)(CH_2)_3CH_3$	8.30	17.25	16.00	4.70	4.40	2.10	2.1	Clear
6-Undecanone	$CH_3(CH_2)_4(CHO)(CH_2)_4CH_3$	8.00	17.21	16.10	4.40	4.20	2.05	1.6	Clear
Diethyl ether	$CH_3CH_2OCH_2CH_3$	4.33	15.64	14.50	2.90	5.10	6.40	N/A	No Gel
Dipropyl ether	$CH_3(CH_2)_2O(CH_2)_2CH_3$	3.34	16.10	15.10	4.20	3.70	6.00	2.2	Clear
Dibutyl ether	$CH_3(CH_2)_3O(CH_2)_3CH_3$	3.22	16.13	15.20	3.40	4.20	5.45	1.5	Clear
Dipentyl ether	$CH_3(CH_2)_4O(CH_2)_4CH_3$	3.10	16.00	15.30	3.30	4.40	5.30	1.4	Clear
Ethanenitrile	CH_3CN	37.50	24.40	15.30	18.00	6.10	15.83	2.3	Opaque
Propanenitrile	CH_3CH_2CN	27.20	21.65	15.30	14.30	5.50	12.39	2.3	Opaque
Butanenitrile	$CH_3(CH_2)_2CN$	20.30	20.40	15.30	12.50	5.10	10.80	2.1	Clear
Hexanenitrile	$CH_3(CH_2)_4CN$	17.26	18.56	15.30	9.50	4.50	8.38	1.9	Clear
Octanenitrile	$CH_3(CH_2)_6CN$	14.70	17.56	15.30	7.60	4.10	7.11	1.5	Clear
Nonanenitrile	$CH_3(CH_2)_7CN$	14.00	17.00	15.30	6.60	3.80	6.62	0.9	Clear
H-Bonding									
1-Butanol	$CH_3(CH_2)_3OH$	17.92	23.20	16.00	5.70	15.80	3.97	N/A	No Gel
1-Pentanol	$CH_3(CH_2)_4OH$	14.50	21.93	15.90	5.90	13.90	3.73	N/A	No Gel
1-Hexanol	$CH_3(CH_2)_5OH$	13.02	21.04	15.90	5.80	12.50	3.54	N/A	No Gel
1-Heptanol	$CH_3(CH_2)_6OH$	11.48	20.52	16.00	5.30	11.70	3.42	N/A	No Gel
1-Octanol	$CH_3(CH_2)_7OH$	9.75	21.01	17.00	3.30	11.90	3.45	N/A	No Gel
1-Nonanol	$CH_3(CH_2)_8OH$	8.58	20.44	16.80	4.80	10.60	3.26	N/A	No Gel
1-Decanol	$CH_3(CH_2)_9OH$	7.70	19.44	16.00	4.70	10.00	3.16	N/A	No Gel
1-Propanoic acid	CH_3CH_2COOH	3.20	19.95	14.70	5.30	12.40	8.43	N/A	No Gel
1-Butanoic acid	$CH_3(CH_2)_2COOH$	2.88	19.11	14.80	5.00	11.00	7.32	N/A	No Gel
1-Pentanoic acid	$CH_3(CH_2)_3COOH$	2.66	18.65	15.00	4.10	10.30	6.39	N/A	No Gel
1-Hexanoic acid	$CH_3(CH_2)_4COOH$	2.82	18.17	15.00	4.10	9.40	5.94	N/A	No Gel
1-Heptanoic acid	$CH_3(CH_2)_5COOH$	3.03	18.48	15.80	3.80	8.80	4.22	N/A	No Gel
1-Octanoic acid	$CH_3(CH_2)_6COOH$	2.82	17.50	15.10	3.30	8.20	5.20	N/A	No Gel
1-Nonanoic acid	$CH_3(CH_2)_7COOH$	1.72	18.05	16.00	3.00	7.80	3.35	N/A	No Gel
1-Pentanethiol	$CH_3(CH_2)_3CHSH$	4.67	17.45	16.30	4.60	4.20	2.05	0.5	Clear
1-Hexanethiol	$CH_3(CH_2)_4CHSH$	4.34	17.25	16.30	4.10	3.90	1.97	0.45	Clear
1-Heptanethiol	$CH_3(CH_2)_5CHSH$	4.11	17.17	16.35	3.70	3.70	1.92	0.45	Clear
1-Octanethiol	$CH_3(CH_2)_6CHSH$	3.95	17.09	16.40	3.30	3.50	1.87	0.4	Clear
1-Decanethiol	$CH_3(CH_2)_8CHSH$	3.84	17.02	16.45	2.90	3.30	1.80	0.3	Clear
1-Butanamine	$CH_3(CH_2)_3NH_2$	4.90	17.78	14.95	4.50	8.50	2.92	N/A	No Gel
1-Pentanamine	$CH_3(CH_2)_4NH_2$	5.36	17.56	15.20	3.87	7.90	2.81	N/A	No Gel
1-Hexanamine	$CH_3(CH_2)_5NH_2$	3.53	17.46	15.40	3.40	7.50	2.74	N/A	No Gel
1-Heptylamine	$CH_3(CH_2)_6NH_2$	3.42	17.42	15.50	3.10	7.30	2.70	N/A	No Gel
1-Octanamine	$CH_3(CH_2)_7NH_2$	3.30	17.37	15.60	2.80	7.10	2.66	N/A	No Gel

For the 56 tested solvents, 32 are capable of forming organogels at concentrations below 3 wt%. An increase in the solvent aliphatic chain length increases the likelihood that a molecular gel will develop. However, beyond this there is no clear correlation between solvent type and the ability to gel, with the exception that neither alcohols nor carboxylic acids form molecular gels.

In an attempt to develop predictive tools to determine which solvents are immobilized by 12HSA, the individual HSPs, total HSP and static relative permittivity are examined as a function of CGC (Fig. 4-2). Solvents that remained as a solution, at concentrations less than 3 wt%, are represented graphically with a CGC of 10. Overall, neither the static relative permittivity, dispersive nor the polar HSP are able to predict gelation ability of 12HSA in the various solvents (Fig. 4-2A, B, E). It is not astonishing that the static relative permittivity is incapable of predicting gelation capacity since it does not account for the complex interactions involving functional groups between the solvent and gelator.[11] Interestingly, the hydrogen-bonding HSP establishes a distinct relationship between gelating capacity and CGC (Fig. 4-2C). Very convincing trends between the hydrogen-bonding HSP and the ability to form clear organogels ($\delta_h < 4.7$ MPa$^{1/2}$), opaque organogels (4.7 MPa$^{1/2} < \delta_h < 5.1$ MPa$^{1/2}$) and solution ($\delta_h > 5.1$ MPa$^{1/2}$) are observed. The turbidity or transparency of an organogel has been correlated to the cross-sectional thickness of the crystalline aggregates, number of junction zones capable of diffracting light, and the number of crystalline aggregates within the self-assembled network.[34,35,36] Zhu and Dordick reported that solvent-gelator interactions weaken gelator-gelator intermolecular hydrogen-bonding interactions and result in thicker crystalline fibers.[13] Further increasing the solvent-gelator interactions cause the fibrous structures to be lost resulting in the complete absence of crystal structure.[13]

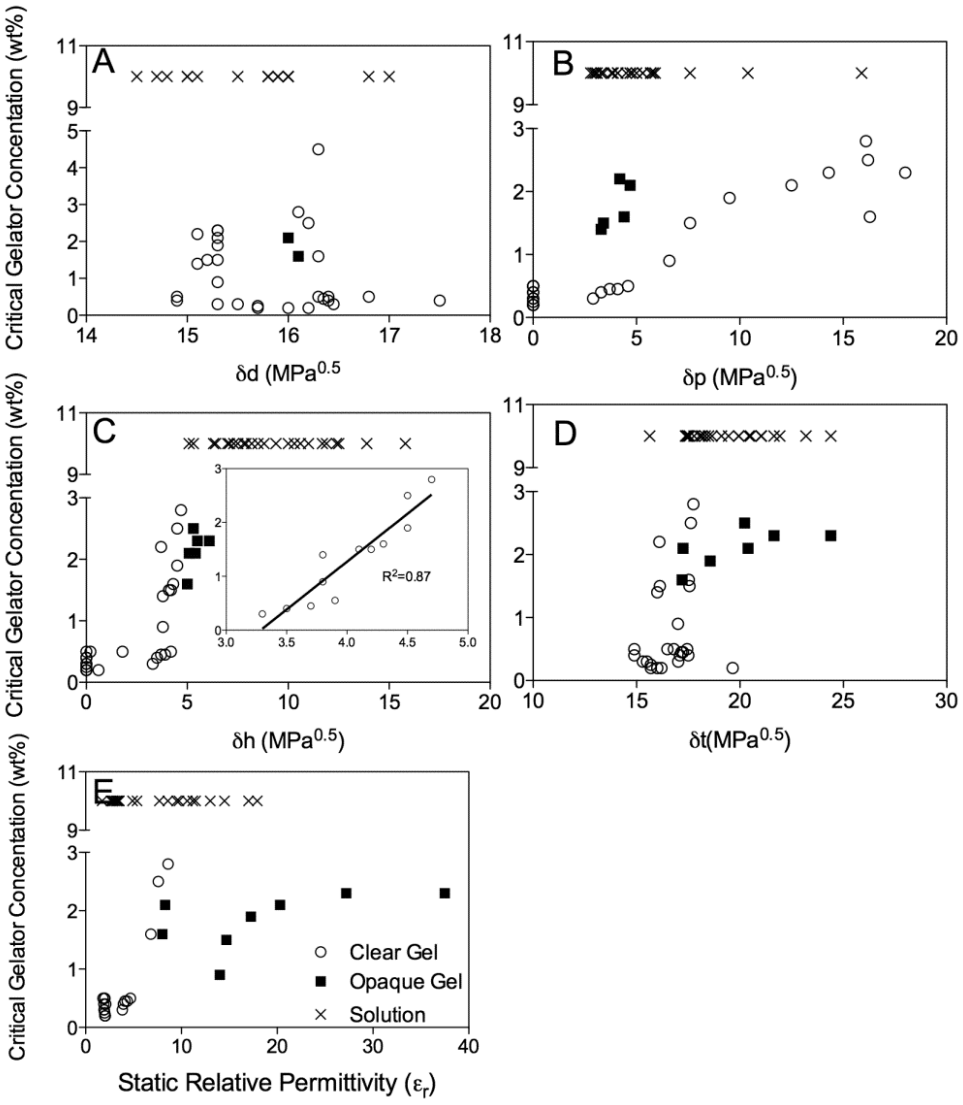

Figure 4-2 CGC as determined using the inverted vial test, as a function of the: dispersive HSP (δ_d) (A); polar HSP (δ_p) (B); hydrogen-bonding HSP (δ_h) (C); total HSP (δ_t) (D); and the static relative permittivity (ε_r) (E). Solvents which did not gel were graphically represented with a CGC of 10.

The intermolecular interactions required for 12HSA to form molecular gels have been very well established[11,14,15,37,38,39,40,41]. 12HSA's cross-sectional fiber width is a multiple of the carboxylic acid dimer length while longitudinal growth occurs via hydrogen bonding between hydroxyl groups at position 12. Hence, if the hydrogen-bonding component is too strong then it will interfere with the formation of gelator-gelator intermolecular hydrogen bonding thus disrupting gel formation. For 12HSA, this occurs at a hydrogen-bonding HSP greater than 4.7 $MPa^{1/2}$ (Fig. 4-2). The CGC also scales with hydrogen-bonding HSP (Fig. 4-2C insert). This confirms that as the solvent-gelator interactions increase, more 12HSA is required to form an organogel. The overall HSP is also useful in distinguishing between which solvents will develop translucent fibrillar networks versus solution (Fig. 4-2D). However, there is an overlap between the HSPs which form opaque gels (very weak structures which break down under force) and which solvents remain as solution. Thus, irrespective of the type of solvent, the individual hydrogen-bonding and total HSP are useful predictive tools for the gelation behavior of molecular gels.

In order to better assess the effect of solvent composition on gelation capacity, Teas diagrams are used to examine correlations between gelation ability and solvent HSPs (Fig. 4-3). Individual HSPs are converted to an average value by dividing each parameter by the sum of the three HSPs:

$$f_d = \frac{\delta_d}{\delta_d + \delta_p + \delta_h}$$

$$f_p = \frac{\delta_p}{\delta_d + \delta_p + \delta_h}$$

$$f_h = \frac{\delta_h}{\delta_d + \delta_p + \delta_h}$$

where f is the percent fraction of the individual HSPs component. The Teas plot shows a

clustering of solvents capable of gelling and another region that remain as solution (Fig. 4-3). Since we are working with apolar solvents, the dispersive parameter is greater than 50% for all solvents tested. The polar component varies from 50% to as low as 10% and does not influence gelation behavior. However, it is extremely clear that the hydrogen-bonding HSP cannot exceed 18% of the total HSP or the system will not form an organogel. Recent work with dicholesterol–linked azobenzene organogels suggests that as the combination of solvents (i.e., greater concentrations of methanol) and gelator move further apart in Hansen space then they interact less becoming more efficient gelators.[9] Since the solvents, which gel cluster in a specific region on the Teas plot, it is reasonable to assume that the role of Hansen space is important in predicting gel formation.

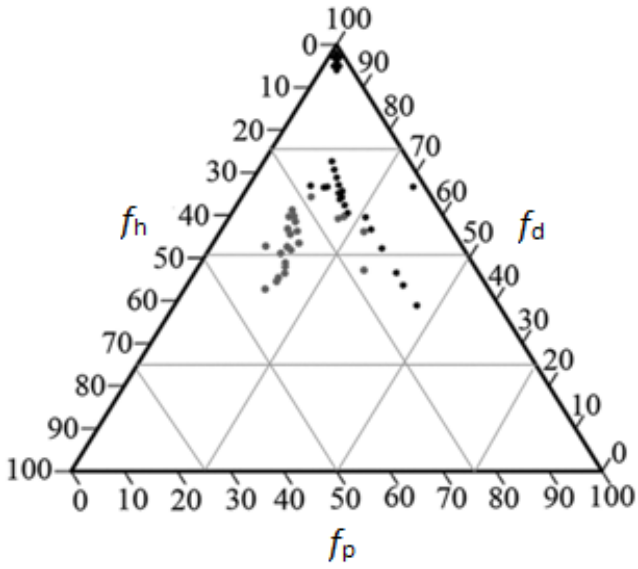

Figure 4-3 Teas plot of calculated solubility parameters for 12HSA in varying solvents. Black circles represent solvents that gelled and grey circles are solvents unable to gel

One distinction between Wu et al.'s,[9] work and ours is that they modified solvent parameters by adjusting the concentration of two mixed solvents while our study examined single solvents with different functional groups and varying alkane chain lengths. The HSPs for 12HSA were calculated using the GCMs (as shown in Equation 3-6, 3-7, 3-8) and the

distance in Hansen space was calculated using Equation 3-9. The distance in Hansen space was not the only factor when deciding if a solvent would form an organogel (Fig. 4-4). Along with the distance in Hansen space, the overall HSP was needed to predict organogel formation. This indicates that there is a limit to how close in Hansen space the solvent and gelator may be (i.e., if they are too close then the solvent-gelator interactions solubilize the gelator). However, the direction in Hansen space is crucial in determining the ability of the gelator to gel the solvent. It becomes clear that HSPs are very powerful tools when trying to understand and predict the likelihood of organogel formation.

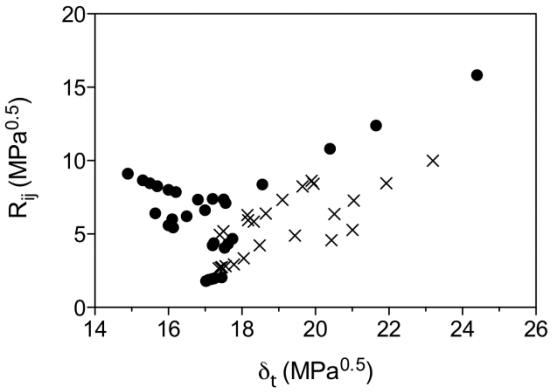

Figure 4-4 Distance in Hansen space between the solvent and 12HSA (δ_d = 17.59 MPa$^{1/2}$, δ_p = 2.86 MPa$^{1/2}$, δ_h = 6.77 MPa$^{1/2}$) versus the total HSP (circles represent gelled solvent, x represent solutions).

In order to confirm that these trends were not specific to 12HSA, CGC reported by Abdallah and Weiss, were examined for ammonium bromide salts where nitrogen was covalently linked to four equal long alkyl chains (ranging from 12 to 18 carbons) (Fig. 4-5).[42] Neither the dispersive HSP nor the polar HSP (Fig. 4-5A, B) were correlated to the CGC. Similar to 12HSA, the CGC is constant below a critical value for the hydrogen-bonding HSP and total HSP. For ammonium bromide salts the hydrogen-bonding HSP is 6 and total HSP is 19 and above these values the CGC increases (Fig. 4-5C, D). It is also worth noting that the

solvents used in Abdallah and Weiss's study (alkanes, benzene, CCl_4, styrene, methyl methacrylate and glycidyl methacrylate) were not the same as we selected for 12HSA suggesting that HSPs universally apply to an even broader group of solvents than tested in this present study.

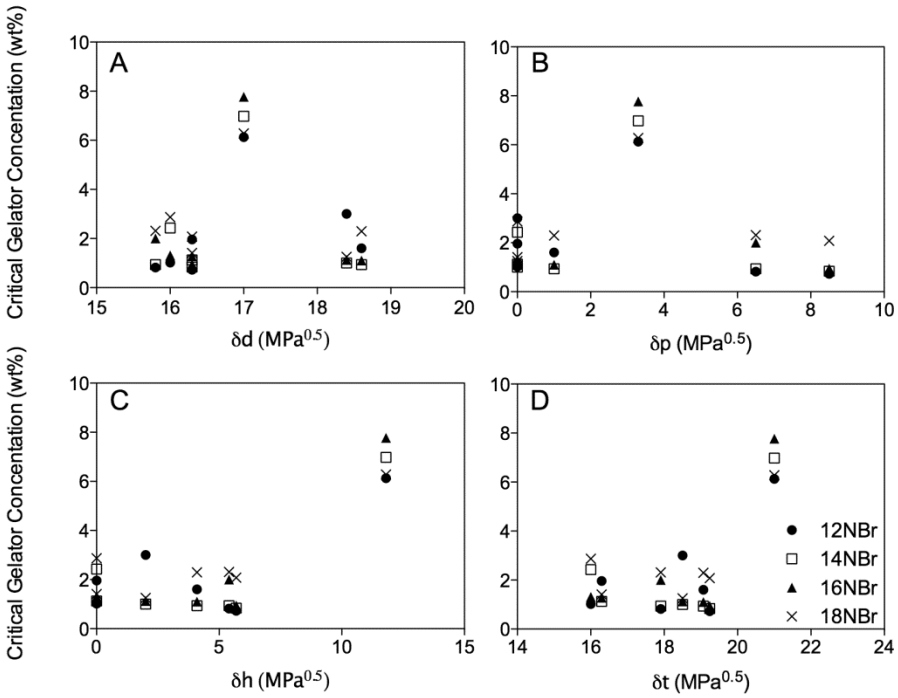

Figure 4-5 CGC for ammonium bromide salts: dispersive HSP (δ_d) (A); polar HSP (δ_p) (B); hydrogen-bonding HSP (δ_h) (C); and total HSP (δ_t) (D).

Although the predictive nature of the HSPs is much stronger than originally anticipated for the wide range of solvents. The parameter becomes even more powerful when observing the CGC as a function of the individual HSPs within the individual classes of solvents. As the carbon length of the solvent increases, the static relative permittivity, the total HSP and the dispersive component of the HSPs increase while the distance in Hansen space decreases (Table 4-1). On the other hand, for polar and hydrogen-bonding solvents, as the chain length increases the static relativity permittivity, the hydrogen-bonding HSP and polar HSP decrease while the dispersive HSP increases (Table 4-1). As the chain length of

the aliphatic solvents increase (i.e., increased static relative permittivity) the CGC decreases (Fig. 4-6A, B). The total HSP and dispersive HSP are inversely correlated to the CGC while the distance in Hansen space is correlated linearly (Fig. 4-6C, D). Only three sets of polar solvents (i.e., aldehydes, ethers, and nitriles) and one set of hydrogen-bonding solvents (i.e., amines) could be observed for correlations between CGC and the solubility parameters due to a lack of samples which gelled. As the chain length increases for polar and hydrogen-bonding solvents, the CGC decreases (Fig. 4-7A, 4-8A). Furthermore, the CGC is inversely proportional to the dispersive HSP, and proportional to the polar (Fig. 4-7D, 4-8D), hydrogen-bonding HSP (Fig. 4-6E, 4-7E), the total HSP (Fig. 4-7F, 4-8F) and the distance in Hansen space (Fig. 4-7G, 4-8G). Upon closer examination of the hydrogen-bonding solvents, as the hydrogen-bonding strength of the primary functional group decreases (i.e., -COOH > -COH > $-NH_2$ > -SH) the CGC decreases (Fig. 4-8A). Therefore, as the hydrogen-bonding strength of the solvent decreases, it is less likely to interfere with the dimerization and longitudinal of 12HSA.

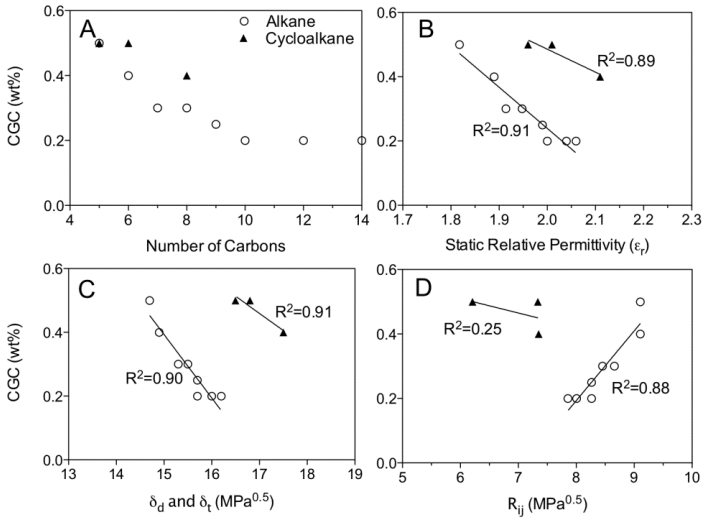

Figure 4-6 CGC versus carbon number (A), static relative permittivity (B), total HSP and the dispersive component of the HSPs (C) and the distance in Hansen space (D) for alkanes.

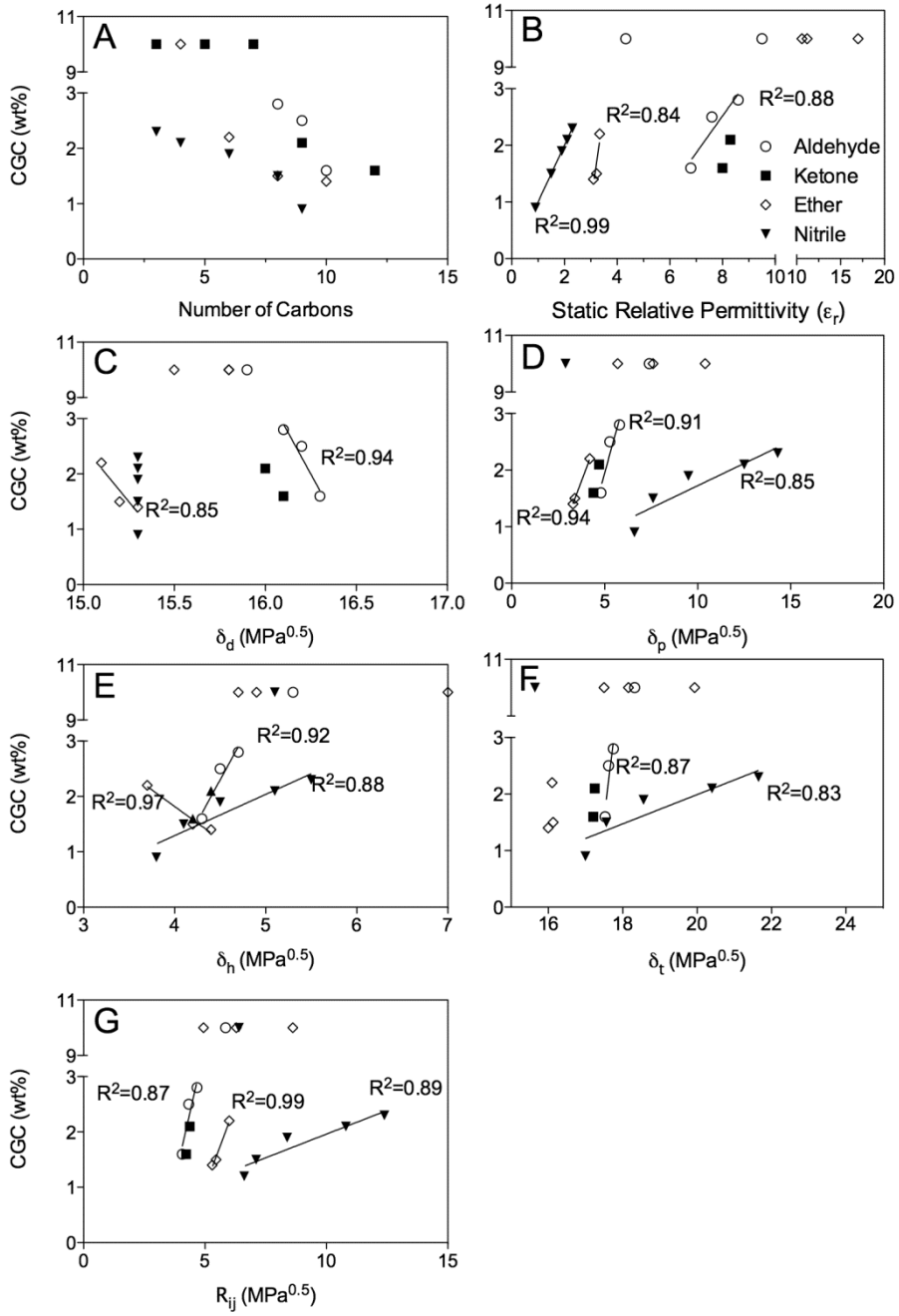

Figure 4-7 CGC versus carbon number (A), static relative permittivity (B), the dispersive component of the HSPs (C), the polar component of the HSPs (D), the hydrogen-bonding component of the HSPs (E), the total HSP (F) and the distance in Hansen space (G) for polar solvents.

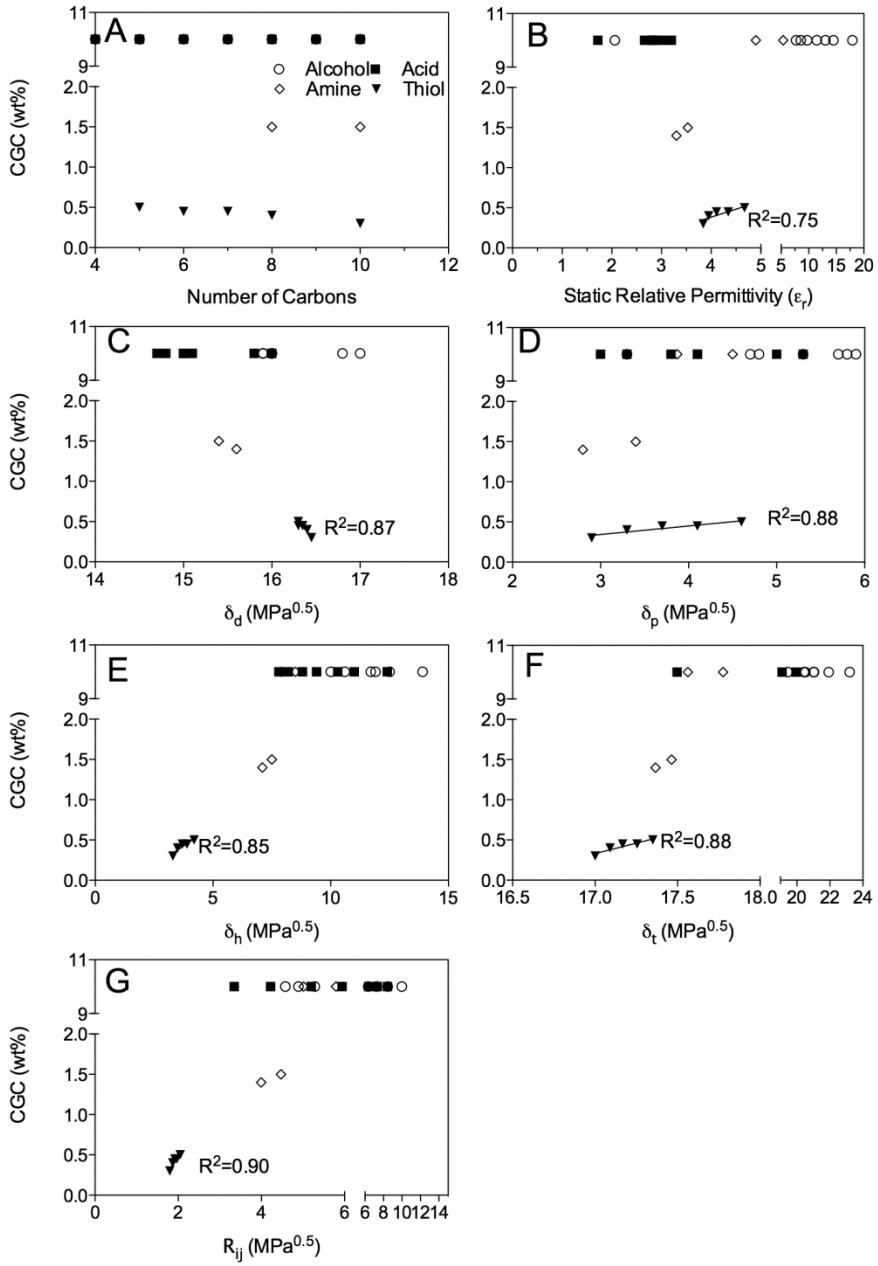

Figure 4-8 CGC versus carbon number (A), static relative permittivity (B), the dispersive component of the HSPs (C), the polar component of the HSPs (D), the hydrogen-bonding component of the HSPs (E), the total HSP (F) and the distance in Hansen space (G) for hydrogen-bonding solvents.

4.5 Conclusions

HSPs are useful in predicting which solvents are immobilized using LMOGs. The prediction ability for 12HSA is related to the hydrogen-bonding HSP (i.e., hydrogen-bonding HSP less than 4.7 $MPa^{1/2}$ produces clear organogels). CGC also scales as a function of the hydrogen-bonding HSP. Solvents with the same functional group, which varied only by chain length, have linear correlations between static relative permittivity, total HSP, dispersive HSP, polar HSP and hydrogen-bonding HSP and the CGC.

4.6 References

1. Mallia, V. A.; Butler, P. D.; Sarkar, B.; Holman, K. T.; Weiss, R. G., Reversible Phase Transitions within Self-Assembled Fibrillar Networks of (R)-18-(n-Alkylamino)octadecan-7-ols in Their Carbon Tetrachloride Gels. *Journal of the American Chemical Society* **2011,** *133*, 15045-15054.
2. Weiss, R. G.; Terech, P., Introduction. In *Molecular Gels: Materials with Self-Assebled Fibrillar Networks*, Weiss, R. G.; Terech, P., Eds. Springer: Dordrecht, The Neatherlands, 2006; pp 1-13.
3. George, M.; Weiss, R. G., Molecular Organogels. Soft Matter Comprised of Low-Molecular-Mass Organic Gelators and Organic Liquids. *Accounts of Chemical Research* **2006,** *39*, 489-497.
4. Fahrländer, M.; Fuchs, K.; Mülhaupt, R.; Friedrich, C., Linear and Nonlinear Rheological Properties of Self-Assembling Tectons in Polypropylene Matrices. *Macromolecules* **2003,** *36*, 3749–3757.
5. Isare, B.; Petit, L.; Bugnet, E.; Vincent, R.; Lapalu, L.; Sautet, P.; Bouteiller, L., The Weak Help the Strong: Low-Molar-Mass Organogelators Harden Bitumen. *Langmuir* **2009,** *25*, 8400-8403.
6. Kubo, W.; Murakoshi, K.; Kitamura, T.; Yodhida, S.; Haruki, M.; Hanabusa, K.; Shirai, H.; Wada, Y.; Yanagida, S., Quasi-Solid-State Dye-Sensitized TiO2 Solar Cells: Effective Charge Transport in Mesoporous Space Filled with Gel Electrolytes Containing Iodide and Iodine. *Journal of Physical Chemisty B* **2001,** *105*, 12809-12815.
7. Sugiyasu, K.; Fujita, N.; Shinkai, S., Visible-Light-Harvesting Organogel Composed of Cholesterol-Based Perylene Derivatives†. *Angewandte Chemie International Edition* **2004,** *43*, 1229-1233.
8. Friggeri, A.; Feringa, B. L.; van Esch, J., Entrapment and release of quinoline derivatives using a hydrogel of a low molecular weight gelator. *Journal of Controlled Release* **2004,** *97*, 241-248.
9. Wu, Y.; Wu, S.; Zou, G.; Zhang, Q., Solvent effects on structure, photoresponse and speed of gelation of a dicholesterol-linked azobenzene organogel. *Soft Matter* **2011,** *7*, 9177-9183.
10. Suzuki, M.; Nakajima, Y.; Yumoto, M.; Kimura, M.; Shirai, H.; Hanabusa, K., Effects of Hydrogen Bonding and van der Waals Interactions on Organogelation Using Designed Low-Molecular-Weight Gelators and Gel Formation at Room Temperature. *Langmuir* **2003,** *19* (21), 8622-8624.
11. Rogers, M. A.; Marangoni, A. G., Solvent-Modulated Nucleation and Crystallization Kinetics of 12-Hydroxystearic Acid: A Nonisothermal Approach. *Langmuir* **2009,** *25* (15), 8556-8566.
12. Hirst, A. R.; Coates, I. A.; Boucheteau, T. R.; Miravet, J. F.; Escuder, B.; Castelletto, V.; Hamley, I. W.; Smith, D. K., Low-molecular-weight gelators: elucidating the principles of gelation based on gelator solubility and a cooperative self-assembly model. *Journal of the American Chemical Society* **2008,** *130*, 9113-9121.
13. Zhu, G.; Dordick, J. S., Solvent Effect on Organogel Formation by Low Molecular Weight Molecules. **2006,** *18* (Chemistry of Materials), 5988-5995.
14. Kuwahara, T.; Nagase, H.; Endo, T.; Ueda, H.; Nakagaki, M., Crystal structure of DL-12-hydroxystearic acid. *Chemistry Letters* **1996,** *25*, 435-436.

15. Lam, R.; Quaroni, L.; Pederson, T.; Rogers, M. A., A molecular insight into the nature of crystallographic mismatches in self-assembled fibrillar networks under non-isothermal crystallization conditions. *Soft Matter* **2010,** *6* (2), 404-408.
16. Li, J. L.; Liu, X. Y.; Wang, R. Y.; Xiong, J. Y., Arichitecture of a Biocompatible Supramolecular Material by Supersaturation-Driven Fabrication of its Network. *Journal of Physical Chemistry B* **2005,** *109*, 24231-24235.
17. Rogers, M. A.; Bot, A.; Lam, R., S.H.; Pedersen, T.; May, T., Multicomponent Hollow Tubules Formeed Using Phytosterol and γ-Oryzanol-Based Compounds: An Understanding of Their Molecular Embrace. *Journal of Physical Chemistry* **2010,** *114*, 8278-8295.
18. Brotin, T.; Devergne, J. P.; Fages, F., Photostationary Fluorescence Emission and Time Resoved Spectroscopy of Symmetrically Disubstituted Anthracenes on teh meso and Side Rings: The Unusual Behavior of the 1,4 Derivative. *Photochemistry and Photobiology* **1992,** *55*, 349-358.
19. Terech, P.; Furman, I.; Weiss, R. G., Structures of Organogels Based Upon Cholesteryl 4-(2-Anthryloxy)Butanoate, A Highly Efficient Luminescing Gelator - Neutron AND X-Ray Small-Angle Scattering Investigations. *Journal of Physical Chemistry* **1995,** *99* (23), 9558-9566.
20. Toro-Vazquez, J. F.; Morales-Rueda, J.; Mallia, V. A.; Weiss, R. G., Relationship Between Molecular Structure and Thermo-mechanical Properties of Candelilla Wax and Amides Derived from (R)-12-Hydroxystearic Acid as Gelators of Safflower Oil. *Food Biophysics* **2010,** *5* (3), 193-202.
21. van Esch, J.; Feringa, B. L., New functional materials based on self-assembling organogels: from serendipity towards design. *Angewandte Chemistry* **2000,** *39*, 2263-2266.
22. Raynal, M.; Bouteiller, L., Organogel Formation Rationalized by Hansen Solubility Parameters. *Chemical Communication* **2011,** *47*, 8271-8273.
23. Aggeli, A.; Bell, M.; Boden, M.; Keen, J. N.; Knowles, P. F.; McLeish, T. C. B.; Pitkeatly, M.; Radford, S. E., Responsive gels formed by the spontaneous self-assembly of peptides into polymeric β-sheet tapes. *Nature* **1997,** *386*, 259-262.
24. Hirst, A. R.; Smith, D. K., Solvent Effects on Supramolecular Gel-Phase Materials: Two-Component Dendritic Gel. *Langmuir* **2004,** *20*, 10851-10857.
25. Hanabusa, K.; Matsumoto, M.; Kimura, M.; Kakehi, A.; Shirai, H., Low Molecular Weight Gelators for Organic Fluids: Gelation Using a Family of Cyclo(dipeptide)s. *Journal of Colloid and Interface Science* **2000,** *224*, 231-244.
26. Grulke, E. A., *Solubility Parameter Values*. 4th edition ed.; John Wiley & Sonds: New York, NewYork, 2005.
27. Hansen, C. M., *Hansen Solubility Parameters*. 2nd ed.; CRC Press: Boca Raton, Fl, 2007.
28. Ham, H. T.; Choi, Y. S.; Chung, I. J., An Explanation of Dispersion States of Single-Walled Carbon Nanotubes in Solvents and Aqueous Surfactant Solutions Using Solubility Paramters. *Journal of Colloid and Interface Science* **2006,** *286*, 216-223.
29. Wohlfahrt, C. H., Pure Liquids: References. In *Landolt-Börnstein - Group IV Physical Chemistry Numerical Data and Functional Relationships in Science and Technology*, Madelung, O., Ed. Springer: 1991; Vol. 6: Static Dielectric Constants of Pure Liquids and Binary Liquid Mixtures.
30. Jang, M.; MKamens, R. M.; Leach, K. B.; Strommen, M. R., A Thermodynamic Approach Using Group Contribution Methods to Model the Partitioning of Semivolatile Organic Compounds on Atmospheric Particulate Matter. *Environmental Science & Technology* **1997,** *31*, 2805-2811.

31. Fedors, R. F., A method for estimating both the solubility parameters and molar volumes of liquids. *Polymer Engineering & Science* **1974,** *14*, 147-154.
32. Lindvig, T.; Michelsen, M. L.; Kontogeorgis, G. M., A Flory–Huggins model based on the Hansen solubility parameters. *Fluid Phase Equilibria* **2002,** *203*, 247-260.
33. van Krevelen, D. W.; Hoftyzer, P. J., Practical Evaluation of the [n]-M relation. *Journal of Applied Polymer Science* **1967,** *11*, 2189-2200.
34. Terech, P.; Pasquier, D.; Bordas, V.; Rossat, C., Rheological properties and structural correlations in molecular gels. *Langmuir* **2000,** *16*, 4485-4494.
35. Tamura, T.; Ichikawa, M., Effect of lecithin on organogel formation of 12-hydroxystearic acid. *Journal of the American Oil Chemists Society* **1997,** *74* (5), 491-495.
36. Abraham, S.; Lan, Y.; Lam, R. S. H.; Grahame, D. A. S.; Kim, J. J. H.; Weiss, R. G.; Rogers, M. A., Influence of Positional Isomers on the Macroscale and Nanoscale Architectures of Aggregates of Racemic Hydroxyoctadecanoic Acids in Their Molecular Gel, Dispersion, and Solid States. *Langmuir* **2012**.
37. Rogers, M. A.; Marangoni, A. G., Non-Isothermal Nucleation and Crystallization of 12-Hydroxystearic Acid in Vegetable Oils. *Crystal Growth & Design* **2008,** *8* (12), 4596-4601.
38. Rogers, M. A.; Wright, A. J.; Marangoni, A. G., Engineering the Oil Binding Capacity and Crystallinity of Self-Assembled Fibrillar Networks of 12-Hydroxystearic Acid in Edible Oils. *Soft Matter* **2008,** *4* (7), 1483-1490.
39. Rogers, M. A.; Wright, A. J.; Marangoni, A. G., Nanostructuring fiber morphology and solvent inclusions in 12-hydroxystearic acid/canola oil organogels (vol 14, pg 33, 2009). *Current Opinion in Colloid & Interface Science* **2009,** *14* (3), 223-223.
40. Terech, P., 12-D-Hydroxyoctadecanoic Acid Organogels - A Small-Angle Neutron-Scattering Study. *Journal De Physique Ii* **1992,** *2* (12), 2181-2195.
41. Terech, P.; Rodriguez, V.; Barnes, J. D.; McKenna, G. B., Organogels and Areogels of Racemic and Chiral 12-Hydroxyoctadecanoic Acid. *Langmuir* **1994,** *10* (10), 3406-3418.
42. Abdallah, A. J.; Weiss, R. G., Organogels and low molecular mass organic gelators. *Advanced Materials* **2000,** *12*, 1237-1247.

5.0 INFLUENCE OF SOLVENT ON THE SUPRAMOLECULAR ARCHITECTURES IN MOLECULAR GELS

Wu, S., Gao, J., Emge, T. J., and Rogers, M. A.

**This chapter is published in *Soft Matter* (DOI: 10.1039/c3sm50936b), Received: April 5, 2013/ Published: July 10, 2013.

5.1 Abstract

Elucidating the molecular structures, responsible for promoting self-assembly of LMOGs into supramolecular fibers, has been an extensive area of study. Although this has been a fruitful endeavor, this study illustrates that the chemical nature of the solvent and solvent-gelator interactions are equally important. The nanostructure, microstructure and supramolecular structures, of 12HSA molecular gels, are all influenced by the chemical nature of the solvent, which correlate to the hydrogen-bonding HSP (δ_h). Depending on the solvent employed, the polymorphic form, arrangement of the carboxylic acid dimers, domain size, fiber morphology, microstructure, thermal properties and visual appearance of the gel all differ. Solvents that have $\delta_h < 4.4$ MPa$^{1/2}$ result in a hexagonal polymorphic form, with the 001 *hlk* spacing greater than the extended bimolecular length of 12HSA. This nanoscale arrangement results in translucent gels that contain fibrillar aggregates corresponding to a higher crystallinity compared to molecular gels formed in solvents that have a $\delta_h > 4.4$ MPa$^{1/2}$.

5.2 Introduction

Numerous practical applications of organogels, ranging from photovoltaics,[1] to light harvesting,[2] templating reactions,[2] controlling oils spills,[3,4] controlled drug release,[5] to reversible photoisomerization are being investigated.[6] However, a lack of fundamental understanding has impeded the development of these materials. Organogels are thermally reversible, quasi-solid materials mainly comprised of organic liquids that are broadly subcategorized into molecular or polymeric gels depending on the size of the gelator.[7,8,9] Molecular gels are further categorized based on their mode of self-assembly and include: liquid crystals, worm-like micelles,[10] platelet crystals[11,12] and SAFiNs.[4,13,14,15,16]

In SAFiNs, a meticulous balance between divergent parameters including solubility

and those intermolecular forces that control epitaxial growth into axially symmetric elongated aggregates are required.[8,17,18] In other words, the capability of a molecule to assemble, resulting in a SAFiN, relies on a precise ratio of gelator-gelator to gelator-solvent interactions. Even though the direct role of solvent on the physical properties has not been established, numerous studies have illustrated the importance of understanding solvent-gelator interactions.[6,19,20,21] It is recognized that as the solvent-gelator interactions increase, the likelihood of directional gelator-gelator interactions decrease, resulting in thicker fibers.[6,22,23] Optimal gelation occurs when limited solvent-gelator intermolecular physical bonds (i.e., hydrogen-bonding,[24,25,26,27] π-π stacking, dipole-dipole,[28,29] and London dispersion forces[11]) form and the SAFiN is comprised of thin entangled fibers.[22] Furthermore, in supramolecular assemblies of disc-like molecules the shape of the solvent molecule can facilitate intercalation into the helical stacks, which alters the conformation of the monomers into the supramolecular structures.[30]

The balance between solvent gelator interactions, which results in SAFiNs formation, has become an active area of study with attempts to correlate solvent parameters to gelation behavior.[15,18,31,32] Raynal and Bouteiller adapted HSPs commonly used in polymer science, to evaluate gelation behavior in SAFiNs.[31] Their meta-analysis revealed that solvents which gelled were clustered in Hansen space (R_{ij}) (i.e., the distance between the gelator and solvent position in Hansen space).[31] Later, the hydrogen-bonding HSP (δ_h) was shown to be positively correlated with the CGC for 12HSA.[15] HSPs, are separated into three main interaction components which sum to the overall energy density, δ_t. The three components of δ_t are the hydrogen bonding, δ_h, the polar, δ_p, and the dispersive, δ_d HSP.[33] Solvents with δ_h < 4.7 $MPa^{1/2}$ produce clear organogels, while opaque organogels form between 4.7 $MPa^{1/2}$ < δ_h < 6.5 $MPa^{1/2}$ and solution remained when the δ_h > 6.5 $MPa^{1/2}$.[15] Similar results were obtained

for pyrenyl-linker-glucono gelators where the CGC was associated with both δ_h and δ_p.[32] The purpose of this study is to examine if solubility parameters are a useful tool in understanding the nanostructure, microstructure and/or the supramolecular network of 12HSA SAFiNs.

5.3 Methods

Varying the aliphatic chain length and/or the functional group of the solvent was used to modify HSPs. The selection criteria for solvents were maintained as simple as possible with the aliphatic chain being linear, saturated, the functional group located in the primary position and the solvent must be in a liquid state between 10 °C and 30 °C. The only exception to these selection criteria was the inclusion of ethers and ketones where the functional group was located in the exact middle of the molecule. HSPs are altered by the functional group present. For example, solvents with the same aliphatic chain length, differing only based on the presence of distinctive functional groups alter the HSPs (i.e., pentane (δ_t = 14.6 $MPa^{1/2}$, δ_d = 14.6 $MPa^{1/2}$, δ_p = 0.0 $MPa^{1/2}$, and δ_h = 0.0 $MPa^{1/2}$); 3-pentone (δ_t = 18.5 $MPa^{1/2}$, δ_d = 15.8 $MPa^{1/2}$, δ_p = 7.6 $MPa^{1/2}$, and δ_h = 4.7 $MPa^{1/2}$); and 1-pentanol (δ_t = 21.3 $MPa^{1/2}$, δ_d = 15.9 $MPa^{1/2}$, δ_p = 5.9 $MPa^{1/2}$, and δ_h = 13.6 $MPa^{1/2}$)). The HSPs are also varied when the functional group is constant but the aliphatic chain length is changed (i.e., propanenitrile (δ_t = 21.6 $MPa^{1/2}$, δ_d = 15.4 $MPa^{1/2}$, δ_p = 14.3 $MPa^{1/2}$, and δ_h = 5.5 $MPa^{1/2}$); hexanenitrile (δ_t = 18.6 $MPa^{1/2}$, δ_d = 15.3 $MPa^{1/2}$, δ_p = 9.5 $MPa^{1/2}$, and δ_h = 4.5 $MPa^{1/2}$); and nonanenitrile (δ_t = 17.0 $MPa^{1/2}$, δ_d = 15.3 $MPa^{1/2}$, δ_p = 6.6 $MPa^{1/2}$, and δ_h = 3.8 $MPa^{1/2}$). General categories of the tested solvents include ketones, aldehydes, nitriles, alkanes, thiols, ethers, amines, carboxylic acids and alcohols. A complete list of the solvents used in this study and their solubility parameters may be found in Gao et al.[15] 2.5 wt% 12HSA was dispersed in each solvent, heated to 100 °C for 20 min, and stored for 24 h at 20 °C until further analysis. All solvents and (*R*)-12HSA were obtained from Sigma-Aldrich (Cherry

Hill, NJ, USA) with purity greater than 95%.

5.3.1 Free Induction Decay-NMR Measurements

Each sample was subjected to T_2 relaxation measurement on a Bruker mq20 Series TD-NMR Analyzer (Bruker, Milton, ON, Canada). A Hahn-echo pulse sequence was used to measure the Free Induction Decay (FID). The operational pulse length was obtained using the calibration procedures recommended by the manufacturer. The 90° pulse was 2.6 μs and the 180° pulse was 5.1 μs. This allowed determination of the gain (64) and recycle delay (5 sec). Tau was selected to be as short as possible (0.5 ms) to minimize chemical exchange and diffusion effects on the decay curves.

5.3.2 Differential Scanning Calorimetry (DSC)

10 mg to 12 mg of 2.5 wt% 12HSA molecular gels were transferred into Alod-Al hermetic DSC pans. Due to the volatility of certain solvent, melting and crystallization temperatures could only be measured for some samples. The DSC chamber (Q2000, TA instruments, New Castle, DE) was pre-cooled to the 20 ℃ before the sample was placed into the chamber, which was continually flushed with nitrogen (0.5 ml/min). The samples were heated and cooled at 2 ℃/min to determine the peak crystallization and melting temperatures as well, the enthalpy of melt was determined by integrating the transition using the tangent skimming method available in the software.

5.3.3 Fourier Transform Infrared Spectroscopy (FT-IR)

The carbonyl (~1700 cm^{-1}) and hydroxyl (~3200 cm^{-1}) signals of the 12HSA gels were measured using a Thermo Nicolet FT-IR and an Attenuated total refraction (ATR) prism (Thermo Fisher Scientific, MA, USA). 256 scans were collected at 4 cm^{-1} resolution. The background used for the IR measurements was the empty cell.

5.3.4 X-Ray Diffraction

The x-ray diffraction (XRD) or wide-angle x-ray scattering (WAXS) patterns of 12HSA gels in different solvents were obtained by use of a Bruker HiStar area detector and an Enraf-Nonius FR571 rotating anode x-ray generator equipped with Rigaku Osmic mirror optic system (~0.06 deg 2q nominal dispersion for Cu Ka; l = 1.5418 Å) operating at 40 kV and 40 mA. All of the data were collected at room temperature over a period of about 300 sec. The sample to detector distance was 10.0 cm and the standard spatial calibration was performed at that distance. Scans were 4 deg wide in omega (w) with fixed detector, or Bragg, angle (2q) of 0 deg, and fixed platform (f and c) angles of 0 and 45 deg, respectively. In all cases, the count rate for the area detector did not exceed 100,000 cps.

5.3.5 Microscopy

The supramolecular structure was imaged using a Linkham Imagining Station (Linkham, Surrey, England) equipped with a Q imagining 2560 x 1920 pixel CCD camera (Micropublisher, Surrey, Canada) and a 10 X Olympus lens (0.25 N.A.) (Olympus, Tokyo, Japan). Samples were placed on a glass slide and a cover slip was placed on top of the sample. The slide was transferred into a peltier temperature control stage (LTS120, Linkham, Surrey, England) and heated to 80 ℃ and was slowly cooled (at 2 ℃/min to 20 ℃) to observe fiber formation.

5.4 Discussion

HSPs are particularly useful in predicting the capacity of a LMOG to immobilize different solvents.[15,31,32] The strong correlation between HSPs and the CGC moved our research group to study the effect of HSPs on the physical properties of molecular gels to provide further insights into the role of solvents and solvent parameters on SAFiNs formation. Previously, for 12HSA, it was found that the hydrogen-bonding HSP (δ_h)

positively correlated to the CGC.[15] However, the mechanism behind the increase in CGC remains unknown.

The relaxation time, obtained from pulsed NMR (pNMR), is a measure of a "degree of crystallinity". A decrease in the crystalline order is influenced by crystallographic mismatches, solvent inclusions, different polymorphic forms and high crystal surface area to volume ratios, which correlate to longer relaxation times.[34] Not surprisingly, as the relaxation time increased, corresponding to a decrease in the "crystallinity", the CGC increased. As a function of HSPs, the relaxation time did not correlate to static relative permittivity (Fig. 5-1A), the dispersive HSP (δ_d) (Fig. 5-1B), polar HSP (δ_p) (Fig. 5-1C) nor distance in Hansen space (Fig. 5-1F). However, a positive correlation between the relaxation time and hydrogen-bonding HSP (δ_h) (Fig. 5-1D) and the total HSP (δ_t) illustrate that the hydrogen-bonding non-covalent interactions between the solvent and gelator effect the ability of a LMOG to assemble into a SAFiN (Fig. 5-1E). Below δ_h ~4.5 $MPa^{1/2}$ the crystallinity is unaffected by changing δ_h, while changes to δ_h between 4.5 $MPa^{1/2}$ to 6.5 $MPa^{1/2}$, correlate to a linear decrease in the crystallinity of the SAFiNs. Beyond 6.5 $MPa^{1/2}$ there was no correlation between the two parameters. It is important to note that beyond δ_h ~ 6.5 $MPa^{1/2}$, 12HSA did not gel the solvents. Transparent organogels have been observed when δ_h was below 4.5 $MPa^{1/2}$, correlating to crystal aggregates that are smaller than the diffraction limit of light (i.e., a fibrillar crystal) and from 4.5 $MPa^{1/2}$ to 6.5 $MPa^{1/2}$, opaque gels with spherulitic structures were observed.[15] The positive correlation between δ_h and the relaxation time suggests that increasing δ_h either causes an increase in the interactions between the solvent and gelator leading to crystallographic mismatches, increased solvent inclusions and/or a change in the polymorphic form. Beyond δ_h ~ 6.5 $MPa^{1/2}$ and the gelator becomes soluble in the solvent and thus incapable of forming a molecular gel. The solvents selected beyond δ_h ~

6.5 $MPa^{1/2}$ include all organic acids, alcohols, and amines as well as short chain ketones (i.e., less than 5 carbons).

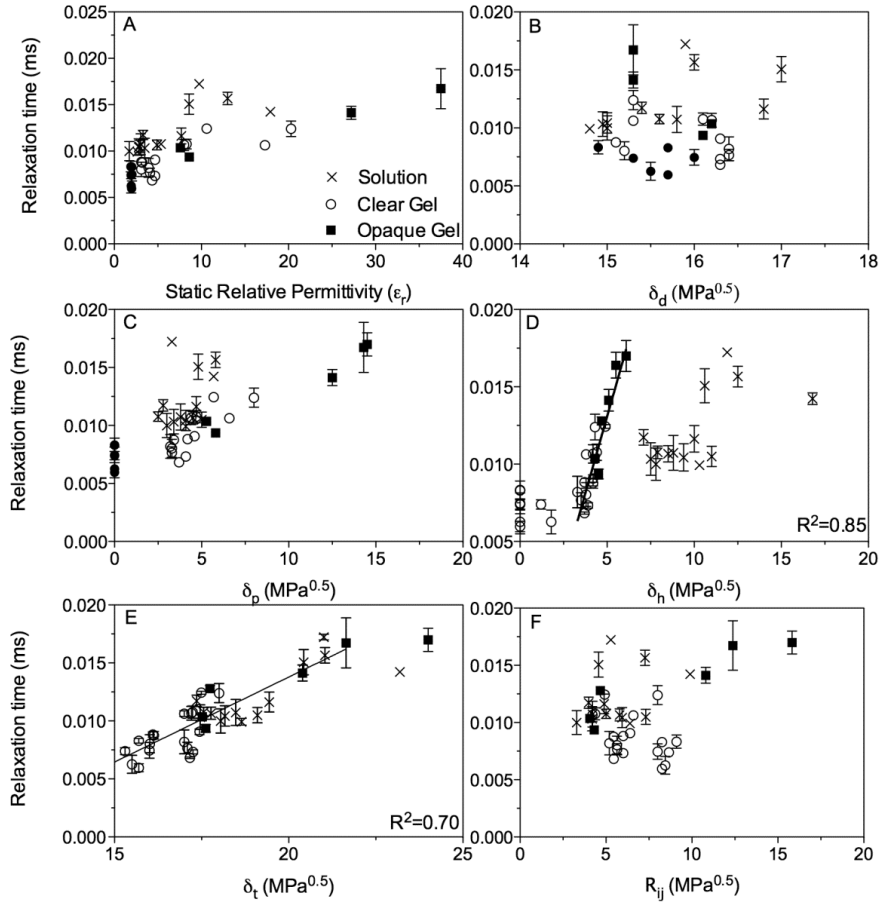

Figure 5-1 T_2 relaxation time as determined using pNMR, as a function of the: static relative permittivity (A); dispersive HSP (δ_d) (B); polar HSP (δ_p) (C); hydrogen-bonding HSP (δ_h) (D); total HSP (δ_t) (E); and distance in Hansen space between the solvent and the gelator (R_{ij}) (F).

The amplitude of the FID relaxation is proportional to the volume of the crystalline phase.[21] As the static relative permittivity, δ_p, δ_h, and δ_t increase so does the solubility of 12HSA, corresponding to a decrease in the FID amplitude (Fig. 5-2A, C, D, E). The decrease in the amplitude also correlates with an increase in the CGC, which may be partially explained by changes in solubility.[15] The amount of crystalline material, or solubility, does not change below δ_h ~ 4.5 $MPa^{1/2}$ (Fig. 5-2D). However, the amplitude decreases above 4.5

$MPa^{1/2}$ corresponding to the transition from translucent to opaque molecular gels.

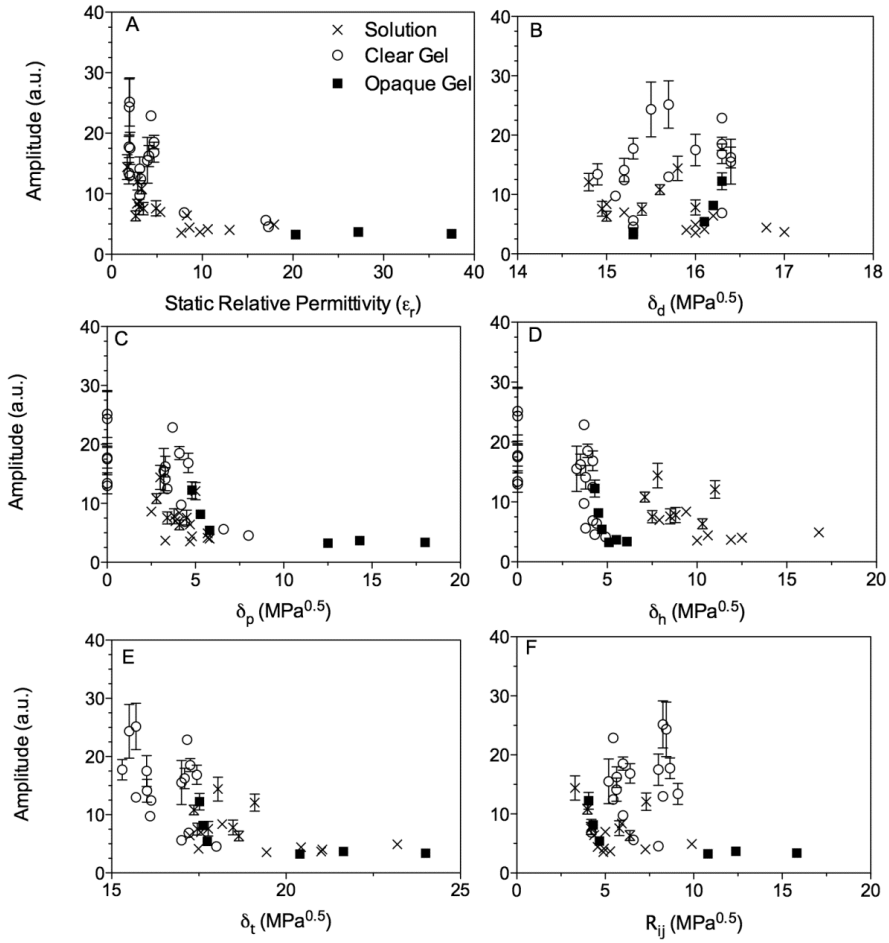

Figure 5-2 Amplitude of the T_2 relaxation time as determined using pNMR, as a function of the: static relative permittivity (A); dispersive HSP (δ_d) (B); polar HSP (δ_p) (C); hydrogen-bonding HSP (δ_h) (D); total HSP (δ_t) (E); and distance in Hansen space between the solvent and the gelator (R_{ij}) (F).

To corroborate the positive correlation between δ_h and the crystallinity, observed using pNMR, the onset of melt determined using DSC was utilized (Fig. 5-3). The melting temperature did not correlate well with the static relative permittivity, δ_d, and Hansen space (R_{ij}) (Fig. 5-3A, B, F). However, as δ_p and δ_h increase, there is a negative correlation with the melting temperature (Fig. 5-3C, D). Gibbs free-energy curves have been used to describe changes in the melting temperatures with crystal perfection.[35] For each new composition of

crystal, a new surface area between the gelator and solvent is created.[36] As the melting point increases, the crystal size and/or the crystals perfection is enhanced. Even though there may be less crystalline mass, the melting point for the 12HSA strands is dependent on either the crystal size (i.e., larger crystals have less interfacial free energy) or the degree of annealing (i.e., they have less crystalline imperfections). It is important to note that only the transition temperatures could be determined on solvent that gelled and that are not too volatile.

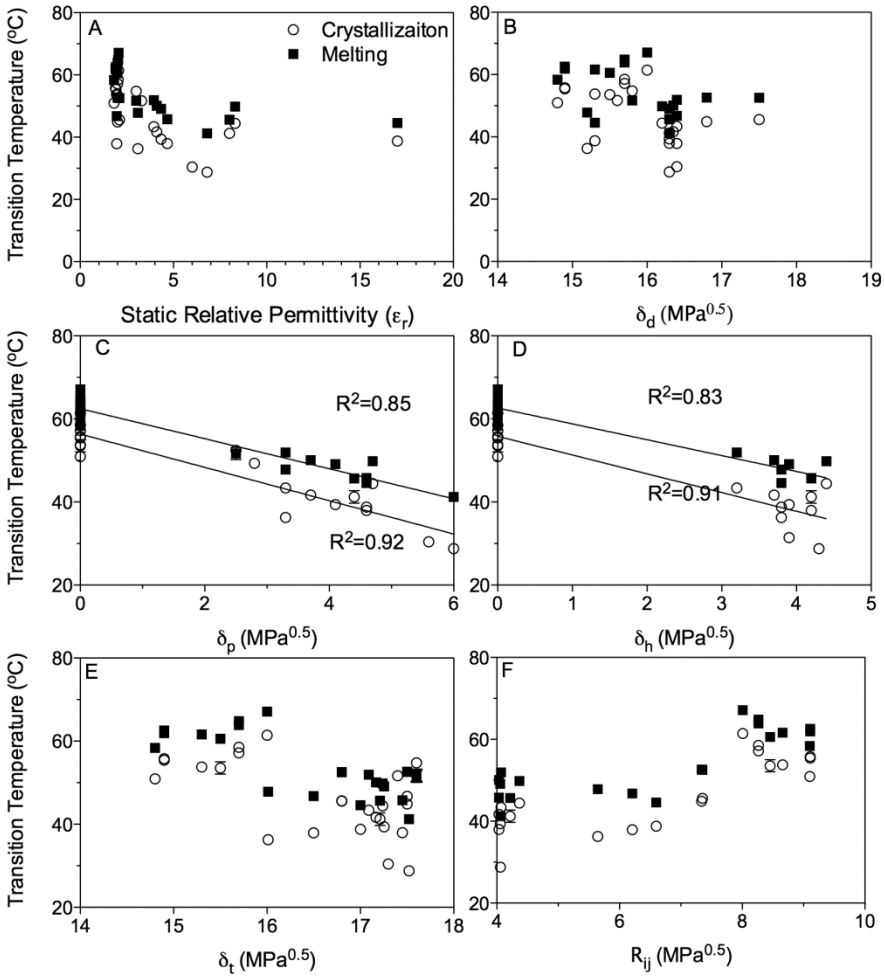

Figure 5-3 Crystallization and melting temperature, as a function of the: static relative permittivity (A); dispersive HSP (δ_d) (B); polar HSP (δ_p) (C); hydrogen-bonding HSP (δ_h) (D); total HSP (δ_t) (E); and distance in Hansen space between the solvent and the gelator (R_{ij}) (F).

The crystallization and melting enthalpy showed no obvious trends between solvent parameters and transition enthalpy (Fig. 5-4). This was expected since the samples were measured at a consistent concentration (2.5 wt%) and the CGC varied depending on the solvent parameters.[15] Along with changes in the CGC, numerous contrasting variables affect the transition enthalpy including: crystal perfect, size, and polymorphic form.[6]

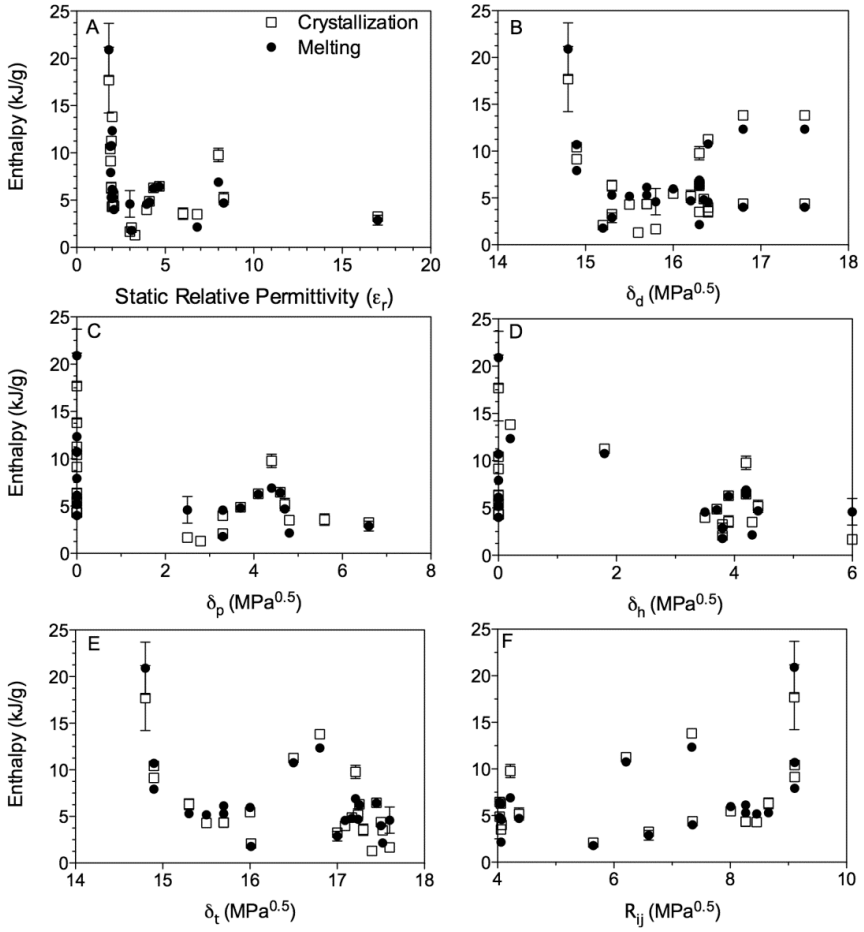

Figure 5-4 Crystallization and melting enthalpy, as a function of the: static relative permittivity (A); dispersive HSP (δ_d) (B); polar HSP (δ_p) (C); hydrogen-bonding HSP (δ_h) (D); total HSP (δ_t) (E); and distance in Hansen space between the solvent and the gelator (R_{ij}) (F).

It is clear that certain macroscopic physical properties (i.e., crystallinity and thermal properties) vary with solvent parameters (Fig. 5-1, 5-2, 5-3, 5-4). However, the cause of the

macroscopic differences must originate from either the micro and/or nanostructure of the SAFiNs. Crystallographic mismatches explain both the observed trends in the relaxation time and the onset of melt. Crystallographic mismatches, in organogels, arise when the crystallographic mismatch nucleation barrier is low allowing gelator molecules to incorporate in a sub-optimal configuration onto the crystal lattice resulting in a branch point.[37,38,39,40] If crystallographic mismatches are responsible for the decrease in crystallinity, then at low δ_h fibrillar aggregates should be observed and as the δ_h increases, the prevalence of mismatches should increase, causing fibrillar aggregates to decrease in length. To experimentally validate this theory, micrographs are presented, in order from low to high δ_h (Fig. 5-5). It is obvious that at low δ_h (i.e., $\delta_h < 4.2$ MPa$^{1/2}$) there is little effect on the fiber morphology (Fig. 5-5). At low δ_h, the crystal morphology is comprised of very fine, long aspect ratio fibers. At δ_h between 4.3 MPa$^{1/2}$ and 4.4 MPa$^{1/2}$ the fiber morphology is present however, the fibers become thicker and individual fibers cluster into aggregates. Beyond 4.4 MPa$^{1/2}$ a drastic reduction in the fiber length is observed and the crystallites undergo a supramolecular transition to spherulites, which may be explained by the crystallographic mismatch theory. The changes observed in the microstructure, as δ_h increases, correspond precisely to the changes in relaxation time measured with pNMR (Fig. 5-1D) and to the CGC which was previously reported.[15]

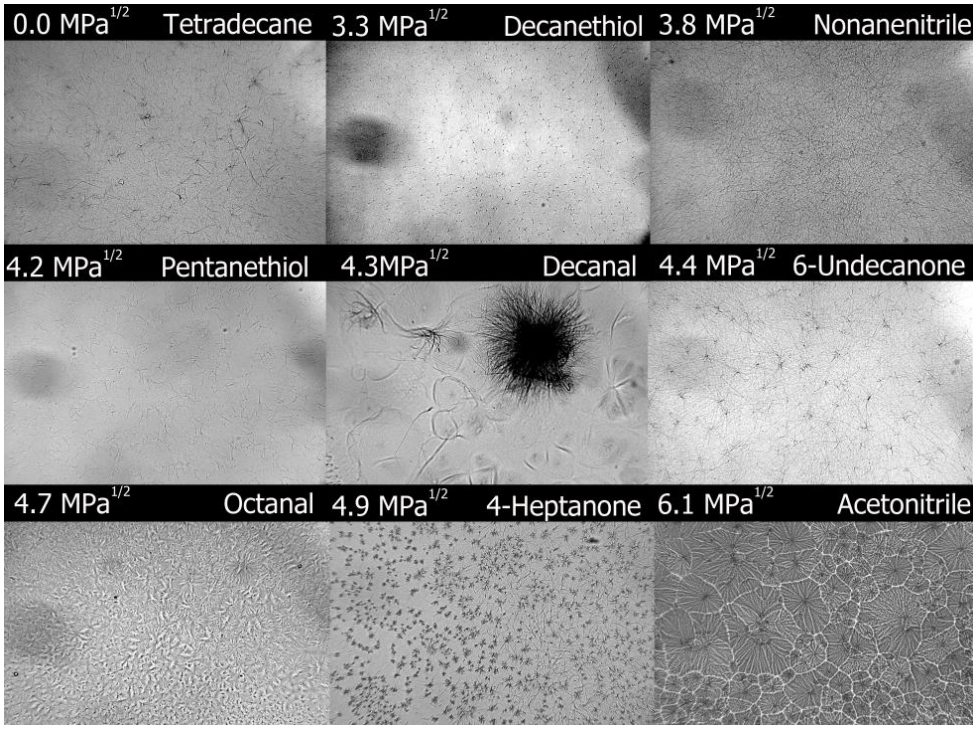

Figure 5-5 Brightfield micrographs of 2.5 wt% 12HSA molecular gels in various solvents. Hydrogen-bonding HSP is indicated in the upper left corner. The width of the micrographs is 120 um.

To observe if the nanostructure of the SAFiNs is influenced by solvent parameters, FT-IR was used to study the chemical state of the 12HSA carboxylic acid (Fig. 5-6, 5-7, 5-8). Three carboxylic acid conformations may be observed. Wave number 1730 cm^{-1} corresponds to a free monomer, 1720 cm^{-1} represents the acyclic dimer and 1690 cm^{-1} indicates a cyclic dimer.[41,42,43] The carboxylic acid peak for 12HSA in amines could not be differentiated from the amine peak at ~1600 cm^{-1} (Fig. 5-8E). The peak position of the carboxylic acid group was plotted against the HSPs (Fig. 5-9). The only correlation between solubility parameters and the chemical state of the carboxylic acid was for δ_h (Fig. 5-9D). Cyclic dimers (~1690 cm^{-1}) were observed when $\delta_h < 4.4$ $MPa^{1/2}$ corresponding to fibrillar crystals (Fig. 5-5, 5-10) and the elevated crystallinity (Fig. 5-1). Acyclic dimers were found at 4.4 $MPa^{1/2} < \delta_h < 6.5$ $MPa^{1/2}$ corresponding to spherulitic crystals (Fig. 5-5, 5-10) and a decrease in the crystallinity (Fig. 5-1). This suggests that, at least in part, crystallographic mismatches arise from a sub-

optimal configuration of the 12HSA head group (Fig. 5-10). Beyond δ_h ~ 6.5 $MPa^{1/2}$ 12HSA was unable to form a molecular gel in these solvents. Two different peaks, associated with carboxylic acid groups, were observed beyond ~ 6.5 $MPa^{1/2}$. A peak at 1710 cm^{-1} and a second weak peak at 1650 cm^{-1} were observed and are attributed to dimer formation; however it is unknown if the dimmer is a 12HSA-solvent dimer, a 12HSA-12HSA dimer or a solvent-solvent dimer (Fig. 5-8A).

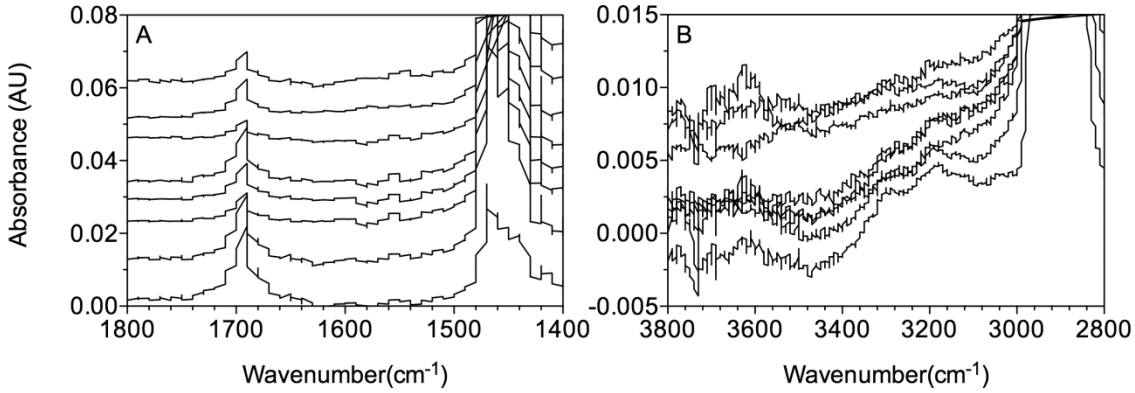

Figure 5-6 Offset FT-IR spectra of 12HSA molecular gels in alkanes. Solvent chain length increases from bottom to top.

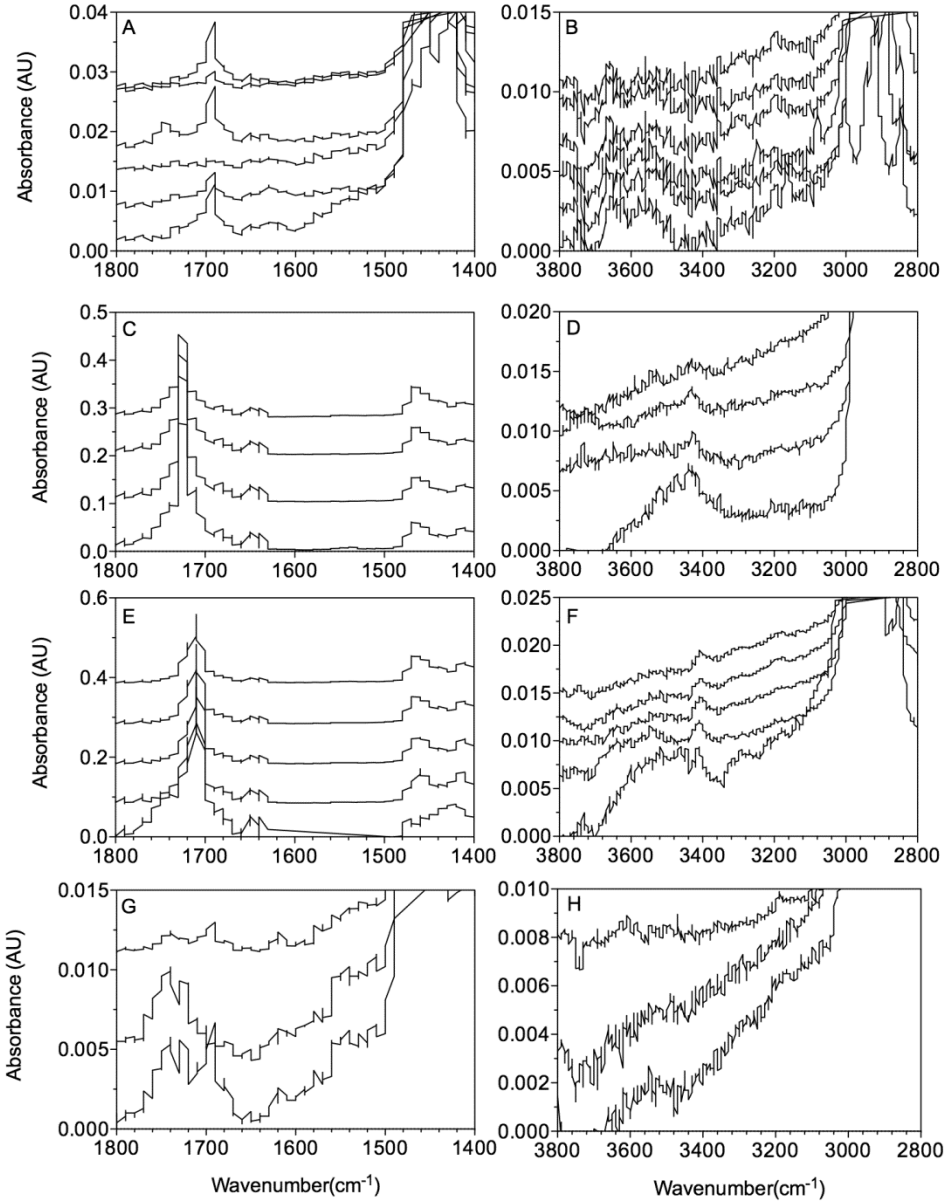

Figure 5-7 Offset FT-IR spectra of 12HSA molecular gels in (A, B) nitriles, (C, D) aldehydes, (E, F) ketones, and (G, H) ethers. Solvent chain length increases from bottom to top.

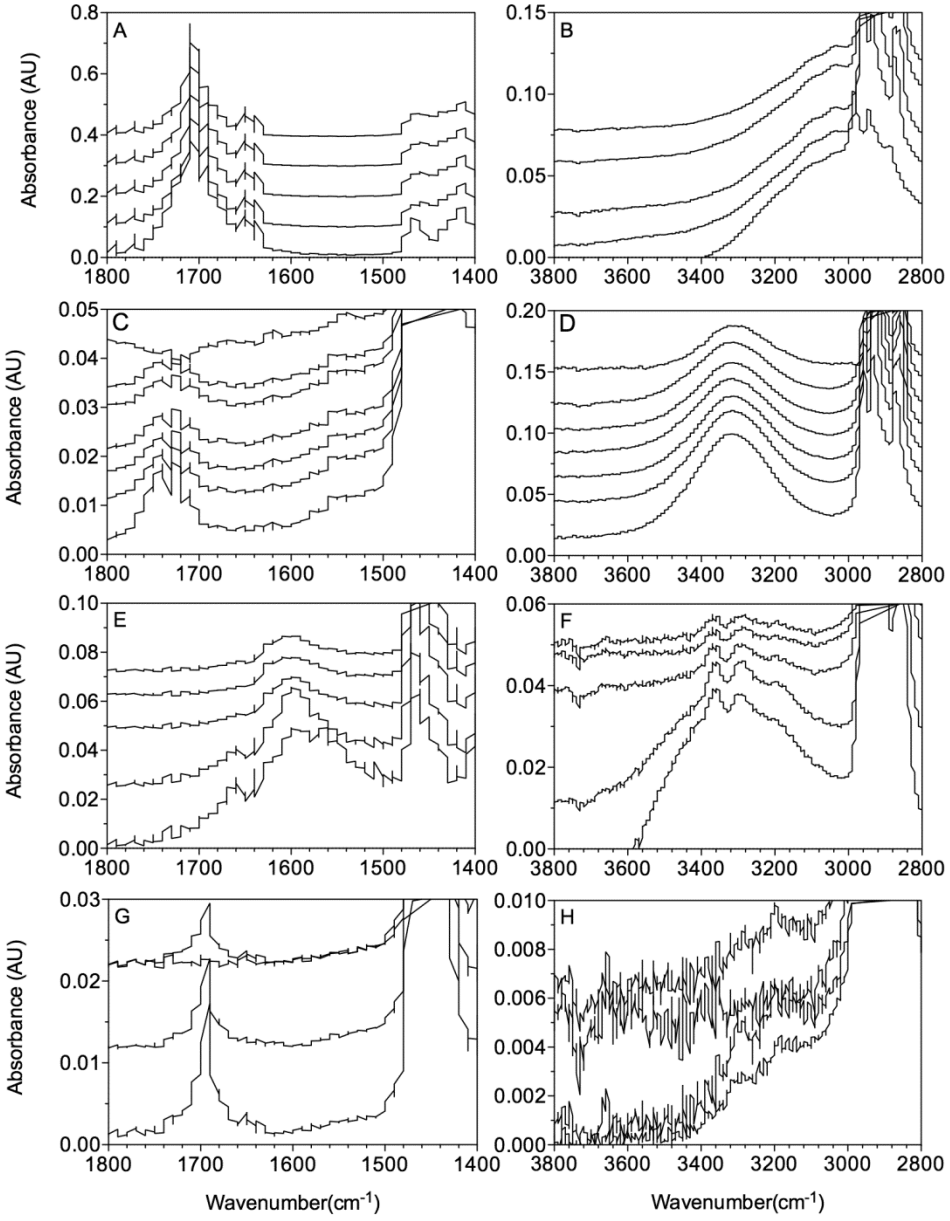

Figure 5-8 Offset FT-IR spectra of 12HSA molecular gels in (A, B) carboxylic acids, (C, D) alcohols, (E, F) amines, and (G, H) thiols. Solvent chain length increases from bottom to top.

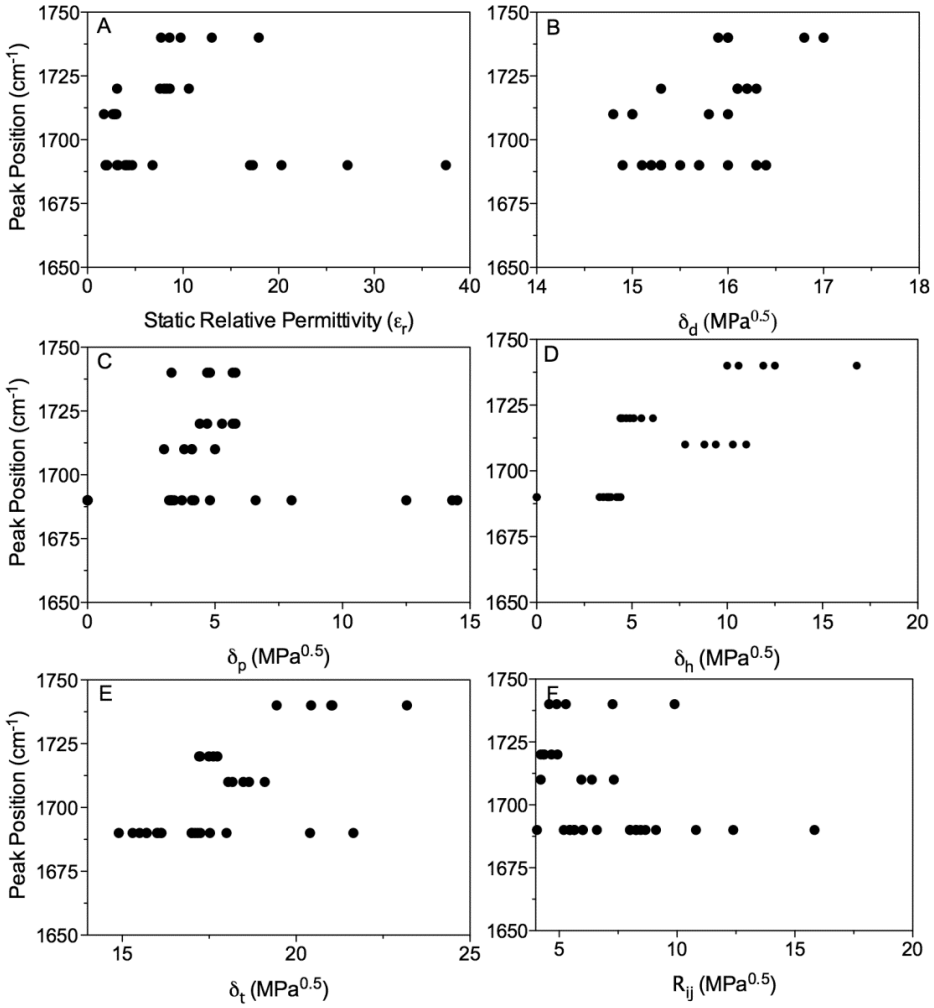

Figure 5-9 FT-IR carboxylic acid peak position, as a function of the: static relative permittivity (A); dispersive HSP (δ_d) (B); polar HSP (δ_p) (C); hydrogen-bonding HSP (δ_h) (D); total HSP (δ_t) (E); and distance in Hansen space between the solvent and the gelator (R_{ij}) (F).

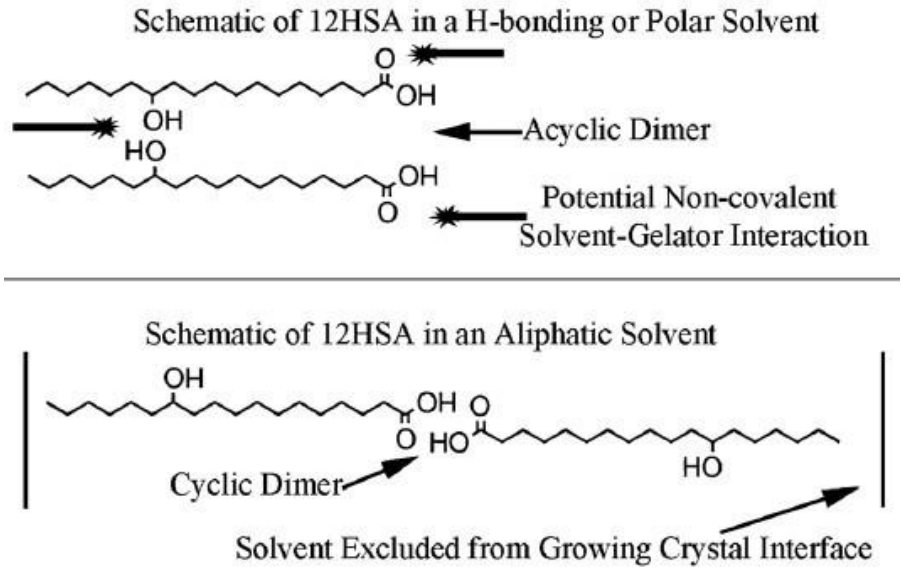

Figure 5-10 Schematic representation of 12HSA in a hydrogen-bonding or polar solvent and 12HSA in an aliphatic solvent

Nanoscale structural changes were studied using different aspects of the XRD spectra (Fig. 5-11, 5-12, 5-13) including: the short angle *d*-spacing (Fig. 5-14), wide angle *d*-spacing (Fig. 5-15) and domain size (Fig. 5-16). Typically, 12HSA molecular gels have the 001 *d*-spacing greater than the bimolecular length of 12HSA (~ 46 Å) at low δ_h, and a *d*-spacing shorter than the bimolecular length at high δ_h.[43] The extended bimolecular length of 12HSA in molecular gels varies with respect to different solvent properties (Fig. 5-14). As the static relative permittivity, δ_p, and δ_t increase, there is a decrease in the *d*-spacing (Fig. 5-14A, C, E). Focusing on δ_h, (Fig. 5-14D) the same trend was observed for the 001 *d*-spacing and the relaxation time (Fig. 5-1D), as well as the chemical state of the carboxylic acid (Fig. 5-9D). It is clear that when the 001 *d*-spacing is greater than the bimolecular length of 12HSA (d > ~ 46 Å), then the 12HSA molecules arrange in a cyclic dimer (1690 cm^{-1}) (Fig. 5-9D). Beyond δ_h ~ 4.4 $MPa^{1/2}$, there is a decrease in the *d*-spacing resulting in an acyclic dimer (i.e., 1720 cm^{-1}) (Fig. 5-9D). This suggests that interdigitation between 12HSA molecules is a result of the formation of an acyclic dimer.

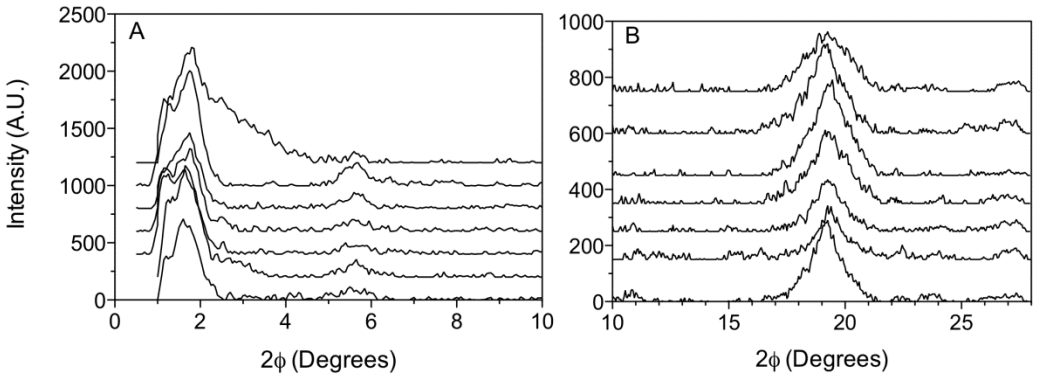

Figure 5-11 Offset short angle (A) and wide angle (B) XRD spectra of 12HSA molecular gels in alkanes. Solvent chain length increases from bottom to top.

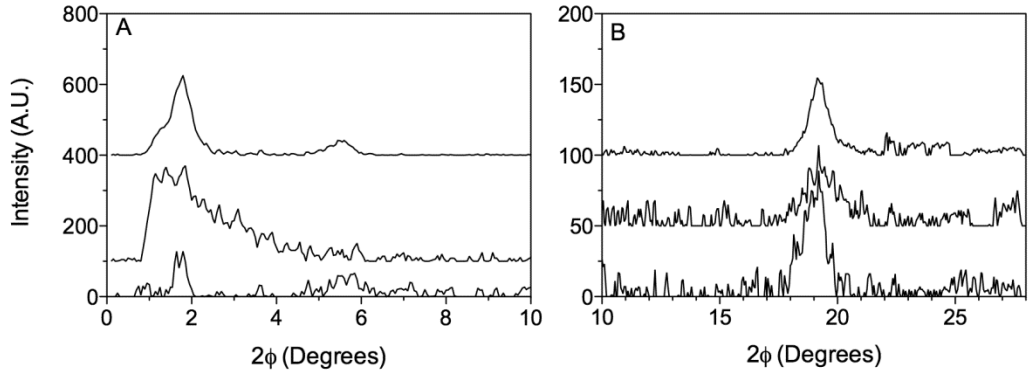

Figure 5-12 Offset short angle (A) and wide angle (B) XRD spectra of 12HSA molecular gels in thiols. Solvent chain length increases from bottom to top.

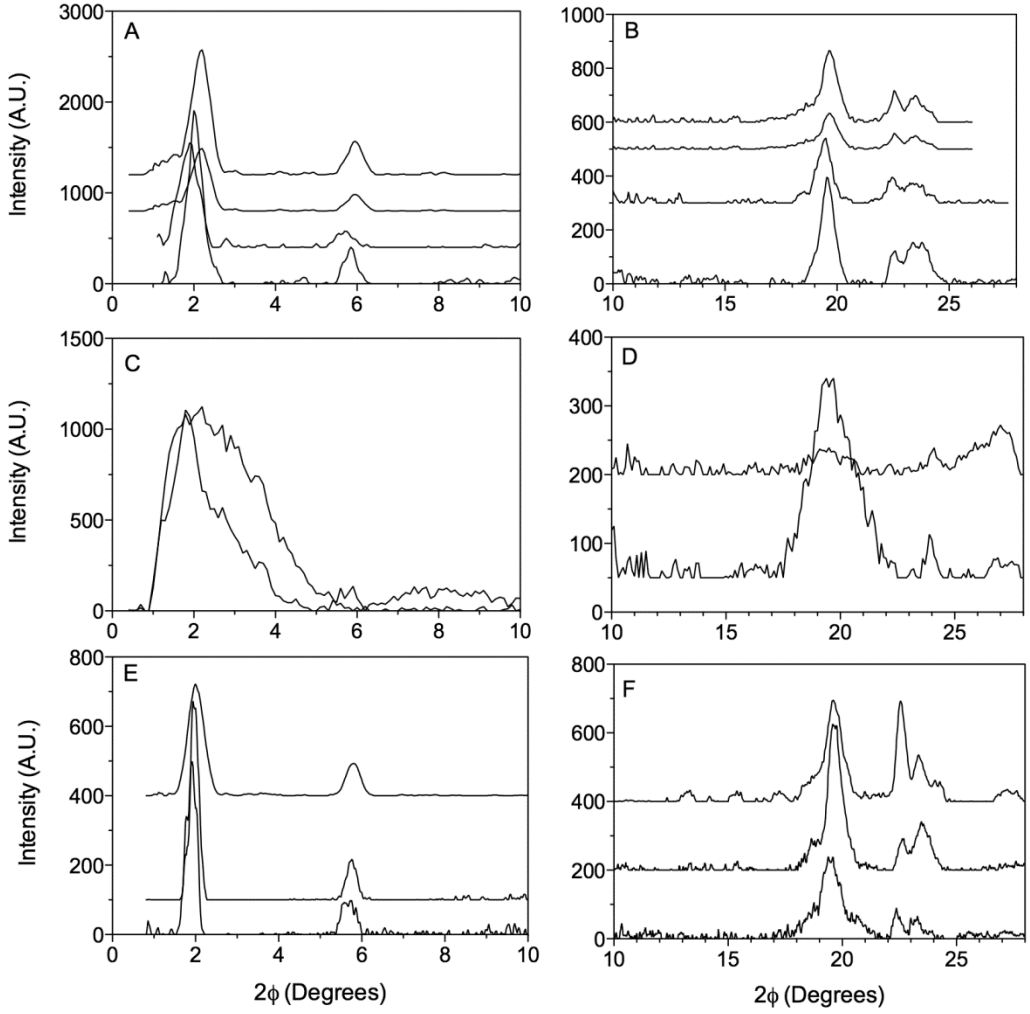

Figure 5-13 Offset short angle (A, C, D) and wide angle (B) XRD spectra of 12HSA molecular gels in (A, B) nitriles, (C, D) aldehydes, and (E, F) ketones. Solvent chain length increases from bottom to top.

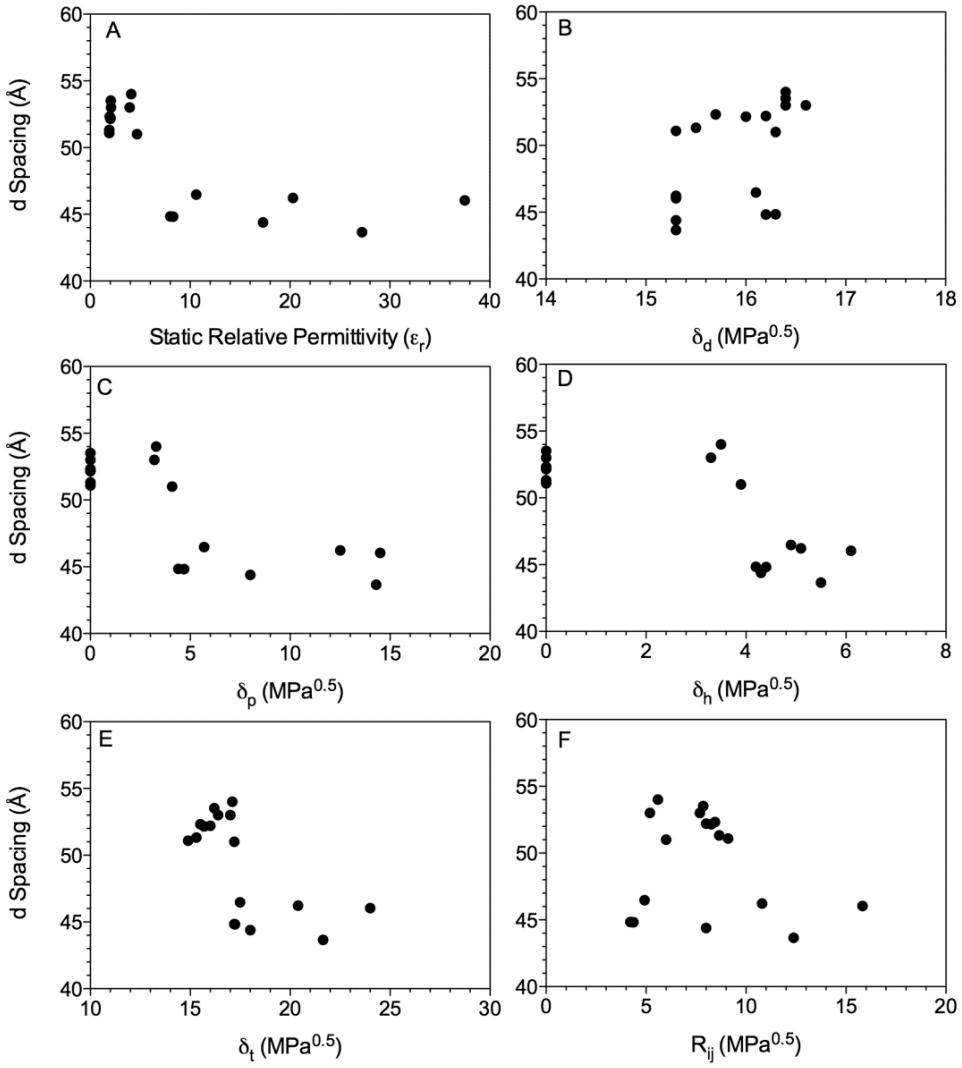

Figure 5-14 Short angle XRD *d*-spacing of the 001 lamellar spacing, as a function of the : static relative permittivity (A); dispersive HSP (δ_d) (B); polar HSP (δ_p) (C); hydrogen-bonding HSP (δ_h) (D); total HSP (δ_t) (E); and distance in Hansen space between the solvent and the gelator (R_{ij}) (F).

Solvent induced polymorphic transitions have recently reported for molecular gels of 12HSA.[44] At low δ_h, the wide-angle spacing was at 4.3 Å corresponding to a hexagonal (~ 4.1 Å) sub-cell spacing (Fig. 5-11, 5-12, 5-15D)[44,45,46] As δ_h increases, a transition from a hexagonal to a triclinic parallel sub-cell (strong peak at 4.6 Å, and two weak peaks at 3.9 Å and 3.8 Å) is observed (Fig. 5-13, 5-15D). The sub-cell transition observed at $\delta_h \sim 4.4$ MPa$^{1/2}$ (Fig. 5-15D) corresponds to a transition from a cyclic to an acyclic dimer (Fig. 5-9D), a decrease in the extended length bimolecular length of 12HSA (Fig. 5-14D), a decrease in the crystallinity (Fig. 5-1D, 5-2D) and a transition from a fibrillar to spherulitic crystal morphology (Fig. 5-5).

The full-width half-max from the XRD spectra, were used to calculate the domain size using the Williamson-Hall equation:[47]

$$FW(S) \times \cos(\theta) = \frac{K \times \lambda}{Size} + (4 \times Strain \times \sin(\theta)) \quad \text{(Equation 5-1)}$$

where FW is the full-width half-max, θ is the diffraction angle, K is the Scherrer constant, λ is the X-ray wavelength. Since few diffraction peaks were observed we had to assume that no strain was present and the slope was set equal to zero (Fig. 5-16). From the *y*-intercept, the domain size was calculated and plotted against solubility parameters (Fig. 5-17). The domain size follows a parabolic shape when plotted against the static relative permittivity (Fig. 5-17A), δ_p (Fig. 5-17C), δ_h (Fig. 5-17D) and δ_t (Fig. 5-17E). The vertex of the parabola corresponds to $\delta_h \sim 4.2$ MPa$^{1/2}$ which is the transition for the nanoscopic, macroscopic and supramolecular changes observed in 12HSA molecular gels.

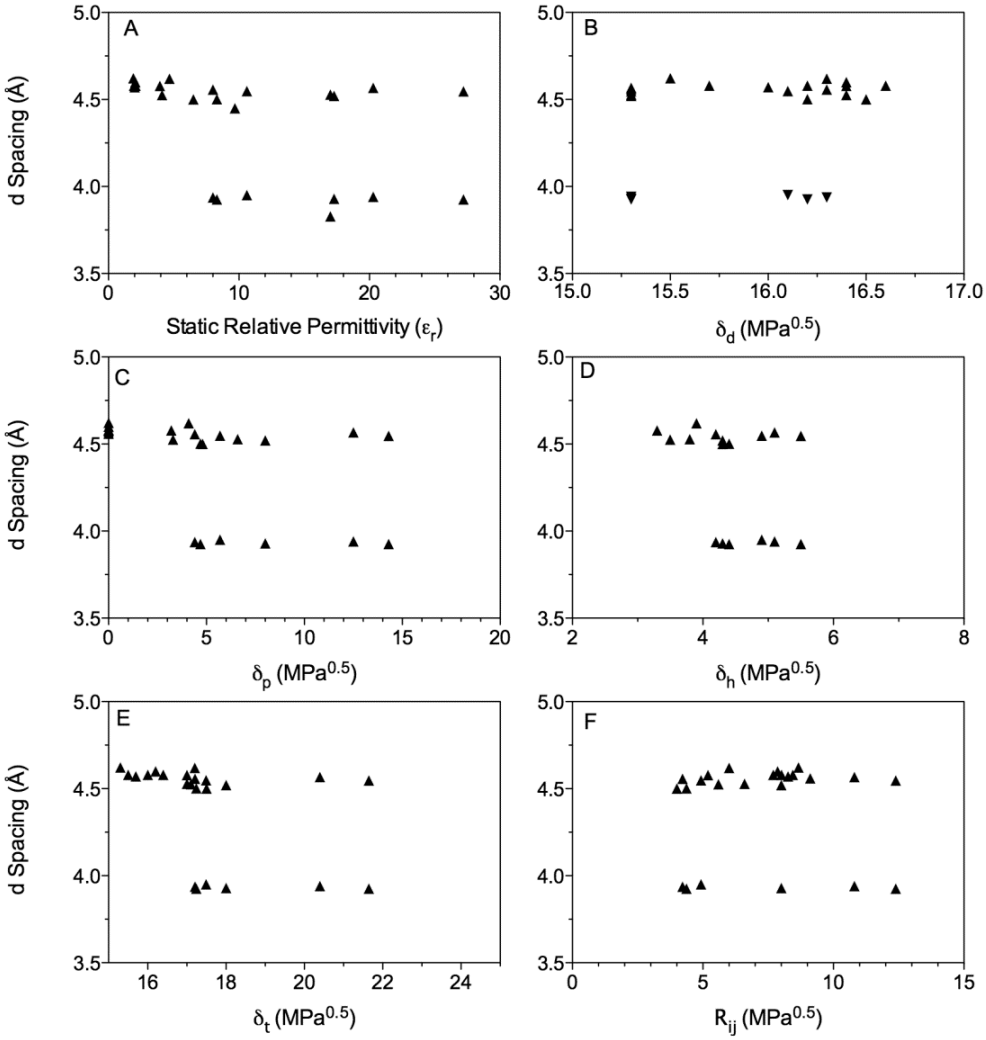

Figure 5-15 Wide angle XRD *d*-spacing, as a function of the: static relative permittivity (A); dispersive HSP (δ_d) (B); polar HSP (δ_p) (C); hydrogen-bonding HSP (δ_h) (D); total HSP (δ_t) (E); and distance in Hansen space between the solvent and the gelator (R_{ij}) (F).

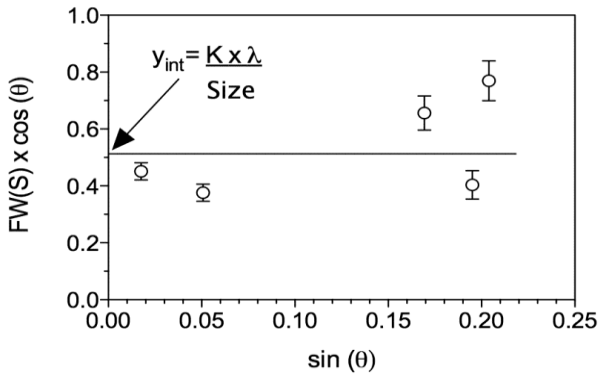

Figure 5-16 Williamson-Hall plot to determine the domain size using the full-width, half-max from XRD patterns. The data shown is for 12HSA in butanenitrile.

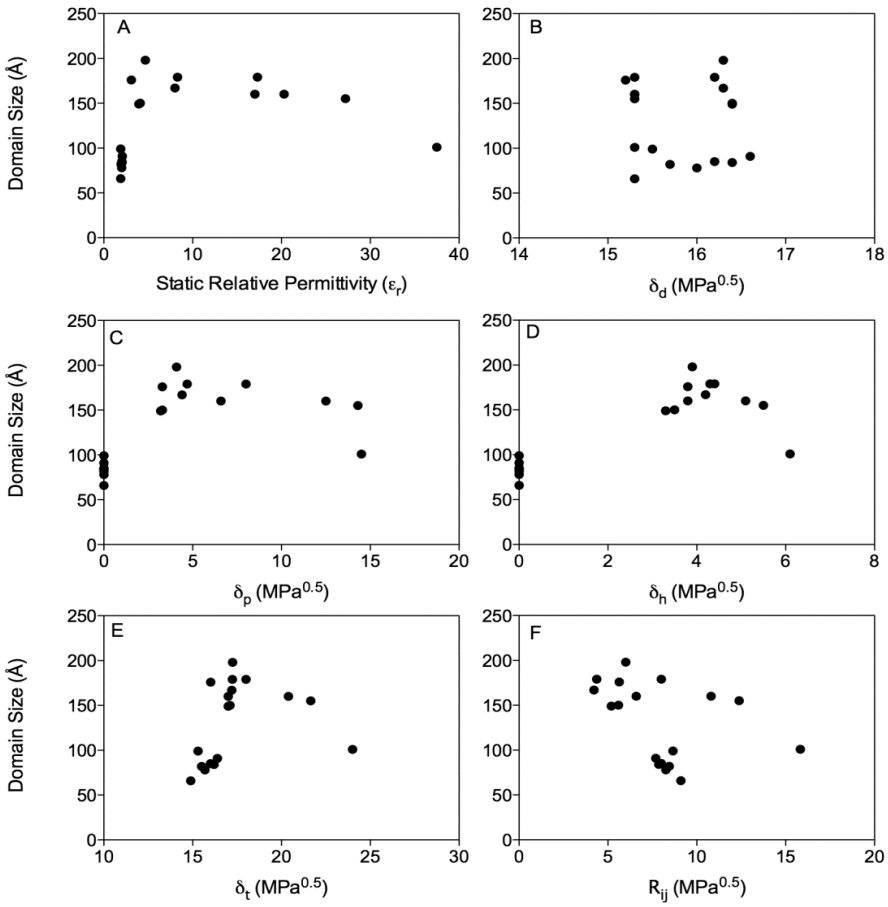

Figure 5-17 Domain size calculated using a Williamson-Hall plot, as a function of the: static relative permittivity (A); dispersive HSP (δ_d) (B); polar HSP (δ_p) (C); hydrogen-bonding HSP (δ_h) (D); total HSP (δ_t) (E); distance in Hansen space between the solvent and the gelator (R_{ij}) (F).

Obviously, solvent affects all levels of structure in molecular gels from polymorphic nanoscale interactions, to the domains size, microstructure, supramolecular structure and to the macroscopic properties of the gel (Fig. 5-18). These new insights provide a new level of tailorability for molecular gels. These drastic changes in the structure will influence practical applications such as hardness, solvent mobility, rate of bioactive release and tortuosity of biological scaffolding.

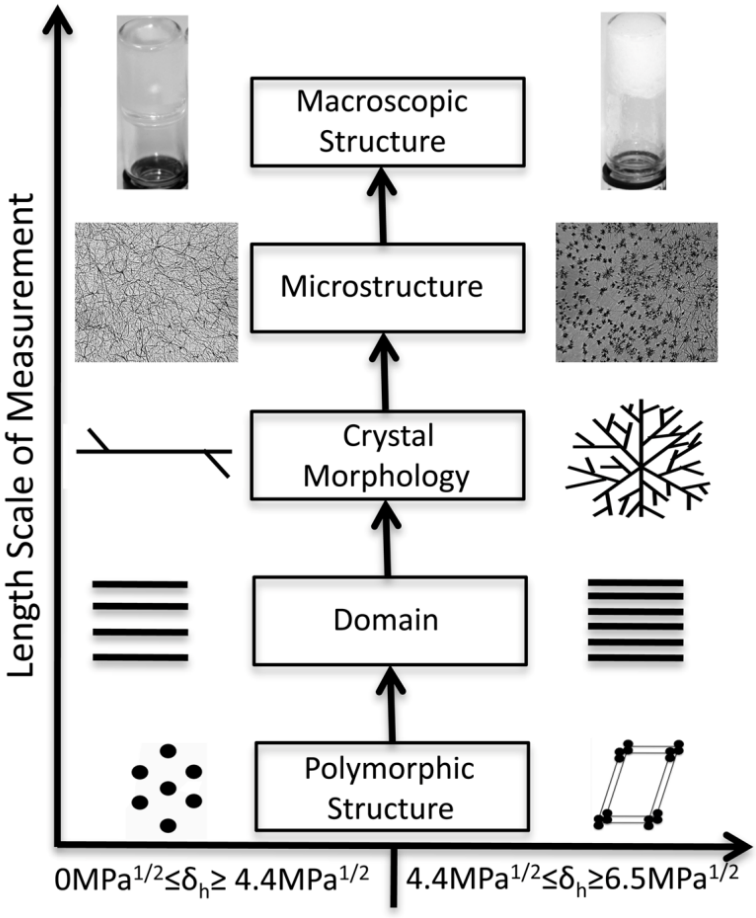

Figure 5-18 Schematic representation of the levels of structure that are altered as the HSPs are varied using solvent selection.

5.5 Conclusions

Numerous reports have worked on elucidating the gelator structures that give rise to molecular gels. However, this study illustrates that without taking into account the chemical structure of the solvent and the solvent-gelator interactions, the likelihood of success is low. The crystalline structure of 12HSA, a structurally simple gelator, is influenced by solvent properties. Different polymorphic forms, dimer structure, domain size, fiber morphology, microstructure, thermal properties and visual appearance are all drastically influenced by solvent parameters. Although this may impede progress on a universal technique for designing new gelators, the ability to manipulate these structures is invaluable and may open new avenues in pharmacology, biomaterials and scaffolds.

5.6 References

1. Kubo, W.; Murakoshi, K.; Kitamura, T.; Yodhida, S.; Haruki, M.; Hanabusa, K.; Shirai, H.; Wada, Y.; Yanagida, S., Quasi-Solid-State Dye-Sensitized TiO2 Solar Cells: Effective Charge Transport in Mesoporous Space Filled with Gel Electrolytes Containing Iodide and Iodine. *Journal of Physical Chemisty B* **2001,** *105*, 12809-12815.
2. Sugiyasu, K.; Fujita, N.; Shinkai, S., Visible-Light-Harvesting Organogel Composed of Cholesterol-Based Perylene Derivatives†. *Angewandte Chemie International Edition* **2004,** *43*, 1229-1233.
3. Bhattacharya, S.; Krishnan-Ghosh, Y., First report of phase selective gelation of oil from oil/water mixtures. Possible implication toward containing oil spills. . *Chemical Communication* **2001**, 185-186.
4. Jadhav, R. S.; Vemula, P. K.; Kumar, R.; Raghavan, S. R.; John, G., Sugar-Derived Phase-Selective Molecular Gelators as Model Solidifiers for Oil Spills. *Angewandte Chemie* **2010,** *49*, 7695 –7698.
5. Friggeri, A.; Feringa, B. L.; van Esch, J., Entrapment and release of quinoline derivatives using a hydrogel of a low molecular weight gelator. *Journal of Controlled Release* **2004,** *97*, 241-248.
6. Wu, Y.; Wu, S.; Zou, G.; Zhang, Q., Solvent effects on structure, photoresponse and speed of gelation of a dicholesterol-linked azobenzene organogel. *Soft Matter* **2011,** *7*, 9177-9183.
7. Mallia, V. A.; Butler, P. D.; Sarkar, B.; Holman, K. T.; Weiss, R. G., Reversible Phase Transitions within Self-Assembled Fibrillar Networks of (R)-18-(n-Alkylamino)octadecan-7-ols in Their Carbon Tetrachloride Gels. *Journal of the American Chemical Society* **2011,** *133*, 15045-15054.
8. Weiss, R. G.; Terech, P., Introduction. In *Molecular Gels: Materials with Self-Assebled Fibrillar Networks*, Weiss, R. G.; Terech, P., Eds. Springer: Dordrecht, The Neatherlands, 2006; pp 1-13.
9. George, M.; Weiss, R. G., Molecular Organogels. Soft Matter Comprised of Low-Molecular-Mass Organic Gelators and Organic Liquids. *Accounts of Chemical Research* **2006,** *39*, 489-497.
10. Duffy, N.; Blonk, H. C. G.; Beindorff, C. M.; Cazade, M.; Bot, A.; Duchateau, G., Organogel-Based Emulsion Systems, Micro-Structural Features and Impact on In Vitro Digestion. *Journal of the American Oil Chemists Society* **2009,** *86* (8), 733-741.
11. Toro-Vazquez, J. F.; Morales-Rueda, J.; Mallia, V. A.; Weiss, R. G., Relationship Between Molecular Structure and Thermo-mechanical Properties of Candelilla Wax and Amides Derived from (R)-12-Hydroxystearic Acid as Gelators of Safflower Oil. *Food Biophysics* **2010,** *5* (3), 193-202.
12. Bot, A.; Veldhuizen, Y. S. J.; den Adel, R.; Roijers, E. C., Non-TAG structuring of edible oils and emulsions. *Food Hydrocolloids* **2009,** *23* (4), 1184-1189.
13. Terech, P.; Aymonier, C.; Loppinet-Serani, A.; Bhat, S.; Banerjee, S.; Das, R.; Maitra, U.; Del Guerzo, A.; Desvergne, J. P., Structural Relationships in 2,3-Bis-n-decyloxyanthracene and 12-Hydroxystearic Acid Molecular Gels and Aerogels Processed in Supercritical CO2. *Journal of Physical Chemistry B* **2010,** *114* (35), 11409-11419.
14. Terech, P., 12-D-Hydroxyoctadecanoic Acid Organogels - A Small-Angle Neutron-Scattering Study. *Journal De Physique Ii* **1992,** *2* (12), 2181-2195.
15. Gao, J.; Wu, S.; Rogers, M. A., Harnessing Hansen Solubility Parameters to Predict Organogel Formation. *Journal of Materials Chemistry* **2012,** *22*, 12651-12658.

16. Bot, A.; den Adel, R.; Roijers, E. C., Fibrils of gamma-Oryzanol plus beta-Sitosterol in Edible Oil Organogels. *Journal of the American Oil Chemists Society* **2008,** *85* (12), 1127-1134.
17. Suzuki, M.; Nakajima, Y.; Yumoto, M.; Kimura, M.; Shirai, H.; Hanabusa, K., Effects of Hydrogen Bonding and van der Waals Interactions on Organogelation Using Designed Low-Molecular-Weight Gelators and Gel Formation at Room Temperature. *Langmuir* **2003,** *19* (21), 8622-8624.
18. Rogers, M. A.; Marangoni, A. G., Solvent-Modulated Nucleation and Crystallization Kinetics of 12-Hydroxystearic Acid: A Nonisothermal Approach. *Langmuir* **2009,** *25* (15), 8556-8566.
19. Hirst, A. R.; Coates, I. A.; Boucheteau, T. R.; Miravet, J. F.; Escuder, B.; Castelletto, V.; Hamley, I. W.; Smith, D. K., Low-molecular-weight gelators: elucidating the principles of gelation based on gelator solubility and a cooperative self-assembly model. *Journal of the American Chemical Society* **2008,** *130*, 9113-9121.
20. Rogers, M. A.; Wright, A. J.; Marangoni, A. G., Nanostructuring Fiber Morphology and Solvent Inclusions in 12-Hydroxystearic Acid/Canola Oil Organogels. *Current Opinion in Colloid & Interface Science* **2009,** *14* (1), 33-42.
21. Rogers, M. A.; Wright, A. J.; Marangoni, A. G., Post-crystallization increases in the mechanical strength of self-assembled fibrillar networks is due to an increase in network supramolecular ordering. *Journal of Physics D-Applied Physics* **2008,** *41* (21), 1-5.
22. Zhu, G.; Dordick, J. S., Solvent Effect on Organogel Formation by Low Molecular Weight Molecules. **2006,** *18* (Chemistry of Materials), 5988-5995.
23. Pinault, T.; Isare, B.; Bouteiller, L., Solvents with Similar Bulk Properites Induce Distinct Supramolecular Architectures. *CHEMPHYSCHEM* **2006,** *7*, 816-819.
24. Kuwahara, T.; Nagase, H.; Endo, T.; Ueda, H.; Nakagaki, M., Crystal structure of DL-12-hydroxystearic acid. *Chemistry Letters* **1996,** *25*, 435-436.
25. Lam, R.; Quaroni, L.; Pederson, T.; Rogers, M. A., A molecular insight into the nature of crystallographic mismatches in self-assembled fibrillar networks under non-isothermal crystallization conditions. *Soft Matter* **2010,** *6* (2), 404-408.
26. Li, J. L.; Liu, X. Y.; Wang, R. Y.; Xiong, J. Y., Arichitecture of a Biocompatible Supramolecular Material by Supersaturation-Driven Fabrication of its Network. *Journal of Physical Chemistry B* **2005,** *109*, 24231-24235.
27. Rogers, M. A.; Bot, A.; Lam, R., S.H.; Pedersen, T.; May, T., Multicomponent Hollow Tubules Formeed Using Phytosterol and γ-Oryzanol-Based Compounds: An Understanding of Their Molecular Embrace. *Journal of Physical Chemistry* **2010,** *114*, 8278-8295.
28. Brotin, T.; Devergne, J. P.; Fages, F., Photostationary Fluorescence Emission and Time Resoved Spectroscopy of Symmetrically Disubstituted Anthracenes on teh meso and Side Rings: The Unusual Behavior of the 1,4 Derivative. *Photochemistry and Photobiology* **1992,** *55*, 349-358.
29. Terech, P.; Furman, I.; Weiss, R. G., Structures of Organogels Based Upon Cholesteryl 4-(2-Anthryloxy)Butanoate, A Highly Efficient Luminescing Gelator - Neutron AND X-Ray Small-Angle Scattering Investigations. *Journal of Physical Chemistry* **1995,** *99* (23), 9558-9566.
30. Nakano, Y.; Hirose, T.; Stals, P. J. M.; Meijer, E. W.; Palmans, A. R. A., Conformational Analysis of Supramolecular Polymerization Process of Disc-like Molecules. *Chemical Science* **2012,** *3*, 148-155.
31. Raynal, M.; Bouteiller, L., Organogel Formation Rationalized by Hansen Solubility Parameters. *Chemical Communication* **2011,** *47*, 8271-8273.

32. Yan, N.; Xu, Z.; Diehn, K. K.; Raghavan, S. R.; Fang, Y.; Weiss, R. G., Pyrenyl-Linker-Glucono Gelators. Correlations of Gel Properties with Gelator Structures and Characterization of Solvent Effects. *Langmuir* **2013,** *29*, 793-805.
33. Hansen, C. M., *Hansen Solubility Parameters*. 2nd ed.; CRC Press: Boca Raton, Fl, 2007.
34. Duval, F. P.; van Duynhoven, J. P. M.; Bot, A., Practical implications of the phasecompositional assessment of lipid-based food products by time-domain NMR. *Journal of the American Oil Chemists Society* **2006,** *83*, 905-912.
35. Farbi, D.; Guan, J.; Cesaro, A., Crystallisation and melting behaviour of poly (3-hydroxybutyrate) in dilute solution: towards an understanding of physical gels. *Thermochimica Acta* **1998,** *321*, 3-16.
36. Rogers, M. A.; Wright, A. J.; Marangoni, A. G., Engineering the Oil Binding Capacity and Crystallinity of Self-Assembled Fibrillar Networks of 12-Hydroxystearic Acid in Edible Oils. *Soft Matter* **2008,** *4* (7), 1483-1490.
37. Liu, X.-L.; Sawant, P. D., Determination of the Fractal Characteristic of Nanofiber-Network Formation in Supramolecular Materials. *CHEMPHYSCHEM* **2002,** *3*, 374-377.
38. Liu, X. Y.; Sawant, P. D., Mechanism of the formation of self-organized microstructures in soft functional materials. *Advanced Materials* **2002,** *14*, 421-426.
39. Li, J. L.; Wang, R. Y.; Liu, X. Y.; Pan, H. H., Nanoengineering of a Biocompatible Organogel by Thermal Processing. *Journal of Physical Chemistry B* **2009,** *113* (15), 5011-5015.
40. Wang, R.; Lui, X.-Y.; Xiong, J.; Li, J., Real-time observation of fiber network formation in molecular organogel: supersaturation-dependent microstructure and its related rheological property. . *Journal of Physical Chemistry B* **2006,** *110*, 7275-7280.
41. Grahame, D. A. S.; Olauson, C.; Lam, R. S. H.; Pedersen, T.; Borondics, F.; Abraham, S.; Weiss, R. G.; Rogers, M. A., Influence of Chirality on the Modes of Self-Assembly of 12-Hydroxystearic Acid in Molecular Gels of Mineral Oil. *Soft Matter* **2011,** *7*, 7359-7365.
42. Lin-Vien, D.; Colthup, N. B.; Fateley, W. G.; Grasselli, J. G., *The Handbook of Infrared and Raman Characteristic Frequencies of Organic Molecules*. Academic Press: London, UK, 1991.
43. Abraham, S.; Lan, Y.; Lam, R. S. H.; Grahame, D. A. S.; Kim, J. J. H.; Weiss, R. G.; Rogers, M. A., Influence of Positional Isomers on the Macroscale and Nanoscale Architectures of Aggregates of Racemic Hydroxyoctadecanoic Acids in Their Molecular Gel, Dispersion, and Solid States. *Langmuir* **2012**.
44. Wu, S.; Gao, J.; Emge. T.; Rogers, M. A., Solvent Induced Polymorphic Nanoscale Transitions for 12-Hydroxyoctadecanoic Acid Molecular Gels. *Crystal Growth & Design* **2013,** *Accepted*.
45. Marangoni, A. G., Crystallization Kinetics. In *Fat Crystal Networks*, Marangoni, A. G., Ed. Marcel Dekker: New York, 2005; pp 21-82.
46. Sato, H.; Ueno, S., Polymorphism in Fats and Oils. In *Bailey's Industrial Oil and Fat Products*, 6th ed.; Shahidi, F., Ed. John Wiley & Sons, Inc: New York, USA, 2005; pp 77-120.
47. Lou, D.; Audebrand, N., Profile Fitting and Diffraction Line-Broadening Analysis. *Advances in X-ray Diffraction* **1997,** (41), 556-565.

6.0 CONCLUSIONS

Organic solvents with various functional groups and aliphatic chain length have different impacts on the gelation capacity of 12HSA. As a new approach to study molecular gels, hydrogen-bonding HSP (δ_h) has found particular use in predicting 12HSA molecular gels formation. Clear gels are able to form in solvents with $\delta_h \leq 4.7$ MPa$^{1/2}$ while opaque gels form between 4.7 MPa$^{1/2}$ $< \delta_h <$ 5.1 MPa$^{1/2}$. When δ_h is greater than 5.1 MPa$^{1/2}$, crystal structures disappear and solution remains. Such trend is consistent with the fact that solvent-gelator interactions are the key factor in mediating 12HSA molecular gels formation. Due to the molecular structure of 12HSA, hydrogen bonding is the major intermolecular force that interacts between 12HSA molecules and brings 12HSA and solvents together. As δ_h of solvents increases, solvent-gelator interactions become stronger, which on the other hand has weakened the gelator-gelator interactions between 12HSA molecules. Gel formation is thus disrupted leading to the formation of thicker crystalline fibers or the disappearance of crystal structure when the solvents' hydrogen-bonding component is too strong. Hence, more 12HSA molecules are required to off-set the interference from solvents and to build up the supramolecular gels network. This can be confirmed by the positive linear correlation revealed in this study between CGC of 12HSA in organic solvents and δ_h. The correlation between CGC and HSPs is even much stronger when observed within the individual class of solvents.

The underlying reason for the changes in 12HSA gelation capacity and CGC is related to the polymorphic transitions that occur in the nanoscopic network structure. Affected by solvents, 12HSA self-assemble into SAFiNs as two different chemical states: cyclic dimers and acyclic dimers, which are strongly correlated to δ_h. Cyclic dimers are observed when $\delta_h <$ 4.4 MPa$^{1/2}$ and acyclic dimers are observed at an elevated δ_h between 4.4

$MPa^{1/2}$ and 5.1 $MPa^{1/2}$. When δ_h goes beyond 5.1 $MPa^{1/2}$, solution remains. Such trend in transition between dimers is consistent with the transition between two polymorphic forms present in 12HSA molecular gels: hexagonal and triclinic parallel, which also occurs at $\delta_h \sim$ 4.4 $MPa^{1/2}$. As δ_h increases, the hexagonal subcell is transformed into the triclinic polymorphic form. Such modifications of nanostructure induced by solvents result in the variations in fiber microstructure and macroscopic physical properties that include crystallinity and thermal properties. Each of these properties is revealed to scale with δ_h, which corroborates the correlation between δ_h and polymorphic transitions in nanostructure. In solvents with δ_h < 4.4 $MPa^{1/2}$, 12HSA transparent organogels form containing fibrillar crystals with the hexagonal subcell. As δ_h of solvents increases, crystallinity of molecular gels decreases mainly due to the increasing solvent-gelator interactions. The stronger interactions between solvents and gelators result in crystallographic mismatches and the change in polymorphic forms that affect the crystalline order. When δ_h is greater than 4.4 $MPa^{1/2}$, transparent fibrillar aggregates are transformed to opaque organogels network with spherulitic crystal morphology and the triclinic parallel subcell.

Aims of this research are achieved. Each level of 12HSA molecular gels structure from nanoscopic scale to supramolecular scale is observed to be influenced by the nature of solvent and solvent-gelator interactions. δ_h has been proved to be closely related to the solvent induced modifications in 12HSA gelation capacity and structural transition and therefore can be a very useful tool in predicting and understanding 12HSA molecular gels formation. In support of the numerous other studies on organogelators, the findings in this research illustrating the crucial role of solvents in organogel formation will provide critical insights into the effects of solvent when attempting to design and manipulate the new kinds of organogels. Since the current research is only focused on the simple solvent system, in the

future, it is possible to scrutinize the relationship between HSPs and molecular gels formation using a more complicated solvent system, such as solvent with more than one functional group, or a mixed solvent system, by means of which the capability of HSPs as a predictive tool in studying molecular gels formation can be better and more thoroughly evaluated.

APPENDIX

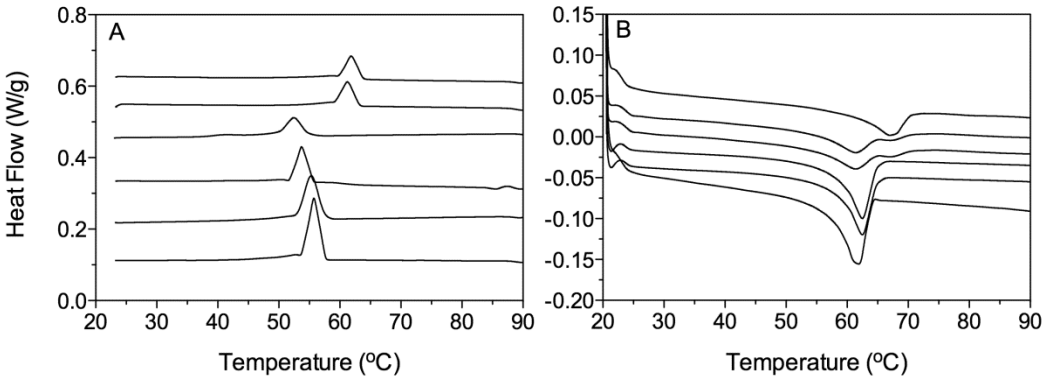

Appendix 1 DSC crystallization (A) and melting (B) thermograms of straight chain aliphatics which have been vertically offset to prevent overlap. The thermograms from bottom to the top are hexane, heptane, octane, decane, dodecane and tetradecane.

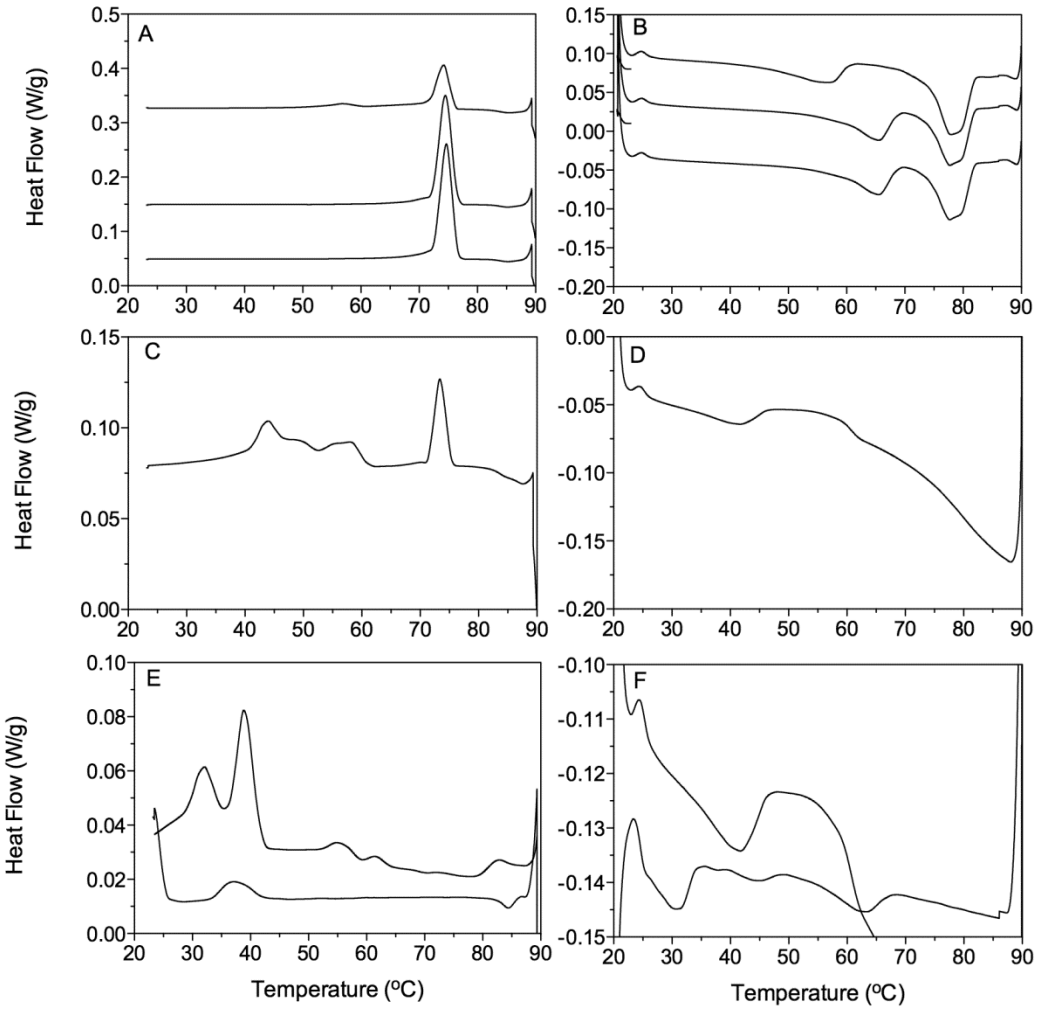

Appendix 2 DSC crystallization (A, C, E) and melting (B, D, E) thermograms of straight chain nitriles (A, B), aldehydes (C, D), and ketones (E, F) which have been vertically offset to prevent overlap. The thermograms from bottom to the top are butylnitrile, heptylnitrile and hexanitrile (A, B), dodecylaldehyde (C, D), and nonanone and undecone (E, F).

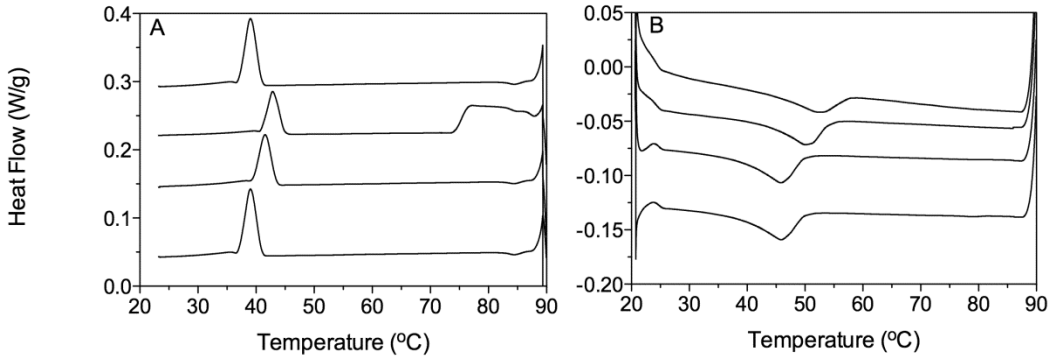

Appendix 3 DSC crystallization (A) and melting (B) thermograms of straight chain thiols, which have been vertically offset, to prevent overlap. The thermograms from bottom to the top are heptylthiol, hexathiol, octanethiol and decanethiol.